Trends in Estuarine Water Quality and Submerged Aquatic Vegetation Invasion

By

ERIN LEE HESTIR
B.A. (University of California, Berkeley), 2004

DISSERTATION

Submitted in partial satisfaction of the requirements for the degree of
DOCTOR OF PHILOSOPHY

in

GEOGRAPHY

in the

OFFICE OF GRADUATE STUDIES

of the

UNIVERSITY OF CALIFORNIA

DAVIS

Approved:

_____
Susan L. Ustin, Chair

_____
Deborah L. Elliott-Fisk

_____
David H. Schoellhamer

Committee in Charge

2010

ProQuest LLC
789 East Eisenhower Parkway
P.O. Box 1346
Ann Arbor, MI 48106-1346

TABLE OF CONTENTS

ACKNOWLEDGEMENTS

First I would like to extend my deep appreciation to my advisor, Susan L. Ustin. Not only has she provided guidance and support for my dissertation research, she has truly been an effective mentor, pushing me toward opportunities and challenges to better myself as a scientist. I hope one day my accomplishments reflect the effort she extended to my education and personal growth.

I could not have conducted this research without invaluable contributions from my co-authors and colleagues: Jonathan Greenberg, David Schoellhamer, Maria Santos, Shruti Khanna, Margaret Andrew, Tara Morgan-King, Joshua Viers, and Sepalika Rajapakse. Between my co-authors and my dissertation committee members, Susan Ustin, David Schoellhamer, and Deborah Elliott-Fisk, my dissertation has been improved and strengthened. I thank them for their hard work, sharp eyes, and keen brains. George Scheer ensured meticulous backup support.

I could not have survived graduate school without loving encouragement from my friends and family: Mom, Dad, Robin, Gerri, Tom and Tom, Eric, Meg, Maria, Jonathan, Lyra, Marcy, David, Abby, and more. I fear listing you all here would take more pages than I have (this paper is expensive!) You know who you are, and rest assured your championship (and patience) means the world to me.

Finally, I would like to especially acknowledge my mother, Dr. Ernestine Lee. I was fortunate enough to watch and learn from my mother as she pursued her doctorate in Chemistry while raising two teenage daughters with my father. She was an effective and inspirational role model for a young teenage girl. Mom, if I can be half as strong,

motivated, and successful a scientist as you, I will be a lucky woman. Thank you for being you.

This research was supported by the Interagency Ecological Program through California Department of Water Resources contract 4600008137-T4. Additional funding was provided by the California Department of Boating and Waterways agreement 03-105-114.

Erin Lee Hestir
June 2010
Geography

Trends in Estuarine Water Quality and Submerged Aquatic Vegetation Invasion

Abstract

The interaction between submerged aquatic vegetation (SAV), turbidity, and water movement is modeled as a feedback in which SAV reduces water flow, thus decreasing turbidity, and promoting growth. This positive feedback can promote ecosystem shifts to an alternative state (e.g. from a high turbidity-low SAV state to low turbidity-high SAV) from which it is unlikely to revert to its previous state (hysteresis). These shifts are usually modeled for SAV and turbidity in shallow lakes. Estuaries have different controls on turbidity that complicate this model, such as high mineral contribution to turbidity, as well as high hydrologic and environmental variability. The objective of this research was to detect feedbacks between SAV and turbidity in an anthropogenically modified estuary given the multiple external controls on turbidity and the variability of the system, and to determine if these feedbacks promote hysteresis.

Remote sensing was necessary to determine SAV distribution. Using a machine learning classifier, SAV was mapped in the Sacramento San Joaquin River Delta from airborne imaging spectroscopy acquired during June-July 2004-2008. Agreement between the map classes and ground reference data was “very good”, although discrimination between water and SAV was difficult when SAV was sparse or deep.

SAV areal cover was analyzed around *in situ* turbidity and velocity stations. Annual maximum water velocities from 2004-2006 that exceeded 0.49 $m \cdot s^{-1}$ controlled SAV cover. SAV cover limits high growing season turbidities from 2004-2008: SAV has

the most significant impact on turbidities ranging from 13.8-15.8 NTU, and this constraint on summertime turbidity is likely reducing habitat quality and quantity for the endemic and endangered fish the Delta smelt (*Hypomesus transpacificus*).

An analysis of historic turbidity data from the same stations showed a significant decline from 1975-2008 (-1.3% of the mean site turbidity/year); the turbidity decline is highly correlated with SAV cover (R2=0.9). The relative contribution of SAV to the decreasing turbidity trend averages between 21-70% of the total trend; this contribution varied with percent SAV cover. Anthropogenic activities in the watershed reduced the sediment supply into the Delta, which favored the expansion of SAV. Turbidity declines were further promoted by expanding SAV.

INTRODUCTION

Turbidity, or the optical clarity of a water body, is an important ecological indicator for inland freshwater and estuarine systems. Three primary constituents contribute to the clarity of an estuary: 1) suspended and dissolved sediment, 2) phytoplankton, and 3) dissolved organic matter (DOM) (Holden and LeDrew 2004). The transport of sediment through estuaries can influence the geomorphology and the rate and type of biogeochemical processes in wetlands and floodplains (Mertes et al. 1993, Jaffe et al. 2007), as well as the penetration of light in the water column which can influence productivity of submerged vegetation and photosynthetic capabilities of phytoplankton (Cloern 1987). Heavy metals and pesticides adsorb onto sediments in estuaries (Ruhl et al. 2001, Schoellhamer et al. 2007), and suspended sediments are cited as the most common pollutant in surface waters of freshwater systems (Schmugge et al. 2002); mercury, polychlorinated biphenyls (PCBs), and organochlorine (OC) pesticides are transported into the system attached to suspended sediment (Schoellhamer et al. 2007). Phytoplankton, often measured by the amount of chlorophyll-a in water, is commonly used as a trophic indicator of aquatic systems, based on nutrient availability. Phytoplankton serve as the base of the aquatic food web, and play an important role in biogeochemical and nutrient cycling (Cloern 1996). In the San Francisco Estuary phytoplankton are commonly light-limited rather than nutrient-limited, and are thus significantly affected by turbidity and suspended sediment. Phytoplankton populations are characterized by temporally and spatially ephemeral blooms (Cloern 1996), many of which are toxic to humans, benthic and pelagic organisms. Dissolved organic matter, primarily dissolved organic carbon, humic, and fluvic acids, is the primary food resource for plankton and nutrient regeneration (Hansell and Carlson 2002), contributes to the

acidity of freshwaters (Akkanen and Kukkonen 2001), decreases light availability in the water column, and also plays an important role in global carbon cycling (Hansell and Carlson 2002).

Submerged aquatic vegetation (SAV) is a subset of aquatic macrophytes; they are rooted, flowering vascular plants that establish in the softer sediments of aquatic habitats (Dennison et al. 1993). SAV is important in coastal estuarine systems; it provides habitat for fisheries and affects biological and physical processes such as nutrient cycling, sediment stabilization, and water turbidity (Dennison et al. 1993). Often, the health of SAV can be used as a "barometer" of an aquatic system's health, and this has become an important legal tool for the protection of coastal and estuarine waters (Bostater et al. 2003). However, in some estuarine systems, growth of submerged macrophytes, or the invasion of these species into new habitat indicate conditions of eutrophication or ecological disturbance (Giardino and Zilioli 2001). In these instances, the apparent health of invasive SAV is indicative of the declining health of the entire estuarine ecosystem. Invading SAV is primarily light limited (Barko et al. 1986), and water clarity is the most significant factor limiting light availability (Hudon et al. 2000, Madsen et al. 2001). However, SAV establishment and growth is also dependent on hydrodynamics (e.g., wave energy, water velocity), sediment characteristics and geochemistry (Madsen et al. 2001). SAV can itself act as an ecosystem engineer (Jones et al. 1994), altering the physical habitat it colonizes and inducing feedback mechanisms (Koch 2001). Once established, SAV can reduce water velocity (Petticrew and Kalff 1992), attenuate wave energy (Koch and Beer 1996), decrease turbidity and increase sedimentation (Madsen et al. 2001), which can all lead to further degradation of estuarine habitat, and increased

invasion by SAV. This feedback between SAV, turbidity, and water movement permeates the trophic structure of aquatic ecosystems, as changes in sediment dynamics, light availability and SAV distribution impact benthic habitat composition and pelagic habitat quality from primary production through to fish. However, it is unclear whether such feedbacks are present in estuaries due to dominance of turbidity by suspended sediment, and spatial and temporal variability of hydrology, turbidity, and SAV distribution. Furthermore it is unknown how influential these feedbacks, if present, are in ecosystem states.

Quantifying SAV distribution has several challenges: field-based methods can be time consuming, logistically precluded by inaccessibility, and direct contact with the vegetation can result in further weed dispersal (Bossard et al. 2000). Remote sensing provides a synoptic solution to quantifying and monitoring SAV over large spatial areas (Ackleson and Klemas 1987). However, for a remote sensing approach to be successful, the analysis must be accurate, repeatable over space and time, and account for the inherent variability in the system. In estuarine systems, meteorological, physical, and biological heterogeneity present problems that must be considered in order to successfully map SAV.

The objective of this dissertation research was to detect feedbacks between water movement, SAV, and turbidity in an anthropogenically modified estuary, to determine whether such feedbacks have permeated the trophic structure of the aquatic ecosystem and contributed to the declining health of the system. My research was conducted in the Sacramento-San Joaquin River Delta ("the Delta"), the upstream component of the San Francisco Estuary, the largest estuary in the Western United States. The estuary drains

over 160,000 km^2 of California into the Pacific Ocean via the San Francisco Bay, provides drinking water to 25 million people, and irrigates over 5 million acres of agricultural land contributing to the state's $31 billion agricultural industry. Once a vast tidal marsh, the Delta now is a mosaic of reclaimed "islands" of agricultural tracts, rip-rap levee-bound rivers connected by man-made sloughs, and flooded islands. Although a highly modified estuary (Nichols et al., 1986), the Delta provides critical habitat for five federally listed threatened or endangered fish, including the Delta smelt (*Hypomesus transpacificus*), which is sensitive to turbidity declines in the estuary (Sommer et al. 2007). The hydrodynamic variability of the system is manifest in a wide range of water depths, tidal fluxes, salinities, and freshwater inflows that exhibit extreme seasonal and inter-annual variability. Saline waters flow upstream into the Delta on flood tides during low-flow, and freshwater inflows from the Sacramento, San Joaquin, and tributary rivers flow downstream at 1700 ± 300 m^3s^{-1} in the winter and 540 ± 40 m^3s^{-1} in the summer (Jassby and Cloern 2000). El Nino-Southern Oscillation influences on precipitation patterns result in extremely dry or wet years, which in turn translate into very low flow (e.g.: 1977 annual mean flow 230 m^3s^{-1}) or high flow (e.g.: 1983 annual mean flow 2700 m^3s^{-1}) water years (Jassby and Cloern 2000).

Projections for climate change predict serious impacts on the Delta. Under even the coolest of climate warming scenarios, earlier snowmelt and reductions in snowpack by 2100 are predicted, which will alter Delta inflows, resulting in wetter winters, and drier summers (Knowles and Cayan 2004). This shift in the hydrograph, aggravated by increasing sea levels, will likely lead to dramatic changes in suspended sediment, salinity, and aquatic foodweb dynamics. Additionally, California's population is expected to

nearly double by 2050 (DWR 2007), placing additional pressure on the Delta for human and agricultural water consumption.

The Delta may be the most invaded estuary in the world (Cohen and Carlton 1998), and has been recently invaded by a fast growing macrophyte, *Egeria densa* which is actively changing the habitat in the Delta (Service 2007). *E. densa* grows in dense, monospecific stands throughout much of the Delta. It is the dominant SAV species in the Delta, and along with several other invasive SAV species (*Myriophyllum spicatum*, *Cabomba caroliniana*, *Potamogeton crispus*) has effectively replaced much of the native SAV. *Egeria densa* contributes 85% to the total biomass of SAV, followed by *Ceratophyllum demersum* (native) and *Myriophyllum spicatum* (invasive*)*. Major invasions of *E. densa* were first reported in the 1980s, and rapid expansion was observed in the 1990s. The estuary is also the site of a rapid decline in several fish populations. Since 2000 there have been record or near-record low abundances of four species, including the endangered Delta smelt (*Hyposemus transpacificus*). The decline in smelt has been attributed, in-part, to expansion of invasive SAV (Brown and Michniuk 2007), declining turbidity in the Delta (Nobriga et al. 2005), as well as recent blooms of toxic algae (Lehman et al. 2005). This research was motivated by the apparent ecological degradation that may have prompted such drastic fish declines. Have possible feedbacks between SAV, turbidity, and water movement contributed to the Delta's current "ecosystem crisis"?

This dissertation presents four manuscripts on remote sensing, SAV, turbidity, and velocity. Chapter 1 (Hestir et al. 2008) is an exploratory analysis of imaging spectroscopy to map invasive aquatic plant communities in the Delta. It introduces the

utility of remote sensing to determine aquatic vegetation distribution, and discusses the unique challenges to detecting submerged aquatic vegetation. Following the initial investigation into SAV detection outlined in Chapter 1, Chapter 2 (Hestir et al. 2010a) presents the method used to map SAV distribution in the Delta using a machine learning classification scheme on airborne imaging spectroscopy. Informed by the conclusions from Chapter 1, a field campaign conducted in summer 2008 concurrent with airborne spectroscopic remote sensing imagery collection provided the data necessary to train and validate an ensemble decision tree classifier to map SAV across 48 flightlines covering the Delta. This classifier was then successfully applied to archive image data from 2004-2007 to map SAV with very good agreement between the maps and ground reference data collected in those respective years. Chapter 2 highlights the necessity of narrow-band data across the visible through the short-wave infrared regions of the reflected spectrum-data provided only by airborne imaging spectroscopy- to SAV detection.

From the SAV distribution maps developed in Chapter 2, it was possible to investigate the interaction between SAV, turbidity and water velocity. Chapter 3 (Hestir et al. 2010b) uses the SAV areal cover around *in situ* turbidity and velocity stations and the data collected at those stations from 2004-2008 to identify annual maximum water velocity thresholds on SAV cover, and to model the limiting effect SAV cover has on growing season Delta turbidity. The results from Chapter 3 indicate the likelihood of positive feedbacks between SAV, turbidity, and water movement that leads to the potential of two ecosystem states reinforced by this feedback. In the first state, SAV cover is low, water velocity is high, sediment resuspension is high, and turbidity is high, thus limiting SAV. Under the second potential state, water velocity is low, SAV cover is

high, and turbidity is low which further promotes SAV growth. Such feedbacks leave aquatic ecosystems open to catastrophic ecosystem regime shift (van Nes et al. 2007). Chapter 4 (Hestir et al. 2010c) investigates the roles that the diminishing sediment supply and the SAV invasion into the Delta have in the declining turbidity trend, and speculates on the possibility of a regime shift.

Collectively, this research is intended to shed light into murky waters. Turbidity in estuaries is important to both the quality of water for human use and consumption, as well as ecosystem health. In the Delta particularly, high turbidity is needed for endangered fish habitat, and it is decreasing. Invasive submerged aquatic vegetation is likely acting as an ecosystem engineer; there are important feedbacks between SAV and water turbidity that have and may further diminish an already impaired ecosystem's health. An understanding of the interaction between SAV and turbidity in estuaries is needed to inform decision making under future climate change and water management and use scenarios, both issues of immediate importance in the San Francisco Estuary.

REFERENCES

Ackleson, S. G. and V. Klemas. 1987. Remote sensing of submerged aquatic vegetation in lower chesapeake bay: A comparison of Landsat MSS to TM imagery. Remote Sensing of Environment **22**: 235-248.

Akkanen, J. and J. Kukkonen. 2001. Effects of water hardness and dissolved organic material on bioavailability of selected organic chemicals. Environmental Toxicology and Chemistry **20**: 2303-2308.

Barko, J. W., M. S. Adams, and N. L. Clesceri. 1986. Environmental factors and their consideration in the management of submersed aquatic vegetation: A review. Journal of Aquatic Plant Management **24**: 1-10.

Bossard, C., J. Randall, and M. Hoshovsky, editors. 2000. Invasive plants of California's Wildlands. University of California Press, Berkeley.

Bostater, C., T. Ghir, L. Bassetti, C. Hall, E. Reyier, R. Lowers, K. Holloway-Adkins, and R. Virnstein. 2003. Hyperspectral remote sensing protocol development for submerged aquatic vegetation in shallow water. Remote Sensing of the Ocean and Sea Ice, Proceedings of SPIE **5233**: 199-215.

Brown, L. and D. Michniuk. 2007. Littoral fish assemblages of the alien-dominated Sacramento-San Joaquin Delta, California, 1980–1983 and 2001–2003. Estuaries and Coasts **30**: 186-200.

Cloern, J. 1996. Phytoplankton bloom dynamics in coastal ecosystems: a review with some general lessons from sustained investigation of San Francisco Bay, California. Reviews of Geophysics **34**: 127-168.

Cloern, J. E. 1987. Turbidity as a control on phytoplankton biomass and productivity in estuaries. Continental Shelf Research **7**: 1367-1381.

Cohen, A. and J. Carlton. 1998. Accelerating invasive rate in a highly invaded estuary. Science **279**: 555-558.

Dennison, W. C., R. J. Orth, K. A. Moore, J. C. Stevenson, V. Carter, P. W. Bergstrom, and R. A. Batiuk. 1993. Assessing water quality with submersed aquatic vegetation. BioScience **43**: 86-94.

DWR, C. 2007. Draft A & E Report for The California Water Plan, 2009. California Department of Water Resources, Sacramento.

Giardino, C. and E. Zilioli. 2001. Imaging Spectrometry for Submerged Vegetation Mapping in Make Garda. IEEE Transactions on Geoscience and Remote Sensing **6:** 2749-2751.

Hansell, D. and C. Carlson. 2002. Biogeochemistry of Marine Dissolved Organic Matter. Academic Press, Burlington.

Hestir, E., S. Khanna, M. Andrew, M. Santos, J. Viers, J. Greenberg, S. Rajapakse, and S. Ustin. 2008. Identification of invasive vegetation using hyperspectral remote sensing in the California Delta ecosystem. Remote Sensing of Environment **112**: 4034-4047.

Hestir, E. L., J. A. Greenberg, and S. L. Ustin. 2010a. Classification Trees for Aquatic Vegetation Community Prediction from Imaging Spectroscopy. IEEE Journal of Applied Remote Sensing **in review**.

Hestir, E. L., D. H. Schoellhamer, J. A. Greenberg, T. Morgan, and S. L. Ustin. 2010b. Interactions between Submerged Vegetation, Turbidity, and Water Movement in a Tidal River Delta. Water Resources Research **in review**.

Hestir, E. L., D. H. Schoellhamer, J. A. Greenberg, T. Morgan, and S. L. Ustin. 2010c. Turbidity Declines and Submerged Aquatic Vegetation Expansion in a Tidal River Delta. Estuaries & Coasts **in review**.

Holden, H. and E. LeDrew. 2004. Effects on the water column on hyperspectral reflectance of submerged coral reef features. Bulletin of Marine Science **69**: 685-699.

Hudon, C., S. Lalonde, and P. Gagnon. 2000. Ranking the effects of site exposure, plant growth form, water depth, and transparency on aquatic plant biomass. Canadian Journal of Fisheries and Aquatic Sciences **57**: 31-42.

Jaffe, B. E., R. E. Smith, and A. C. Foxgrover. 2007. Anthropogenic influence on sedimentation and intertidal mudflat change in San Pablo Bay, California: 1856-1983. Estuarine, Coastal and Shelf Science **73**: 175-187.

Jassby, A. and J. Cloern. 2000. Organic sources and rehabilitation of the Sacramento-San Joaquin Delta (California, USA). Aquatic Conservation: Marine and Freshwater Ecosystems **10**: 323-352.

Jones, C. G., J. H. Lawton, and M. Shachak. 1994. Organisms as Ecosystem Engineers. Oikos **69**: 373-386.

Knowles, N. and D. Cayan. 2004. Elevational Dependence of Projected Hydrologic Changes in the San Francisco Estuary and Watershed. Climate Change **62**: 319-336.

Koch, E. 2001. Beyond light: physical, geological, and geochemical parameters as possible submersed aquatic vegetation habitat requirements. Estuaries **24**: 1-17.

Koch, E. W. and S. Beer. 1996. Tides, light and the distribution of Zostera marina in Long Island Sound, USA. Aquatic Botany **53**: 97-107.

Lehman, P. W., G. Boyer, C. Hall, S. Waller, and K. Gehrts. 2005. Distribution and toxicity of a new colonial Microcystis aeruginosa bloom in the San Francisco Bay Estuary, California. Hydrobiologia **541**: 87-99.

Madsen, J. D., P. A. Chambers, W. F. James, E. W. Koch, and D. F. Westlake. 2001. The interaction between water movement, sediment dynamics and submersed macrophytes. Hydrobiologia **444**: 71-84.

Mertes, L., M. Smith, and J. Adams. 1993. Estimating suspended sediment concentration in surface waters of the Amazon river wetlands from Landsat images. Remote Sensing of Environment **43**: 281-301.

Nobriga, M., F. Feyrer, R. Baxter, and M. Chotkowski. 2005. Fish community ecology in an Altered River delta: Spatial patterns in species composition, life history strategies, and biomass. Estuaries and Coasts **28**: 776-785.

Petticrew, E. L. and J. Kalff. 1992. Water flow and clay retention in submerged macrophyte beds. Canadian Journal of Fisheries and Aquatic Sciences **49**: 2483-2489.

Ruhl, C. A., D. H. Schoellhamer, R. P. Stumpf, and C. L. Lindsay. 2001. Combined Use of Remote Sensing and Continuous Monitoring to Analyse the Variability of Suspended-Sediment Concentrations in San Francisco Bay, California. Estuarine, Coastal and Shelf Science **53**: 801-812.

Schmugge, T. J., W. P. Kustas, J. C. Ritchie, T. J. Jackson, and A. Rango. 2002. Remote sensing in hydrology. Advances in Water Resources **25**: 1367-1385.

Schoellhamer, D. H., T. E. Mumley, and J. E. Leatherbarrow. 2007. Suspended sediment and sediment-associated contaminants in San Francisco Bay. Environmental Research **105**: 119-131.

Service, R. F. 2007. Delta Blues, California Style. Science **317**: 4444.

Sommer, T., C. Armor, R. Baxter, R. Breuer, L. Brown, M. Chotkowski, S. Culberson, F. Feyrer, M. Gingras, B. Herbold, W. Kimmerer, A. Mueller-Solger, M. Nobriga, and K. Souza. 2007. The Collapse of Pelagic Fishes in the Upper San Francisco Estuary: El Colapso de los Peces Pelagicos en La Cabecera Del Estuario San Francisco. Fisheries **32**: 270-277.

van Nes, E., W. Rip, and M. Scheffer. 2007. A Theory for Cyclic Shifts between Alternative States in Shallow Lakes. Ecosystems **10**: 17-28.

· Chapter 1 ·

Identification of Invasive Vegetation Using Hyperspectral Remote Sensing in the California Delta Ecosystem

Identification of Invasive Vegetation Using Hyperspectral Remote Sensing in the California Delta Ecosystem

Erin L. Hestir[a], Shruti Khanna[a], Margaret E. Andrew[a], Maria J. Santos[a], Joshua H. Viers[b], Jonathan A. Greenberg[a], Sepalika S. Rajapakse[a], Susan L. Ustin[a].

[a] Department of Land, Air, and Water Resources, University of California, Davis, One, Shields Ave., Davis, CA 95616.

[b] Department of Environmental Science and Policy, University of California, Davis, One Shields Ave., Davis, CA 95616.

ABSTRACT

Estuaries are among the most invaded ecosystems on the planet. Such invasions have led to the formation of a massive $1 billion restoration effort in California's Sacramento-San Joaquin River Delta. However, invasions of weeds into riparian, floodplain, and aquatic habitats threaten the success of restoration efforts within the watershed and jeopardize economic activities. The doctrine of early detection and rapid response to invasions has been adopted by land and water resource managers, and remote sensing is the logical tool of choice for identification and detection. However meteorological, physical, and biological heterogeneity in this large riverine system present unique challenges to successfully detecting invasive weeds. We present three hyperspectral case studies which illustrate the challenges, and potential solutions, to mapping invasive weeds in riverine and wetland systems: 1) Perennial pepperweed was mapped over one portion of the Delta using a logistic regression model to predict weed occurrence. 2) Water hyacinth and 3) submerged aquatic vegetation (SAV), primarily composed of Brazilian waterweed, were mapped over the entire Delta using a binary decision tree that incorporated spectral mixture analysis (SMA), spectral angle mapping (SAM), band indexes, and continuum removal products. Perennial pepperweed detection was moderately successful; phenological stage influenced detection rates. Water hyacinth was mapped with modest accuracies, and SAV was mapped with high accuracies. Perennial pepperweed and water hyacinth both exhibited significant spectral variation related to plant phenology. Such variation must be accounted for in

order to optimally map these species, and this was done for the water hyacinth case study. Submerged aquatic vegetation was not mapped to the species level due to complex nonlinear mixing problems between the water column and its constituents, which was beyond the scope of the current study. We discuss our study in the context of providing guidelines for future remote sensing studies of aquatic systems.

1. INTRODUCTION

Invasions of aquatic weeds into freshwater, estuarine, and floodplain habitats can decrease biodiversity, threaten critical habitat, alter nutrient cycles, and degrade water quality. An estimated USD $100 million per year is spent on control and eradication programs targeting aquatic weeds in the United States (Pimentel et al., 2000). Systematic, comprehensive monitoring programs are needed to detect invasions in order to effectively control aquatic weeds. Traditional methods of monitoring weed infestations are costly, time consuming, and often require direct contact with the weeds which can result in further weed dispersal (Bossard et al., 2000). Additionally, aquatic ecosystems are often inaccessible or logistically difficult for field-based monitoring methods. Remote sensing provides a synoptic solution for monitoring aquatic weed infestations over large spatial areas (Ackleson and Klemas, 1987). To be successful, a remote sensing approach must be accurate, repeatable over space and time, and account for the inherent spatial and environmental heterogeneity of a system.

We present three case studies that illustrate how these problems can be addressed to develop regional-scale monitoring of invasive aquatic and wetland weeds in the Sacramento-San Joaquin Delta: the terrestrial riparian weed, perennial pepperweed (*Lepidium latifolium*); the floating aquatic weed, water hyacinth (*Eichhornia crassipes*); and the submerged aquatic weed, Brazilian waterweed (*Egeria densa*). Each case study highlights the complexities of remote sensing of aquatic and wetland systems. They also demonstrate a range of techniques that can be used, and often integrated, to produce accurate maps that can be used by wetland and estuarine resource managers. Our examples are from a study to map these invasive species at high spatial

resolution (3 m) over a regional area of 2500 km^2. The challenge of analyzing airborne hyperspectral remote sensing over a large study region notwithstanding, we demonstrate that the techniques presented can be applied consistently to all flightlines in the study region over multiple years, thus creating an effective and comprehensive monitoring program.

In estuarine systems, meteorological, physical, and biological heterogeneity present serious challenges that must be resolved to successfully map and monitor distributions of aquatic vegetation species. Meteorological heterogeneity is one challenge to invasive species monitoring. Factors such as weather conditions, sun, and view angle determine the bidirectional reflectance distribution function (BRDF), which complicates remote sensing of aquatic vegetation, especially submerged aquatic vegetation (SAV) such as Brazilian waterweed. Sunglint is light specularly reflected off the water surface which effectively impedes retrieval of a useable signal (Bostater et al., 2004; Mertes et al., 1993; Morel and Belanger, 2006). Variable sun angles and wind speeds contribute differing flightline effects that confound region-wide analyses. The spectral detection of SAV is also affected both by the apparent optical properties of water, such as surface reflectance and vertical diffuse attenuation, and inherent optical properties that do not depend on the ambient radiance distribution in the water column (Mobley, 1994). Water depths change with tidal stage and runoff; suspended and dissolved materials vary over geomorphological gradients, meteorological conditions, flow conditions, and land use practices. All of these effects influence remote sensing of aquatic systems by limiting the detection of SAV as light attenuates with depth, altering the water leaving reflectance.

Another challenge to monitoring this system is its biological heterogeneity. Plant phenology varies across the large gradients present in this system. Water hyacinth and perennial pepperweed life histories must be accounted for to capture key phenological attributes such as flowering and senescence. Different phenologic states, combined with differences in leaf and canopy structure can be present over short distances, creating intra-species variation that can result in overlapping spectral features between co-occurring species. Additionally, weed species

may be present in subpixel mixtures even at high spatial scales. Hyperspectral imaging may provide sufficient information to overcome these challenges, allowing the application of more complex spectral analyses and spectral unmixing techniques (Becker et al., 2007; Bostater et al., 2004; Hirano et al., 2003; Schmidt and Skidmore, 2003; Williams et al., 2003).

To summarize, detecting and monitoring invasive weed species in wetland and aquatic ecosystems at the region-wide scale is complicated by considerable physical and environmental variability. The spatial heterogeneity of these systems requires moderate to high spatial resolution (< 5m) imagery (Becker et al., 2007). High spectral resolution imaging (> 100 bands with narrow bandwidths) can be used to improve discrimination of target species and resolve complex mixing problems. Flightline effects also contribute additional variability. We overcame this variability by incorporating multiple widely available techniques into novel classification schemes for water hyacinth and SAV detection, and by using a logistic regression model to map perennial pepperweed.

2. STUDY SITE

The Sacramento-San Joaquin River Delta (hereafter the "Delta") is formed by the confluence of the Sacramento and San Joaquin Rivers and drains into the Pacific Ocean via the San Francisco Bay (Figure 1). The Bay-Delta is the largest estuary in the western United States and its watershed drains over 160,000 km^2 of California. The hydrodynamic heterogeneity of the Delta system is manifest in a wide range of salinities, tidal fluxes, water depths, and freshwater inflows with extreme seasonal and interannual variability (Jassby and Cloern, 2000). Saline waters flow upstream into the Delta on flood tides, and freshwater inflows from the Sacramento, San Joaquin, and tributary rivers flow downstream at an average of 1700 ± 300 m^3s^{-1} in the winter and $540 \pm 40 m^3s^{-1}$ in the summer (Jassby and Cloern, 2000). The El Niño-Southern Oscillation influences precipitation patterns, resulting in extremely dry or wet years, that respectively translate into very low flow (e.g.: 230 m^3s^{-1} in 1977) or high flow (e.g.: 2700 m^3s^{-1} in 1983) water years (Jassby and Cloern, 2000). This study focuses on the Central Delta (2,139 km^2),

which contains the confluence of the Sacramento and San Joaquin Rivers and the network of small channels, rivers, and lakes formed by flooded agricultural tracts that connects them.

The Delta provides drinking water, agricultural water and land, recreational opportunities in the form of boating and fishing, and shipping access to the cities of Stockton and Sacramento. The Delta is a major hub for freshwater conveyance systems in the state, providing drinking water for 25 million people and important irrigation resources for California's $32 billion agricultural industry (CDFA, 2006). The estuary contains habitat for waterfowl along the Pacific flyway as well as threatened and endangered fish species such as Delta smelt, steelhead, and chinook salmon. Unfortunately, the Delta may have the largest number of invasive species of any estuary in the world (Cohen and Carlton, 1998) and is the focus of a massive coordinated ecosystem restoration program, with direct expenditures exceeding USD $1 billion beginning in the mid-1990s (Lund et al., 2007). Invasions of aquatic weeds into the Delta negatively impact ecosystem health, drinking and agricultural water quality, pumping, recreation, and shipping (Bossard et al., 2000), and may prevent the success of native habitat restoration projects within the Delta (Simenstad et al., 2000). The three focal invasive species (perennial pepperweed, water hyacinth, and Brazilian waterweed; Figure 2) are all considered problems in the Delta, and have been granted high visibility and threat status according to the California Invasive Plant Council (Cal-IPC) and the California Department of Food and Agriculture (CDFA).

3. REMOTELY SENSED DATA

To map perennial pepperweed, water hyacinth and SAV (dominated by Brazilian waterweed), we acquired 64 HyMap flightlines encompassing the entire Delta (Figure 1). HyMap is an airborne hyperspectral imager that collects 128 bands in the visible and near-infrared (VNIR; 0.45-1.50 μm) through the shortwave infrared (SWIR; 1.50-to 2.5 μm), at bandwidths from 10 nm in the VNIR to 15-20 nm in the SWIR (Cocks et al., 1998). The spatial resolution of the data is 3 m, with a swath width of 1.5 km. The area was flown in an east-west orientation, at an altitude of approximately 1510 m. Imagery was collected during late morning

and early afternoon low tides between June 22 and July 5, 2005, and June 21 and June 26, 2006 (Figure 1). The HyMap images were converted to apparent surface reflectance using the HyCorr atmospheric correction software (Hyvista Corp., Sydney, Australia), a modified version of the Atmospheric Removal (ATREM) algorithm (Gao et al., 1993). We used an orthorectification algorithm (Analytical Imaging and Geophysics, Boulder, CO) to orthorectify the imagery using the United States Geologic Survey National Elevation Set Digital Elevation Models and a set of 1-foot (covering 30 flightlines) and 1-meter (covering 34 flightlines) color orthophotos. A minimum of 20 ground control points with a total RMSE $\leq$ 1.0 were used for each flightline. Visual inspection of image registration accuracy confirmed a registration error of $\simeq$ 1 pixel. For a detailed report of image data collection and preprocessing steps please see Ustin et al. 2006.

4. GROUND REFERENCE DATA

4.1. Perennial Pepperweed

Field observations were recorded between 2002 and 2006 with a comprehensive inventory of perennial pepperweed populations on selected Cosumnes River Preserve (CRP) lands (Viers et al., 2005). Mapped botanical surveys of perennial pepperweed were conducted during flowering to aid in the identification of pepperweed patches, which were defined as areas containing a minimum of one individual and located at least 3 meters from another patch. For each perennial pepperweed patch, GPS polygons delineating the patch, the number of individuals, areal percent cover, and patch area were recorded (1 m^2 minimum). A total of 345 patches over 15.5 ha were mapped by the inventory.

4.2. Water Hyacinth and SAV

Field data collection efforts for both water hyacinth and SAV were conducted simultaneously with hyperspectral image acquisition. GPS locations of large ($\geq$ 3 x 3 meters), homogenous patches of aquatic vegetation (submerged and floating or emergent species), patch size, percent cover of target and co-occurring species, algal cover, and presence of inflorescences were recorded by survey crews in six boats. Eight emergent or floating species and five

submerged aquatic species were selected for field identification. Emergent and floating species included water hyacinth, pennywort (*Hydrocotyle ranunculoides*), water primrose (*Ludwigia* spp.), California tule (*Schoenoplectus acutus*), cattail (*Typha* spp.), the wetland common reed (*Phragmites australis*), azolla (*Azolla*), and duckweed (*Lemma minor*). Submerged aquatic vegetation species recorded included Brazilian waterweed, Eurasian watermilfoil (*Myriophyllum spicatum*), coon's tail (*Ceratophyllum demersum*), Carolina fanwort (*Cabomba caroliniana*), and pondweed (*Potamogeton* spp.). We also collected GPS locations of water with no apparent algae or vegetation and assessed turbidity with a Secchi disk. A total of 2,631 points over 33,000 ha were collected in 2005, and 3,285 points over the same area were collected in 2006. Field data points were screened *a posteriori* for accuracy in species identification, homogeneity in patch size and percent cover, and geographic error associated with the movement of boats with wind and currents during point collection. This resulted in 2,381 ground reference points for 2005, and 2,962 for 2006.

5. CASE STUDIES

The novel analysis approaches used in these case studies integrated many well-established tools used in hyperspectral remote sensing that have previously been applied to a variety of remote sensing studies, including invasive weed mapping (Table 1).

5.1. Cosumnes River Floodplain Perennial Pepperweed Case Study

Perennial pepperweed is an herb of Eurasian origin that was introduced into the USA in the 1930s and is now found throughout California (Figure 2 a; Bossard et al., 2000). The weed grows in several environments, including freshwater, brackish to saline, and alkaline, and in a wide range of habitats including riparian areas, wetlands, marshes, meadows, and floodplains (Bossard et al., 2000; Renz and Blank, 2004; Young et al., 1997; Young et al., 1995). It is also often found in hypersaline conditions (Spenst, 2006), although it is not an obligate halophyte. The natural history of perennial pepperweed, which spreads via prolific seed production (Young

et al., 1997) and highly friable root fragments (Young et al., 1998), enables highly effective propagation and establishment in riparian and floodplain areas.

The Cosumnes River Preserve (CRP) is a collection of parcels (18,000 ha) in the Delta that are managed as a combination of working and natural landscapes by a consortium of state, federal, and non-profit organizations. The preserve includes a lowland river floodplain that is the focus of an ongoing study to characterize the successional trajectory following reconnection of the Cosumnes River with its floodplain. Restoration of the river floodplain was initiated by an accidental levee breach (ca. 1985), and subsequently by intentional breaching of levees during the late-1990s (Florsheim and Mount, 2003). Since then, the river channel and its floodplain have undergone considerable geomorphic change (Florsheim and Mount, 2002, 2003) that has increased the habitat heterogeneity due to colonization of riparian and floodplain vegetation on sand deposits. However, invasion by non-native plant species including perennial pepperweed threatens the long-term success of this restoration project.

Perennial pepperweed frequently reveals mixed, degraded spectra due to its sparse architecture, and the features that lend spectral distinctness at the canopy scale (chiefly, high reflectance throughout the visible imparted by characteristic white inflorescences (Andrew and Ustin, 2006); resemble vegetation mixed with litter or soil at the pixel scale. We therefore limited our classification to pixels dominated by perennial pepperweed selected defined as those where perennial pepperweed covers at least 75% of the total pixel area. Because of the wide range in environmental and hydrological conditions throughout the CRP, at the time of image acquisition, perennial pepperweed exhibited vegetative, flowering, fruiting, and senescing phenologies. The large amount of spectral variation caused by flightline effects, environmental variability, and multiple phenologic stages, in combination with other natural environmental variations, precluded the use of sophisticated unmixing techniques that have been successful at other sites (notably mixture-tuned matched filtering, Andrew and Ustin, 2007). Instead, our mapping strategy used a two-tiered approach: first we generated a continuous map of the probability of perennial

pepperweed presence using a logistic regression model, and second we set a threshold to classify all pixels with > 75% perennial pepperweed cover as being "perennial pepperweed dominated".

5.1.1. Methods

Eight of the 64 2005 HyMap flightlines of the Delta (acquired 23 June 2005 and 28-29 June 2005) contained the CRP. The portions of these flightlines encompassing CRP were cropped and mosaicked together. A minimum noise fraction (MNF) transformation was applied to the hyperspectral mosaic. Logistic regression models were developed in JMP IN (v. 5.0, SAS Institute, Cary, NC) to predict the per-pixel probability of the occurrence of perennial pepperweed. The regression was trained and validated using a random sample of pixels with >75% cover from the CRP inventory (n=930) as well as a random sample of pseudo-absence points (n=63,439). The pseudo-absence points were a random sample of pixels selected from the region most comprehensively surveyed for perennial pepperweed. Known perennial pepperweed pixels were excluded from the random sample, and remaining pixels were assumed to indicate perennial pepperweed absence. 75% of the presence (n=693) and pseudo-absence points (n=47,553) were used to train the regression. MNF bands containing negligible information were excluded from analysis. MNF bands were visually inspected and those exhibiting severe flightline effects were discarded. The remaining bands were chosen through stepwise entry into the logistic regression model. A prediction formula using MNF bands 2-11, 15, and 17 optimized the discrimination of perennial pepperweed from other land cover types (evaluated using R^2). This model was assessed by regressing the estimated probability of perennial pepperweed occurrence (p) against percent cover estimates from the CRP inventory data. The value of p corresponding to 75% cover by perennial pepperweed was identified and pixels were classified as "perennial pepperweed dominated" if their predicted value exceeded this threshold.

Classification accuracy was assessed with the remaining perennial pepperweed presence (n=219) and pseudo-absence points (n=15,886). To assess the contribution of phenological variation to omission errors, we divided all perennial pepperweed dominated pixels into

phenological classes using a K-means unsupervised classification on the same MNF bands as used by the regression model. Phenology of these classes was determined through visual inspection and verified with three physiological indexes: the normalized difference vegetation index (NDVI; Tucker, 1979), the normalized difference water index (NDWI; Gao, 1996), and the cellulose absorption index (CAI; Nagler et al., 2000).

5.1.2. Results

The predicted value (p) provided a reasonably good indicator of the percent cover of perennial pepperweed within a pixel (p=-0.084253 + 0.0072013[% cover perennial pepperweed], $R^2 = 0.41$, n = 2,787). The final classification distinguished perennial pepperweed from pseudo-absence pixels (Table 2) with user's and producer's accuracies of perennial pepperweed detection of 75.8% and 63.0% respectively, and Kappa coefficient relative to the perennial pepperweed class of 0.68.

The K-means classifier found five distinct groups of perennial pepperweed dominated pixels (Table 3). These groups fell out along a gradient of dryness/senescence and were interpreted as completely senescent (n=1), shaded by or under a tree canopy (n=77), flowering (n=277), fruiting (n=363), and senescing (n=190). These interpretations were supported by the physiological indexes. NDVI, NDWI, and CAI all showed significant effect of group ($p<0.0001$; ANOVA) and, for each index, all groups were significantly different from each other at the p=0.05 level (Tukey test, Sokal and Rohlf, 2000). The detection rate of these classes ranged from 0% (senescent) to 85% (fruiting), with fruiting and flowering phenologies showing the highest detection rate (Table 3) in both the training and test sets. The fruiting, flowering, and senescing phenology classes are the most relevant to a remote sensing study. When just these three classes were used to evaluate the classifier performance, the producer's accuracy of the classifier increased to 76.6%.

5.2. California Delta Water Hyacinth Case Study

Introduced to the Sacramento River in 1904 by horticulturalists (Cohen and Carlton, 1995; Finlayson, 1983; Toft et al., 2003) water hyacinth now obstructs navigable waterways, degrades water quality, fouls water pumps, blocks irrigation channels, and has caused significant changes to ecological assemblages throughout the Delta (Bossard et al., 2000; Toft et al., 2003). The California Department of Boating and Waterways is the management agency responsible for controlling water hyacinth in the Delta (Cohen and Carlton, 1995), which is done through the application of chemical herbicides and mechanical removal.

One of the fastest growing plant species in the world (> one ton dry matter day^{-1} ha^{-1}; (Bossard et al., 2000), water hyacinth is a floating aquatic plant forming dense stands that exhibit diverse leaf and canopy morphologies, dependent on patch location and mat density (Figure 2b). Within a single mat of water hyacinth several different leaf morphologies and phenologies can be found (Gopal, 1987). In the Delta, water hyacinth often occurs alongside other floating emergent species like pennywort and water primrose.

As with perennial pepperweed, the spectral signature of water hyacinth is highly variable as the plant can exhibit many contemporaneous phenologies including vegetative, flowering, stressed, and senescent forms that result from herbicide application and frost damage to overwintering plants. The spectral variability of water hyacinth results in spectral overlap with the co-occurring floating plant species pennywort and water primrose, which leads to mixed pixels with spectrally similar constituents. Spectral mixture analysis (SMA; Smith et al., 1990), Spectral Angle Mapper (SAM; Kruse et al., 1993) and continuum removal (Clark and Roush, 1984) have been demonstrated as an effective technique for species-level vegetation detection. Before using these techniques for water hyacinth mapping, we explicitly eliminated other sources of confusion (e.g. terrestrial pixels, mixing with water, SAV, and other emergent plant species) from the analysis area.

5.2.1. Methods

The strategy for water hyacinth classification was to develop a binary decision tree, where each node reduces the variance in the remaining pixels until a map of hyacinth presence and absence was achieved, using the 2005 HyMap data (64 flightlines). The 2005 field data was separated into training (n=1,027) and validation (n=1,354) data for the decision tree. This same methodology was also applied to the 2006 HyMap data using 2006 field data separated into 158 training and 2,804 validation points. Figure 3 depicts a schematic of the water hyacinth decision tree.

In order to discriminate aquatic versus terrestrial land cover types, we first created a mask of the water boundaries (which includes submerged and emergent aquatic vegetation) by manually adjusting the US Bureau of Reclamation GIS layer of waterways. In ArcGIS (version 9.2, ESRI Inc, Redlands, CA) the line map of waterways was overlaid on a color infrared composite of the HyMap images and the edge of the water boundary was matched with the image data. An unconstrained spectral mixture analysis (SMA) was used to identify and exclude any levee banks that may not have been removed by the watermask. The SMA was performed using spectral endmembers of aquatic vegetation, water, and soil derived from the imagery using ground reference data (Figure 4). All pixels in which the SMA fraction for water was < 10% or average albedo between 1.5995 μm – 1.764 μm was higher than 4% were identified as aquatic vegetation. The average reflectance of bands in the shortwave infrared wavelengths 1.5995 μm – 1.764 μm (HyMap bands 78-91) was used to discriminate floating emergent species from submerged aquatic vegetation, sparse tule, and turbid water. Floating emergent species have distinctively high albedo in the SWIR whereas submerged aquatic vegetation, sparse tule and turbid water have muted albedo in the SWIR due to strong infrared absorption by water. Thus, pixels with SWIR reflectance values less than 4% were classified as submerged aquatic vegetation, sparse tule, or turbid water. All other pixels were classified as emergent aquatic vegetation. Note that although tule is an emergent plant, under moderate to low percent cover its

reflectance values across the spectrum are usually lower than those of floating emergent species as it has an erectophile canopy structure and often occurs in mixed pixels with water.

In order to separate darker emergent vegetation such as tule and cattail with high percent cover from bright floating emergent vegetation such as water hyacinth, pennywort, and primrose, the average reflectance value in the near infrared 1.0451 μm – 1.1186 μm (HyMap bands 42-47) was calculated. Pixels identified as emergent aquatic vegetation by the previous node in the decision tree were further classified as "dark" emergent aquatic vegetation if their NIR reflectance value was less than 40% otherwise they were classified as "bright" floating emergent aquatic vegetation. This is a necessary step as many of the pixels classified as water hyacinth "spectral class 2" (Figure 5) are significantly darker in the near-infrared, and must be separated from brighter emergent aquatic vegetation before being classified to the species level. We next set the NIR reflectance threshold even lower to separate tule from other emergent species. Dark emergent aquatic vegetation pixels with less than 24% reflectance in 1.0451 μm – 1.1186 μm were classified as tule.

The final nodes of the decision tree used both the Spectral Angle Mapper (SAM) technique and a water absorption feature to separate water hyacinth from co-occurring floating and emergent species in both classes of vegetation (bright and dark). Water hyacinth is a fleshy, succulent plant, having greater foliar water content than the co-occurring floating species. To take advantage of this difference, we used continuum removal (Clark and Roush, 1984) to quantify the water absorption feature located between 0.907 μm – 1.0746 μm (HyMap bands 33-44). Lower continuum-removed values indicate greater water content. Spectral Angle Mapper is appropriate for species-level monitoring at the regional scale as it is not sensitive to albedo differences across the 64 flightlines; SAM can identify subtle differences in pixel spectra while being insensitive to gain factors. SAM was applied to a subset of the visible and NIR bands (0.45 μm to 0.9541 μm) to reduce noise contributed to the pixel spectra from mixing with water. The SAM technique used endmembers derived from the image data that were representative of

different phenological states and geographic locations throughout the dataset, as determined from the field data (Figure 5). In the dark emergent class identified by low NIR average reflectance, pixels with a continuum removal value less than 0.86, when coupled with the SAM water hyacinth classification output were classified as water hyacinth spectral class 1. In the bright class, pixels were first classified using the SAM output to identify water hyacinth spectral class 2 and the remaining pixels from the continuum removal were classified as water hyacinth spectral class 1 if their value was less than 0.83, otherwise they were classified as pennywort or water primrose. These thresholds were determined empirically based on our field data.

Classification results for validation pixels were extracted from the classified imagery using STARSPAN (http://starspan.casil.ucdavis.edu), an algorithm developed to provide fast, selective pixel extraction from raster and vector data (Rueda and Greenberg, 2004). The accuracy of the emergent classification was assessed with a confusion matrix and kappa statistics were calculated (Lillesand et al., 2004).

5.2.2. Results

In 2005, water hyacinth infested 167.07 ha in the Delta. Out of the 204 field points of water hyacinth that were used for validation, 141 were correctly classified as water hyacinth and 63 were misclassified, resulting in a producer's accuracy of 69.1%. 16 pixels were erroneously classified as water hyacinth, resulting in a user's accuracy of 89.8%. The estimated Kappa coefficient relative to the water hyacinth class is 0.81 (Table 4), a value considered to show strong agreement (Congalton, 1996). We interpret water hyacinth spectral class 1 to be either stressed or flowering water hyacinth due to its darker reflectance in the near-infrared (Hardisky et al., 1986) and a shallower water absorption feature at 0.907 µm – 1.0746 µm (Peñuelas et al., 1993). Based on field observations, these mats have sparser canopies and smaller leaves, resulting in greater confusion with other floating emergent species. When considering the detection rate of these two spectral classes, the producer's accuracy of the healthy/robust water hyacinth class increases to 93.3%, and the producer's accuracy of the other class is 85.1%. Of the 16

commission pixels, 6 were mistakenly identified as healthy/robust water hyacinth, and 10 were incorrectly classified as stressed or flowering water hyacinth.

5.2.3. 2006 Water Hyacinth Classification

A decision tree containing these same variables but with different thresholds determined from 2006 field data was applied to the 2006 HyMap imagery. The areal infestation of hyacinth increased in 2006, where 303 ha of water hyacinth were identified. Out of the 218 water hyacinth field points used for classification validation, 112 pixels were correctly classified as water hyacinth, and 106 were misclassified, producing a user's accuracy of 51.4%. Sixty-nine pixels were incorrectly identified as water hyacinth, resulting in a producer's accuracy of 61.9% (Table 5). The estimated Kappa coefficient relative to the water hyacinth class is 0.49, a value considered to show moderate agreement (Congalton, 1996). The producer's accuracies of the healthy/robust water hyacinth and the stressed/flowering hyacinth are 86.5% and 44.9%, respectively; only 10 comissed pixels were erroneously classified as healthy or robust water hyacinth, whereas 59 commission pixels were misclassified as stressed or flowering water hyacinth. Thus, the decision tree approach described above accounts for the variability inherent in such a dynamic ecosystem; successfully identifying the target species over multiple flightlines, and with minor modifications, over multiple years without requiring enormous training sets for each new year. Nearly half of the 2005 field data were needed to train the 2005 decision tree, whereas only about a tenth was needed in 2006.

5.3. California Delta SAV Case Study

Brazilian waterweed is an SAV species that is the focus of considerable concern in the Delta. Delta aquatic habitats are generally considered degraded (Meng and Moyle, 1995), but more specifically, Brazilian waterweed infested areas hinder the movement of threatened and endangered fishes such as anadromous salmonids, splittail, and Delta smelt (Brown, 2003), and it may prove to make restoration of native habitat nearly impossible where it is firmly established (Simenstad et al., 2000). Furthermore, dense mats of Brazilian waterweed interfere with

recreational and commercial activities such as fishing, boating, swimming, and urban water and irrigation pumping (Bossard et al., 2000). The California Department of Boating and Waterways is again the responsible agency for controlling Brazilian waterweed in order to maintain navigable waterways in the Delta.

Brazilian waterweed forms thick, mono-specific stands of long, intertwining stems and has small white flowers that float at the water surface (Figure 2 c), spreading via fragmentation (Bossard et al., 2000). Its stems can grow as long as 4.5 m, branch frequently, and although usually rooted to the substrate as deep as 7 m below the water surface (Parsons and Cuthbertson, 1992), it can also be found as a free floating mat (Bossard et al., 2000). Brazilian waterweed is adapted to low-light conditions and turbid water appears to favor growth, but it has also been found to thrive under red light, suggesting an affinity for the water surface (Bossard et al., 2000).

The remote sensing signal of SAV at the water surface can become degraded due to attenuation of light with water depth, which varies widely based on bathymetric variability and tidal variability (Underwood et al., 2006), and increased concentrations of water constituents which also vary across the region. Additionally, non-linear spectral mixing occurs as epiphytic algae often grow on Brazilian waterweed and other species of SAV, and emergent algae mats form on top of SAV canopies, obscuring the spectral target. SMA has been successfully applied to Brazilian waterweed discrimination at local sites (single flightlines) in the Delta since 2003 (Mulitsch and Ustin, 2003; Underwood et al., 2006). After reducing other sources of variance from turbid water and very low cover tule in an approach similar to the water hyacinth case study (section 5.2), a combination of spectral unmixing and SAM were used to overcome the mixing problem and to discriminate Brazilian waterweed dominated SAV from other water constituents and isolate it from algae while taking flightline effects into account.

5.3.1. Methods

A decision tree approach was used to map SAV across the 64 2005 HyMap flightlines (Figure 6). Training (n=1,027) and validation data (n=1,354) are described above. All pixels

previously classified by the SMA and the SWIR reflectance value threshold (section 4.2.1.) as SAV, turbid water, or tule were analyzed using this tree.

The classic "red edge" reflectance feature, indicative of chlorophyll in vegetation (Curran et al., 1991; Filella and Peñuelas, 1994; Gitelson and Merzlyak, 1997) was quantified with HyMap bands 19 and 16 (0.7313 µm and 0.6736 µm) in a normalized difference band index which separated turbid water pixels from vegetated pixels. Hoogenboom et al. (1998) found that turbid water bodies with relatively high total suspended solids (TSS) and low phytoplankton concentrations, such as the Delta, display high reflectance up to 0.72 µm. Thus it is relatively easy to separate the red edge from visibly "bright" turbid water.

Although most emergent aquatic species were screened using the SMA and SWIR thresholds described in the water hyacinth decision tree, it was necessary to isolate tule pixels of low percent cover that were classified as SAV because of the spectral dominance of water. The average reflectance of the SWIR bands (1.5995 µm – 1.764 µm) from section 4.2.1. was used, and the threshold was lowered so that pixels with SWIR reflectance less than 3% were classified as submerged aquatic vegetation.

SMA is most successful when just a few endmembers that are spectrally distinct are used to train the SMA. When more similar endmembers are included, the RMSE of the estimated fractions increases (Roberts et al. 1993). To circumvent this problem, a second SMA was conducted on pixels with a water fraction of 10% or greater as determined by the first SMA (section 4.2.1.) and the low SWIR albedo (4.3.1.). The second SMA was trained with four endmembers selected from the imagery using ground reference points of clear water, turbid water, SAV, and emergent algae. Although the endmembers appear spectrally similar (Figure 7), they effectively encompassed the range of spectral variation present in pixels analyzed, which was itself limited, resulting in acceptably accurate (based on validation data) SMA fractions. However, SMA and classic chlorophyll absorption characteristics could not fully identify SAV and discriminate it from other constituents of the water column. In order to further discriminate

water from submerged aquatic vegetation and to isolate SAV from emergent algae on the water surface, SAM was conducted using the visible and NIR wavelengths (as described in section 4.2.1.). This step was included as the final node in the SAV decision tree.

At the time of this analysis, we were unable to identify individual SAV species accurately. Even in pixels with 100% SAV cover at the water surface, pixel reflectance is still dominated by the very strong absorption of water and the spectral variability between species is slight. Nevertheless, Brazilian waterweed has been successfully discriminated from co-occurring SAV species using SMA at very small-scale sites (Mulitsch, 2005). However, given the large scale of the entire Delta, and the extensive variation resulting from the many confounding factors discussed, we have not yet demonstrated that the subtle spectral differences between SAV species are consistently detectable.

5.3.2. Results

In 2005 2,246.5 hectares of Delta waterways were infested with SAV. Out of 316 validation points collected of submerged aquatic vegetation, 187 were correctly classified as SAV, 50 were misclassified as water, and 79 were incorrectly classified as emergent vegetation, resulting in a producer's accuracy of 59.2%; 16 field points were misclassified as SAV, resulting in a user's accuracy of 92.1%. The Kappa coefficient relative to the SAV class is 0.86 (Table 6), indicating strong agreement (Congalton, 1996).

5.3.3. 2006 SAV decision tree

Although we were not able to differentiate SAV to the species level, we were able to develop a method that, like the water hyacinth decision tree, is repeatable across multiple flightlines and multiple years for the same geographic location. A slightly modified decision tree was developed for 2006 imagery that could detect three different SAV classes based on the output of Spectral Angle Mapper. However, other than the additional SAM classes (see Figure 8 for SAM endmembers), the decision tree contained the same variables as the 2005 tree. Areal infestation of SAV decreased to 1,722.8 hectares in 2006. Out of the 1218 SAV field points used

for validation, 844 were correctly identified as SAV, 255 were misclassified as emergent vegetation, and 119 were misclassified as water, resulting in a producer's accuracy of 69.3%. Sixty-one field points were incorrectly classified at SAV, resulting in a user's accuracy of 93.3%. The Kappa coefficient relative to the SAV class is 0.87 (Table 7), a value considered to show strong agreement (Congalton, 1996).

6. DISCUSSION & CONCLUSIONS

The approaches in these case studies provide useful solutions for overcoming the spectral heterogeneity inherent to aquatic and wetland ecosystems. We found that hyperspectral remote sensing can be used to map invasive weeds in extensive dynamic ecosystems such as the Delta, and that multiple hyperspectral tools can be combined to accommodate high variability. Our case studies have demonstrated that both traditional and novel approaches to species mapping and monitoring are effective for use with large datasets, composed of many flightlines with sometimes severe flightline effects and multiple sources of variability. While we encourage the use of the methodology presented, we highlight the challenges involved so that they might serve as guidelines for future studies.

6.1. Meteorological and Illumination Geometry Variability

A certain amount of spectral degradation can be attributed to specular reflection from the water surface received by the sensor, which can distort or block the features of interest. We used careful flight planning to avoid specular reflectance; we controlled for meteorological conditions, such as wind velocities and time of day (Lillesand et al., 2004; Masuda et al., 1988) during data acquisition. In the Delta, summer meteorological conditions are characterized by morning low cloud cover, followed by moderate to high winds in the late mornings and early afternoons. The need for optimal weather conditions within a narrow range of sun angles forced imagery to be acquired over the course of two weeks in 2005, which increased inter-flightline variability due to differences in BRDF, ground conditions and environmental conditions. This variability had to be overcome with a decision tree approach for water hyacinth and Brazilian waterweed and limited

the use of MNF, which is very sensitive to flightline effects, to the local-scale perennial pepperweed analysis. However, it may not be possible, or cost-effective, to control for sunglint by careful flight planning in all studies. Correction techniques, which minimize the effects of sunglint and information loss, are available to reduce this impact (Hedley et al., 2005; Hochberg et al., 2003) but were not used in this study.

Previous studies have shown that the contribution of SAV to the water-leaving reflectance received by the sensor decreases as the depth of the water column between macrophytes and the sensor increases (Han and Rundquist, 2003), thus degrading the measured spectral signature of the target species (Han, 2002). Some hyperspectral remote sensing analyses of benthic organisms have applied water depth corrections based on a homogenous water column (Holden and LeDrew, 2001) or more sophisticated techniques that use spectral libraries created from radiative transfer computations (Hedley and Mumby, 2003; Louchard et al., 2003; Mobley et al., 2005). Our image acquisition protocol attempted to address some of this issue by further restricting the image acquisition to low tide conditions.

6.2. Pixel Constituent Variability

In the three case studies presented, pixel composition presents a common problem. The architecture and patchy distribution of perennial pepperweed reduce the strength and distinctiveness of its spectral signature due to mixing with other vegetation, litter, and soil. Water hyacinth is commonly found in mixed patches with pennywort and water primrose, and the SAV class is characterized by mixing among multiple submerged species and mixing with the water column itself. Multiple approaches have been proposed to improve class separation including improving endmember collection (Tompkins et al., 1997), using stochastic mixture models (Eismann and Hardie, 2004), and applying multiple endmember spectral mixture analysis (MESMA) that can account for phenological changes (Dennison and Roberts, 2003) or water quality.

SAV presents additional mixture problems due to the overlying water column. The Delta has high turbidity and there are gradients in water quality throughout the system caused by tidal flux and run-off. This added pixel constituent creates a most decidedly non-linear, three-dimensional mixing problem that reduces the signal of the target species; 20.9% of SAV field points were misclassified as water. In addition, emergent algae, which have a distinct spectral signature, occur epiphytically on the SAV canopy, making it necessary to exclude pixels identified as emergent algae from the SAV class. This in turn results in an underestimate of SAV distribution. When present on the water surface, supported by understory SAV, emergent algae resemble emergent aquatic vegetation (Underwood et al., 2006). Our results corroborate this pattern: nearly 10% of SAV field points, which were generally covered in algae, were classified as emergent vegetation. Our methods largely assume that planktonic algae play an insignificant role in the turbidity of the Delta. However, there are regional locations of very high phytoplankton content that further confound SAV detection. For example, chlorophyll concentrations in the shallow eastern Delta sloughs and lower San Joaquin River are high and variable (Ball and Arthur, 1979). Although we were not able to successfully discriminate SAV species, several studies that have been used to successfully resolve benthic substrates and species through a variety of water variables and depths (Kutser et al., 2003; Legleiter et al., 2004; Louchard et al., 2003; Louchard et al., 2002; Vahtmäe et al., 2006) suggest this may be possible upon further investigation. From our experience mapping SAV, we recommend future research to adequately identify sources of variability, characterize planktonic vs. SAV chlorophyll, and continue to investigate species-level spectral differences of SAV.

6.3. Biological Variability

Species life history stages have different spectral characteristics. Whenever possible, data collection (both field and remotely sensed) must consider the life history of the target species (Figure 9). The three species in our case studies all differ phenologically. Brazilian waterweed flowers early in the summer, at the time of data acquisition, however, these flowers are relatively

small and sparse in the weed mat. Brazilian waterweed has two peaks in its growth, an initial one during the beginning of the summer, and a stronger peak once again during late summer. An acquisition later in the summer may reduce omission errors as plants may be given more time to grow to the water surface, and may help improve classification to the species level.

Of the perennial pepperweed phenological classes identified by the K-means classifier, the classes interpreted as flowering, fruiting, and senescing are relevant to a remote sensing study, and the classifier performance improved when just these were considered (resulting in a producer's accuracy of 76.6%). Accuracy can be improved by mapping each phenological state individually. As senescence of this sparse weed progresses, the similarity of its signal to surrounding litter and soil increases. Andrew and Ustin (2006) were able to resolve both flowering and fruiting phenologies of perennial pepperweed from co-occurring species with spectral data, and suggested that this weed is most tractably mapped between flowering in late spring and senescence in late summer (Figure 10).

Water hyacinth life stages are distinct in color and can occur simultaneously in the same mat. Accounting for water hyacinth phenological states in the decision tree allowed us to better map the weed. We observed two distinct spectral classes. Of the 67 field points classified as "stressed" water hyacinth, 10 were identified in the field as pennywort or water primrose (error of commission = 14.9%). The second spectral class is interpreted as vegetative or "healthy" water hyacinth, and is well characterized by the spectral angle mapping algorithm, with an error of commission of just 6.7%. However, significant growth of water hyacinth in the Delta does not occur until August through September (Figure 10), which may be limiting the success of water hyacinth detection. We suggest that timing data acquisition to coincide with the peak occurrence of vegetative water hyacinth in the late summer will improve the detection of this target weed.

6.4. Conclusions: Applications of Mapping and Monitoring Invasive Aquatic Weeds

We describe the challenges of mapping aquatic and riparian weeds in this study as ecohydrological constraints, and although they were considered in flight planning for this study, it

is impossible to account for all spatial and temporal variability over such a large study area (213,900 ha). From the results of our case studies, we present several conclusions that may serve as guidelines for future regional-scale wetland mapping strategies: 1) incorporating multiple methods in a decision tree approach can account for variability in large datasets; 2) MNF-based approaches should be used in smaller areas, especially when sensitivity to subtle spectral differences is required; 3) mapping accuracy is improved by partitioning species variability into phenological stages.

A further complication to remote sensing of wetlands is that land managers must often request *post facto* analyses of image data that has been acquired without consideration paid to the characteristics of the target species or with field data that was not acquired with remote sensing in mind (e.g. discounting phenological state or percent cover), as was the case with the perennial pepperweed mapping study. This being said, rarely are managers in the position of having unlimited resources and adequate foresight: more typically, managers must adaptively respond to emerging crises, such as non-native plant invasions. Therefore, remote sensing practitioners must continue to develop methodologies that overcome the challenges inherent in riparian, wetland, and floodplain systems, and must do so in support of early detection and rapid response.

One of the most pressing issues for managers of complex, highly invaded ecosystems such as the Delta is to assess infestation cover and the spatial distribution of invasive species. In spite of the intrinsic variability of the Delta, hyperspectral remote sensing provides a powerful set of tools that can be applied to produce maps of species distributions. Our approach provides a comprehensive, timely, and repeatable product that assesses areal cover of very diverse invasive weeds. The use of hyperspectral imagery to detect and map invasive aquatic and riparian weeds has shown that the technology and its methodologies have reached a stage of maturity; it is being successfully applied to meet operational goals for weed management. For instance, California state agencies are using the results described herein to monitor the spatial and temporal dynamics of weed populations under their prescribed control programs.

7. ACKNOWLEDGEMENTS

This research was supported by the California Department of Boating and Waterways Agreement 03-105-114, the California Bay-Delta Authority U-04-SC-005, and the California Bay-Delta Authority Ecological Restoration Program (ERP-01-NO1, ERP-02D-P66) for funding.

The authors gratefully acknowledge M. Carlock of California Department of Boating & Waterways; D. Kratville, J.R.C. Leavitt, P. Akers, and the field crews of the California Department of Food & Agriculture; M. Lay, N. Noujdina, E. Tom, M. Whiting, Y.-B. Cheng, K. Olmstead, D. Darling, L. Chan, F. Anderson, C. Rueda, K. Keightley, W. Sprague, N. Doyle, M. Trombetti, D. Riaño, C. Ramirez, E. Zhong, S. Reed, W. Stockard, and A. Cook for assistance in the field. We also thank H. Manaker, R. McIlvaine, G. Scheer, and L. Ross for administrative support. JHV would like to thank the following for field assistance: I. Hogle, R. Hutchinson, J. Cuixart, J. Bonilla, B. Harbert, L. Kashiwase, A. Holguin, W. Miller, A. Jacobs, E. Lee, & N. Jensen.

8. REFERENCES

Ackleson, S.G., and V. Klemas. 1987. Remote sensing of submerged aquatic vegetation in lower Chesapeake bay: A comparison of Landsat MSS to TM imagery. Remote Sensing of Environment **22**:235-248.

Adams, J.B., D.E. Sabol, V. Kapos, R. Almeida Filho, D.A. Roberts, M.O. Smith, and A.R. Gillespie. 1995. Classification of multispectral images based on fractions of endmembers: Application to land-cover change in the Brazilian Amazon. Remote Sensing of Environment **52**: 137-154.

Alberotanza, L. 1999. Hyperspectral aerial images. A valuable tool for submerged vegetation recognition in the Orbetello Lagoons, Italy. International Journal of Remote Sensing **20**: 523 – 533.

Andrew, M.E., and S.L. Ustin. 2006. Spectral and physiological uniqueness of perennial pepperweed (Lepidium latifolium). Weed Science **54**: 1051-1062

Andrew, M.E., and S.L. Ustin. 2007. The role of environmental context in mapping Lepidium latifolium with hyperspectral image data. Remote Sensing of Environment **112**: 4301-4317.

Ball, M.D., and J.F. Arthur. 1979. Planktonic chlorophyll dynamics in the Northern San Francisco Bay and Delta. . In T.J. Conomos (Ed.), San Francisco Bay: the Urbanized Estuary (pp. 265-285). AAS, San Francisco.

Becker, B.L., D.P. Lusch, and J. Qi. 2007. A classification-based assessment of the optimal spectral and spatial resolutions for Great Lakes coastal wetland imagery. Remote Sensing of Environment **108**: 111-120.

Boardman, J.W. 1994. Geometric mixture analysis of imaging spectrometry data. IGARSS '94. Surface and Atmospheric Remote Sensing: Technologies, Data Analysis and Interpretation., International **4**: 2369-2371.

Boochs, F., G. Kupfer, K. Dockter, and W. Kuhbauch. 1990. Shape of the red edge as vitality indicator for plants. International Journal of Remote Sensing **11**: 1741-1753.

Bossard, C.C., J.M. Randall, and M.C. Hoshovsky, editors. 2000. Invasive plants of California's Wildlands. University of California Press, Berkeley.

Bostater, C.R., T. Ghir, L. Bassetti, C. Hall, E. Reyeier, R. Lowers, K. Holloway-Adkins, and R. Virnstein. 2004. Hyperspectral remote sensing protocol development for submerged aquatic vegetation in shallow waters. Remote Sensing of the Ocean and Sea Ice 2003, Proceedings of SPIE **5233**: 199-215.

Brown, L.R. 2003. Will Tidal Wetland Restoration Enhance Populations of Native Fishes? San Francisco Estuary & Watershed Science **1**: 1-42.

California Department of Food and Agriculture. 2006. California Agricultural Resource Directory. California Department of Food and Agriculture, Sacramento.

Clark, R.N., and T.L. Roush. 1984. Reflectance spectroscopy - Quantitative analysis techniques for remote sensing applications. Journal of Geophysical Research **89**: 6329-6340.

Cocks, T., R. Jenssen, A. Stewart, I. Wilson, and T. Shields. 1998. The HyMap airborne hyperspectral sensor: the system, calibration, and performance. Proceedings of the 1st EARSEL Workshop on Imaging Spectroscopy, Zurich.

Cohen, A.N., and J.T. Carlton. 1995. Nonindigenous aquatic species in a United States estuary: a case study of the biological invasions of the San Francisco Bay Delta. United States Fish and Wildlife Service National Sea Grant College Program.

Cohen, A.N., and J.T. Carlton. 1998. Accelerating Invasion Rate in a Highly Invaded Estuary. Science **279**: 555-558.

Congalton, R.G. 1996. Accuracy assessment: a critical component of land cover. In T.H.T. J.M. Scott, F.W. Davis, editors. Gap analysis: a landscape approach to biodiversity planning. American Society for Photogrammetry and Remote Sensing, Bethesda.

Cunningham, A., P. Wood, and D. McKee. 2002. Brewster-angle measurements of sea-surface reflectance using a high resolution spectroradiometer. Journal of Optics A: Pure and Applied Optics **4**: S29-S33.

Dennison, P.E., and D.A. Roberts. 2003. The effects of vegetation phenology on endmember selection and species mapping in southern California chaparral. Remote Sensing of Environment **87**: 295-309.

Dennison, W.C., R.J. Orth, K.A. Moore, J. Court Stevenson, V. Carter, S. Kollar, P.W. Bergstrom, and R.A. Batiuk. 1993. Assessing water quality with submersed aquatic vegetation. BioScience **43**: 86-94.

Eismann, M.T., and R.C. Hardie, R.C. 2004. Stochastic spectral unmixing with enhanced endmember class separation. Applied Optics **43**: 6596-6608.

Ferguson, R.L., and K. Korfmacher. 1997. Remote sensing and GIS analysis of seagrass meadows in North Carolina, USA. Aquatic Botany **58**: 241-258.

Ferrari, G.M. 1991. Influence of pH and heavy metals in the determination of yellow substance in estuarine areas. Remote Sensing of Environment **37**: 89-100.

Fililla, I., and J. Peñuelas. 1994. The red edge position and shape as indicators of plant

chlorophyll content, biomass and hydric status International Journal of Remote Sensing **15**: 1459-1470.

Finlayson, B.J. 1983. Water hyacinth: threat to the Delta? Outdoor California **44**: 10-14.

Foody, G.M., and D.P. Cox. 1994. Sub-pixel land cover composition estimation using a linear mixture model and fuzzy membership functions International Journal of Remote Sensing **15**: 619-631.

Gamon, J.A., C.B. Field, M.L. Goulden, K.L. Griffin, A.E. Hartley, G. Joel, J. Penuelas, and R. Valentini. 1995. Relationships Between NDVI, Canopy Structure, and Photosynthesis in Three Californian Vegetation Types. Ecological Applications **5**: 28-41.

Gao, B.-C., K.B. Heidebrecht, and A. Goetz. 1993. Derivation of scaled surface reflectances from AVIRIS data. Remote Sensing of Environment **44**: 165-178.

Gitelson, A.A., and M.N. Merzlyak. 1997. Remote estimation of chlorophyll content in higher plant leaves. International Journal of Remote Sensing **18**: 2691 – 2697.

Glenn, N.F., J.T. Mundt, K.T. Weber, T.S. Prather, L.W. Lass, and J. Pettingill. 2005. Hyperspectral data processing for repeat detection of small infestations of leafy spurge. Remote Sensing of Environment **95**: 399-412.

Gopal, B. 1987. Water hyacinth. Elsevier Science, New York.

Green, A.A., M. Berman, P. Switzer, and M.D. Craig. 1988. A transformation for ordering multispectral data in terms of image quality with implications for noise removal. IEEE Transactions on Geoscience and Remote Sensing **26**: 65-74.

Hall, C.R., C.R. Bostater, and R. Virnstein. 2004. Plant pigment types, distributions, and influences on shallow water submerged aquatic vegetation mapping. Remote Sensing of the Ocean and Sea Ice 2004, Proceedings of SPIE-Volume **5569**: 183-193.

Han, L. 2002. Spectral reflectance of Thalassia testudinum with varying depths. IGARSS **2124**: 2123-2125.

Han, L., and D.C. Rundquist. 2003. The spectral responses of Ceratophyllum demersum at varying depths in an experimental tank. International Journal of Remote Sensing **24**: 859 – 864.

Hardisky, M.A., M.F. Gross, and V. Klemas. 1986. Remote sensing of coastal wetlands. BioScience **36**: 453-460.

Hedley, J.D., A.R. Harborne, and P. Mumby. 2005. Technical note: Simple and robust removal of sun glint for mapping shallow-water benthos. International Journal of Remote Sensing **26**: 2107 – 2112.

Hedley, J.D., and P. Mumby. 2003. A remote sensing method for resolving depth and subpixel composition of aquatic benthos. Limnology and Oceanography **48**: 480-488.

Hirano, A., M. Madden, and R. Welch. 2003. Hyperspectral image data for mapping wetland vegetation. Wetlands **23**: 436-448.

Hochberg, E.J., S. Andrefouet, and M. Tyler. 2003. Sea surface correction of high spatial resolution Ikonos images to improve bottom mapping in near-shore environments. IEEE Transactions on Geoscience and Remote Sensing **41**: 1724-1729.

Holden, H., and E. LeDrew. 2001. Effects of the water column on hyperspectral reflectance of submerged coral reef features. Bulletin of Marine Science **69**: 685-699.

Hoogenboom, H.J., A. Dekker, and I. Althuis. 1998. Simulation of AVIRIS Sensitivity for Detecting Chlorophyll over Coastal and Inland Waters. Remote Sensing of Environment **65**: 333-340.

Huang, Z., B. Turner., S.J. Dury, I.R. Wallis, and W.J. Foley. 2004. Estimating foliage nitrogen concentration from HYMAP data using continuum removal analysis. Remote Sensing of Environment **93**: 18-29.

Jassby, A.D., and J.E. Cloern. 2000. Organic matter sources and rehabilitation of the Sacramento-San Joaquin Delta (California, USA). Aquatic Conservation: Marine and Freshwater Ecosystems **10**: 323-352.

Jassby, A.D., J.E. Cloern, and B.E. Cole. 2002. Annual Primary Production: Patterns and Mechanisms of Change in a Nutrient-Rich Tidal Ecosystem. Limnology and Oceanography **47**: 698-712.

Kokaly, R.F., D.G. Despain, R.N. Clark, and K.E. Livo. 2003. Mapping vegetation in Yellowstone National Park using spectral feature analysis of AVIRIS data. Remote Sensing of Environment **84**: 437-456.

Kruse, F.A., A.B. Lefkoff, J. W. Boardman, K.B. Heidebrecht, A.T. Shapiro, P.J. Barloon, and A. Goetz. 1993. The spectral image processing system (SIPS)-interactive visualization and analysis of imaging spectrometer data. Remote Sensing of Environment **44**: 145-163.

Kutser, T., A.G. Dekker, and W. Skirving, 2003. Modeling spectral discrimination of Great Barrier Reef benthic communities by remote sensing instruments. Limnology and Oceanography **48**: 497-510.

Lass, L.W., D.C. Thill, B. Shafii, B., and T. Prather. 2002. Detecting spotted knapweed (Centaurea maculosa) with hyperspectral remote sensing technology. Weed Technology **16**: 426-432.

Lawrence, R.L., S.D. Wood, and R.L. Sheley. 2006. Mapping invasive plants using hyperspectral

imagery and Breiman Cutler classifications (randomForest). Remote Sensing of Environment **100**: 356-362.

Legleiter, C., D.A. Roberts, W.A. Marcus, and M.A. Fornstad. 2004. Passive optical remote sensing of river channel morphology and in-stream habitat: physical basis and feasibility. Remote Sensing of Environment **93**: 493-510.

Lillesand, T.M., and R.W. Kiefer. 2000. Remote Sensing and Image Interpretation. John Wiley & Sons, Inc, New York.

Louchard, E.M., R. Reid, F. C. Stephens, C. Davis, R. Leathers, T. Downes, and R. Maffione. 2002. Derivative analysis of absorption features in hyperspectral remote sensing data of carbonate sediments. Optics Express **10**: 1573-1584.

Louchard, E.M., R. Reid, F.C, Stephens, C.O. Davis, R.A. Leathers, and T.V. Downes. 2003. Optical remote sensing of benthic habitats and bathymetry in coastal environments at Lee Stocking Island, Bahamas: A comparative spectral classification approach. Limnology and Oceanography **48**: 511-521.

Lund, J., E. Hanak, W. Fleenor, R. Howitt, J. Mount, and P. Moyle. 2007. Envisioning Futures for the Sacramento-San Joquin Delta. Public Policy Institute of California, San Francisco.

Masuda, K., T. Takashima,and Y. Takayama. 1988. Emissivity of pure and sea waters for the model sea surface in the infrared window regions. Remote Sensing of Environment **24**: 313-329.

Meng, L., and P.B. Moyle. 1995. Status of Splittail in the Sacramento-San Joaquin Estuary. Transactions of the American Fisheries Society **124:** 538-549.

Merenyi, E., W.H. Farrand, L.E. Stevens, T.S. Melis, and K. Chibber. 2000. Studying the potential for monitoring Colorado River ecosystem resources below Glen Canyon Dam using low-altitude AVIRIS data. 9th AVIRIS Earth Science and Applications Workshop. Pasadena, CA.

Mertes, L., M.O. Smith, and J.B. Adams. 1993. Estimating suspended sediment concentrations in surface waters of the Amazon River wetlands from Landsat images. Remote Sensing of Environment **43**: 281-301.

Mobley, C.D., L.K. Sundman, C.O. Davis, J.H. Bowles, T.V. Downes, R.A. Leathers, M.J. Montes, W.P. Bissett, D. Kohler, R.P. Reid, E.M. Louchard, and A. Gleason. 2005. Interpretation of hyperspectral remote-sensing imagery by spectrum matching and look-up tables. Applied Optics **44**: 3576-3592.

Morel, A., and S. Belanger. 2006. Improved detection of turbid waters from ocean color sensors information. Remote Sensing of Environment **102**: 237-249.

Mulitsch, M.J. 2005. Remote sensing of California's estuaries: Monitoring climate change and invasive species. Graduate Group of Ecology. University of California, Davis.

Mulitsch, M.J., and S.L. Ustin. 2003. Mapping invasive plants species in the Delta region using hyperspectral imagery. California Department of Boating and Waterways, Sacramento.

Muller, E., H. DeCamps, and M. Dobson. 1993. Contribution of space remote sensing to river studies. Freshwater Biology **29**: 301-312.

Mundt, J.T., N.F. Glenn, K.T. Weber, T.S. Prather, L.W. Lass, and J. Pettingill. 2005. Discrimination of hoary cress and determination of its detection limits via hyperspectral image processing and accuracy assessment techniques. Remote Sensing of Environment **96**: 509-517.

Nagler, P.L., C. Daughtry, and S.N. Goward. 2000. Plant litter and soil reflectance. Remote Sensing of Environment **71**: 207-215.

Parker Williams, A., and E.R. Hunt. 2002. Estimation of leafy spurge cover from hyperspectral imagery using mixture tuned matched filtering. Remote Sensing of Environment **82**: 446-456.

Penfound, W.T., and T.T. Earle. 1948. The biology of the water hyacinth. Ecological Monographs **18**: 447-472.

Pimentel, D., L. Lach, R. Zuniga, and D. Morrison. 2000. Environmental and economic costs of nonindigenous species in the United States. BioScience **50**: 53-65.

Pinnel, N., T. Heege., and S. Zimmermann. 2004. Spectral discrimination of submerged macrophytes in lakes using hyperspectral remote sensing data. SPIE Proceedings Ocean Optics **17**: 1-16.

Pontius, J., R. Hallett, and M. Martin. 2005. Using AVIRIS to assess hemlock abundance and early decline in the Catskills, New York. Remote Sensing of Environment **97**: 163-173.

Renz, M.J., and R.R. Blank. 2004. Influence of Perennial Pepperweed (Lepidium latifolium) Biology and Plant–Soil Relationships on Management and Restoration. Weed Technology **18**: 1359-1363.

Roberts, D.A., M.O. Smith, and J.B. Adams. 1993. Green vegetation, nonphotosynthetic vegetation, and soils in AVIRIS data. Remote Sensing of Environment **44**: 255-269.

Sawaya, K.E., L.G. Olmanson, N.J. Heinert, P.L. Brezonik, and M.E. Bauer. 2003. Extending satellite remote sensing to local scales: land and water resource monitoring using high-resolution imagery. Remote Sensing of Environment **88**: 144-156.

Schlerf, M., C. Atzberger, and J. Hill. 2005. Remote sensing of forest biophysical variables using

HyMap imaging spectrometer data. Remote Sensing of Environment **95**: 177-194.

Schmidt, K.S., and A.K. Skidmore. 2003. Spectral discrimination of vegetation types in a coastal wetland. Remote Sensing of Environment **85**: 92-108.

Simenstad, C., J. Toft, H. Higgins, J. Cordell, M. Orr, P. Williams, L. Grimaldo, Z. Hymanson, and D. Reed. 2000. Sacramento-San Joaquin Delta Breached Levee Wetland Study (BREACH). University of Washington, School of Fisheries, Seattle.

Sims, D.A., and J.A. Gamon. 2002. Relationships between leaf pigment content and spectral reflectance across a wide range of species, leaf structures and developmental stages. Remote Sensing of Environment **81**: 337-354.

Smith, M.O., S.L. Ustin, J.B. Adams, and A.R. Gillespie. 1990. Vegetation in deserts: I. A regional measure of abundance from multispectral images. Remote Sensing of Environment **31**: 1-26.

Sokal, R.R., and F.J. Rohlf. 2000. Biometry. Freeman and Company, New York.

Spenst, R.O. 2006. The biology and ecology of Lepidium latifolium L., in the San Francisco estuary and their implications for eradication of this invasive weed. Graduate Group of Ecology. University of California, Davis.

Tanner, C.C., J.S. Clayton, and R. Wells. 1993. Effects of suspended solids on the establishment and growth of Egeria densa. Aquatic Botany **45**: 299-310.

Toft, J.D., C. Simenstad, J.R. Cordell, and L.F. Grimaldo. 2003. The effects of introduced water hyacinth on habitat structure, invertebrate assemblages, and fish diets. Estuaries **26**: 746-758.

Underwood, E., M. Mulitsch, J. Greenberg, M. Whiting, S. Ustin, and S. Kefauver. 2006. Mapping invasive aquatic vegetation in the Sacramento-San Joaquin Delta using hyperspectral imagery. Environmental Monitoring and Assessment **121**: 47-64.

Underwood, E., S. Ustin, and D. DiPietro. 2003. Mapping nonnative plants using hyperspectral imagery. Remote Sensing of Environment **86**: 150-161.

Ustin, S.L., J.A. Greenberg, E.L. Hestir, S. Khanna, M.J. Santos, M.E. Andrew, M. Whiting, S. Rajapakse, and M. Lay. 2006. Mapping invasive plant species in the Sacramento-San Joaquin Delta using hyperspectral imagery. Department of Boating and Waterway: Aquatic Weed Control, Sacramento.

Vahtmäe, E., T. Kutser, G. Martin, and J. Kotta. 2006. Feasibility of hyperspectral remote sensing for mapping benthic macroalgal cover in turbid coastal waters-a Baltic Sea case study. Remote Sensing of Environment **101**: 342-351.

Valta-Hulkkonen, K., P. Pellikka, H. Tanskanen, A. Ustinov, and O. Sandman. 2003. Digital false colour aerial photographs for discrimination of aquatic macrophyte species. Aquatic Botany, **75**: 71-88.

Viers, J.H., I.B. Hogle, D. DiPietro, S. Arora, M. Gubaydullin, and J.F. Quinn. 2005. Geodatabase application for invasive plant tracking and coordinated habitat restoration. ESRI International User's Conference, San Diego.

Vis, C., C. Hudon, and R. Carignan. 2003. An evaluation of approaches used to determine the distribution and biomass of emergent and submerged aquatic macrophytes over large spatial scales. Aquatic Botany **77**: 187-201.

Ward, D.H., A. Morton, T.L. Tibbitts, D.C. Douglas, E. Carrera-Gonzalez. 2003. Long-term change in eelgrass distribution at Bahia San Quintin, Baja California, Mexico, using satellite imagery. Estuaries **26**: 1529-1539.

Williams, D.C., and J.G. Lyon. 1997. Historical aerial photographs and a geographic information system (GIS) to determine effects of long-term water level fluctuations on wetlands along the St. Marys River, Michigan, USA. Aquatic Botany **58**: 363-378.

Williams, D.J., N.B. Rybicki, A.V. Lombana, T.M. O'Brien, and R.B. Gomez. 2003. Preliminary Investigation of Submerged Aquatic Vegetation Mapping using Hyperspectral Remote Sensing. Environmental Monitoring and Assessment **81**: 383-392.

Young, J.A., D.E. Palmquist, and R.R. Blank. 1998. The Ecology and Control of Perennial Pepperweed (Lepidium latifolium L.). Weed Technology **12**: 402-405.

Young, J.A., D.E. Palmquist, and S.O. Wotring. 1997. The invasive nature of Lepidium latifolium: a review. In J.H. Brock, M. Wade, P. Pysek & D. Green, editors. Plant Invasions: Studies from North America and Europe. Backhuys, Leiden.

Young, J.A., C.E. Turner, and L.F. James. 1995. Perennial pepperweed. Rangelands **17**: 121-123.

Zhang, X. 1998. On the estimation of biomass of submerged vegetation using Landsat thematic mapper (TM) imagery: a case study of the Honghu Lake, PR China. International Journal of Remote Sensing **19**: 11-20.

Table 1. Hyperspectral remote sensing tools used in case studies

Analysis tool	Summary	Relevant applications
Minimum noise fraction (MNF)	Essentially a two-tiered principal components analysis that segregates noise and reduces data dimensionality for subsequent analyses (Green et al., 1988). Demonstrated to be effective for mapping invasive weeds with HyMap data.	Mundt et al., 2005 Underwood et al., 2003
Band indexes	Augment spectral differences between bands, highlighting specific physiological characteristics of vegetation (Sims and Gamon, 2002).	Pontius et al., 2005 Schlerf et al., 2005 Underwood et al., 2003
Spectral mixture analysis (SMA)	Solves for the fraction of endmembers contained within a pixel (Smith et al., 1990; Foody and Cox, 1994; Adams et al., 1995). Has been successfully applied to SAV detection in the Delta since 2003.	Mulitsch and Ustin, 2003 Underwood et al., 2006
Spectral Angle Mapper (SAM)	Measures the similarity between image spectra and a reference spectrum by treating the spectra as vectors with a dimensionality equal to the number of bands in the image (Kruse et al., 1993). Effective for identifying aquatic vegetation.	Alberotanza, 1999 Hirano et al., 2003 Merenyi et al. 2000
Continuum removal	Quantifies useful absorption features which can be used to characterize and identify vegetation (Clark and Roush, 1984).	Huang et al., 2004 Kokaly et al., 2003 Underwood et al., 2003

Table 2. Confusion matrix and classification accuracy of the perennial pepperweed logistic regression model training and validation points.

			Ground Reference				
			Perennial Pepperweed	Pseudo-absence	Total	Producer's accuracy	User's accuracy
Training	Map Classes	Perennial pepperweed	458	130	588	66.1%	77.9%
		Unclassified	235	47,423	47,658	99.7%	99.5%
		Total	693	47,553	48,246	Perennial pepperweed Kappa = 0.71	
Validation	Map Classes	Perennial pepperweed	138	44	182	63.0%	75.8%
		Unclassified	81	15,842	15,923	99.7%	99.5%
		Total	219	15,886	16,105	Perennial pepperweed Kappa = 0.68	

Table 3: Classes of perennial pepperweed dominated pixels as determined by a K-means classification, along with the phenological interpretation; mean NDVI, NDWI, and CAI for each group and proportion of each group classified as perennial pepperweed dominated by the regression model during training and validation.

						% classified	
Group	Phenology	n	NDVI	NDWI	CAI	Training	Test
1	Senescent	1	0.331	-0.093	247.0	0	0
2	Trees, shaded	77	0.864	0.071	6.4	1.7	0
3	Flowering	277	0.765	0.042	1.0	68.9	73.5
4	Fruiting	363	0.637	-0.016	36.3	76.3	84.9
5	Senescing	190	0.494	-0.062	102.9	59.6	64.6

Table 4: Condensed confusion matrix and classification accuracy of the 2005 water hyacinth decision tree. The Kappa coefficient relative to the water hyacinth class is 0.81.

		Ground Reference				
		Water hyacinth	Other emergent & floating vegetation	Total	Producer's accuracy	User's accuracy
Map Classes	Water hyacinth	141	16	157	69.1%	89.8%
	Other emergent & floating vegetation	63	211	274	93.0%	77.0%
	Total	204	227	431		

Table 5: Condensed confusion matrix and classification accuracy of the 2006 water hyacinth decision tree. The Kappa coefficient relative to the water hyacinth class is 0.49.

		Ground Reference				
		Water hyacinth	Other emergent & floating vegetation	Total	Producer's accuracy	User's accuracy
Map Classes	Water hyacinth	112	106	181	51.4%	61.9%
	Other emergent & floating vegetation	106	592	698	89.6%	84.8%
	Total	218	661	879		

Table 6: Condensed confusion matrix and classification accuracy of the 2005 SAV decision tree. The Kappa coefficient relative to the SAV class is 0.86.

		Ground Reference					
		SAV	Water	Emergent & floating vegetation	Total	Producer's accuracy	User's accuracy
Map Classes	SAV	187	2	14	203	59.2%	92.1%
	Water	50	37	16	103	90.2%	35.9%
	Emergent & floating vegetation	79	2	349	430	92.1%	81.2%
	Total	316	41	379	736		

Table 7: Condensed confusion matrix and classification accuracy of the 2006 SAV decision tree. The Kappa coefficient relative to the SAV class is 0.87.

		Ground Reference					
		SAV	Water	Emergent & floating vegetation	Total	Producer's accuracy	User's accuracy
Map Classes	SAV	844	12	49	905	69.3%	93.3%
	Water	255	337	57	649	96.3%	51.9%
	Emergent & floating vegetation	119	1	779	899	88.0%	86.6%
	Total	1218	350	885	2453		

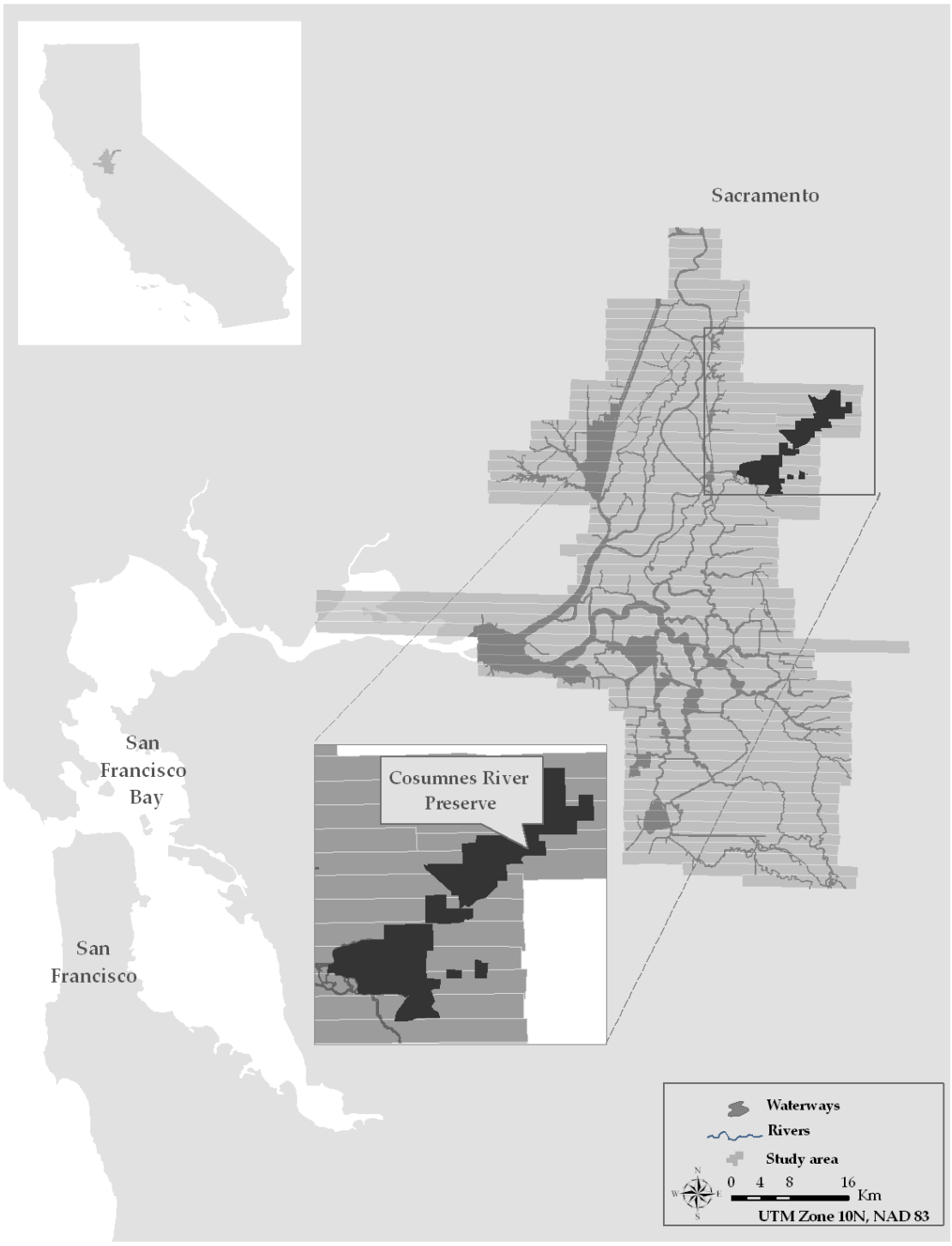

Figure 1: Map of the California Bay-Delta. Overlaid are the boundaries of the HyMap flightlines across which water hyacinth and submerged aquatic vegetation were mapped. An inset highlights the Cosumnes River Preserve, where perennial pepperweed was mapped.

Figure 2: The three focal invasive species for monitoring in the Delta a) perennial pepperweed, b) Brazilian waterweed, c) water hyacinth.

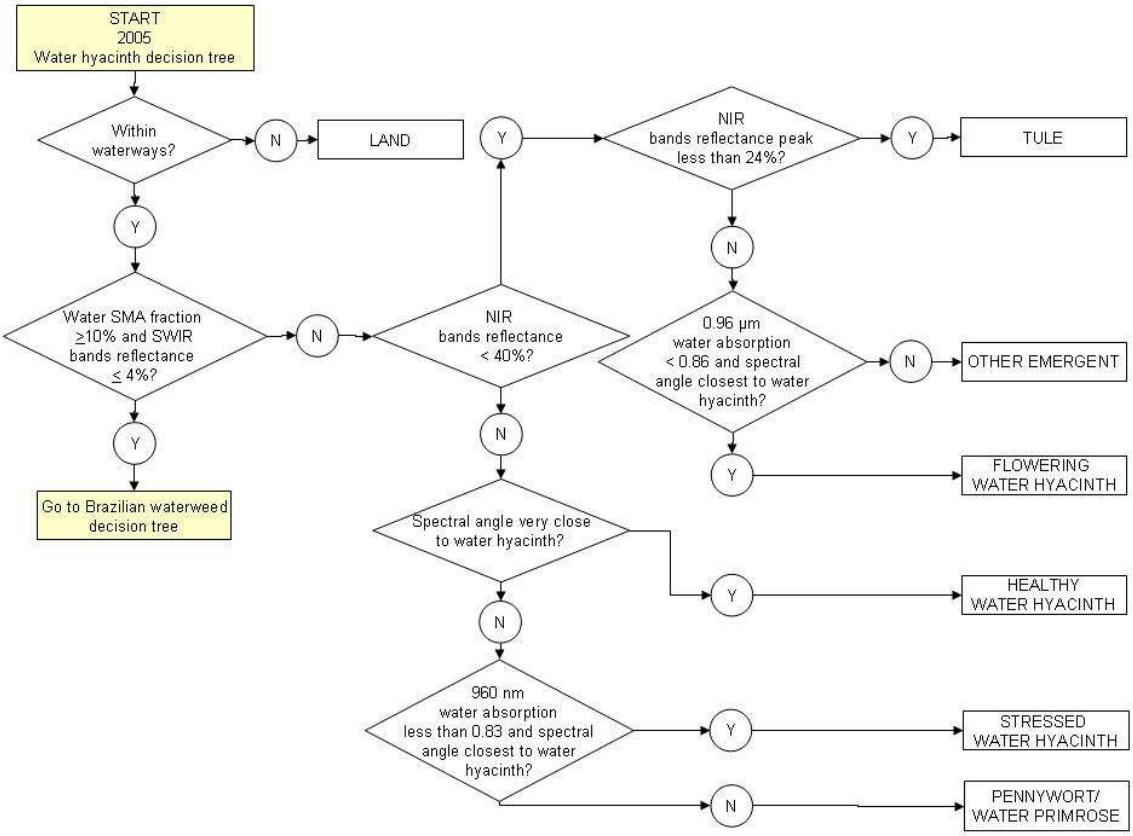

Figure 3: Schematic of the decision tree used to identify water hyacinth in 2005 across 64 HyMap flightlines

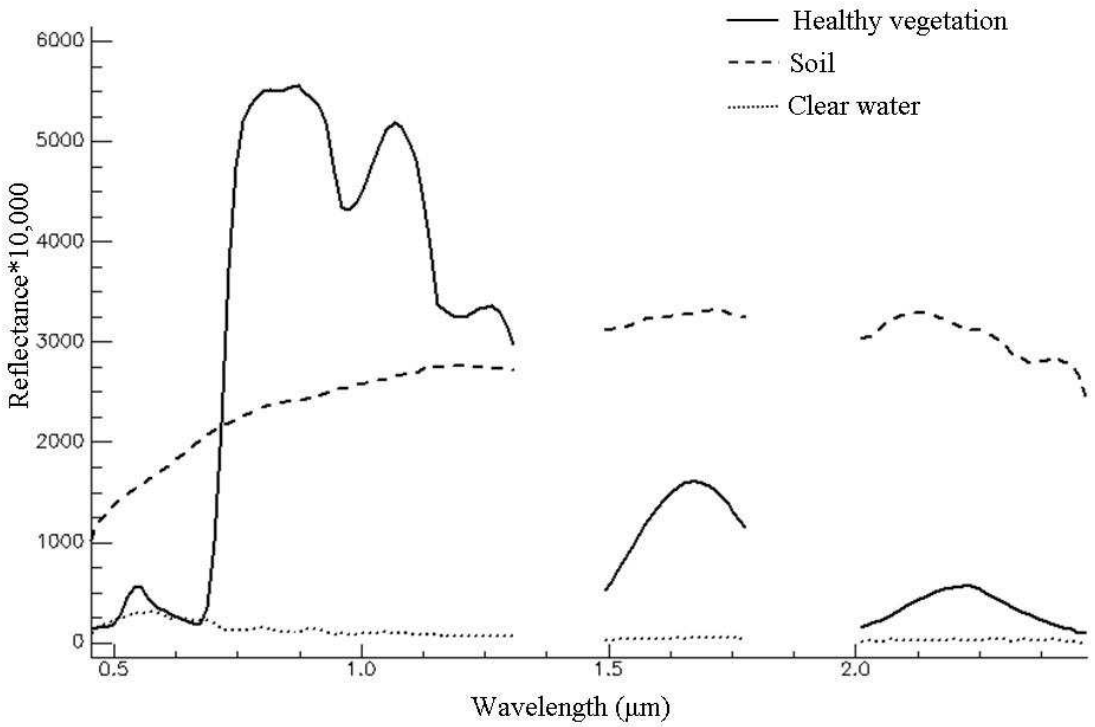

Figure 4: Endmembers of healthy vegetation, soil, and water as used in the first spectral mixture analysis. Spectra were extracted from the HyMap imagery from ground reference data points.

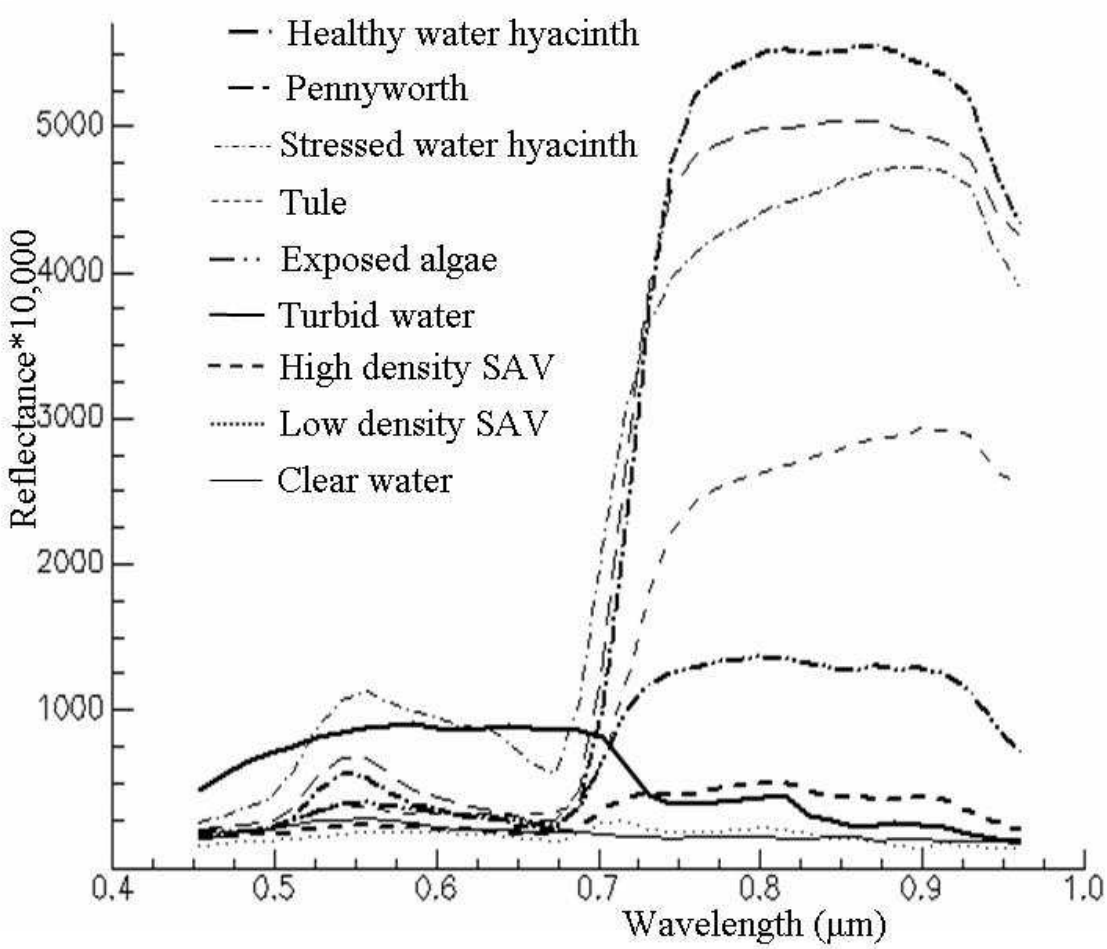

Figure 5: Training endmembers for the Spectral Angle Mapper node of the 2005 decision tree. Spectra were extracted from the HyMap imagery from ground reference data points.

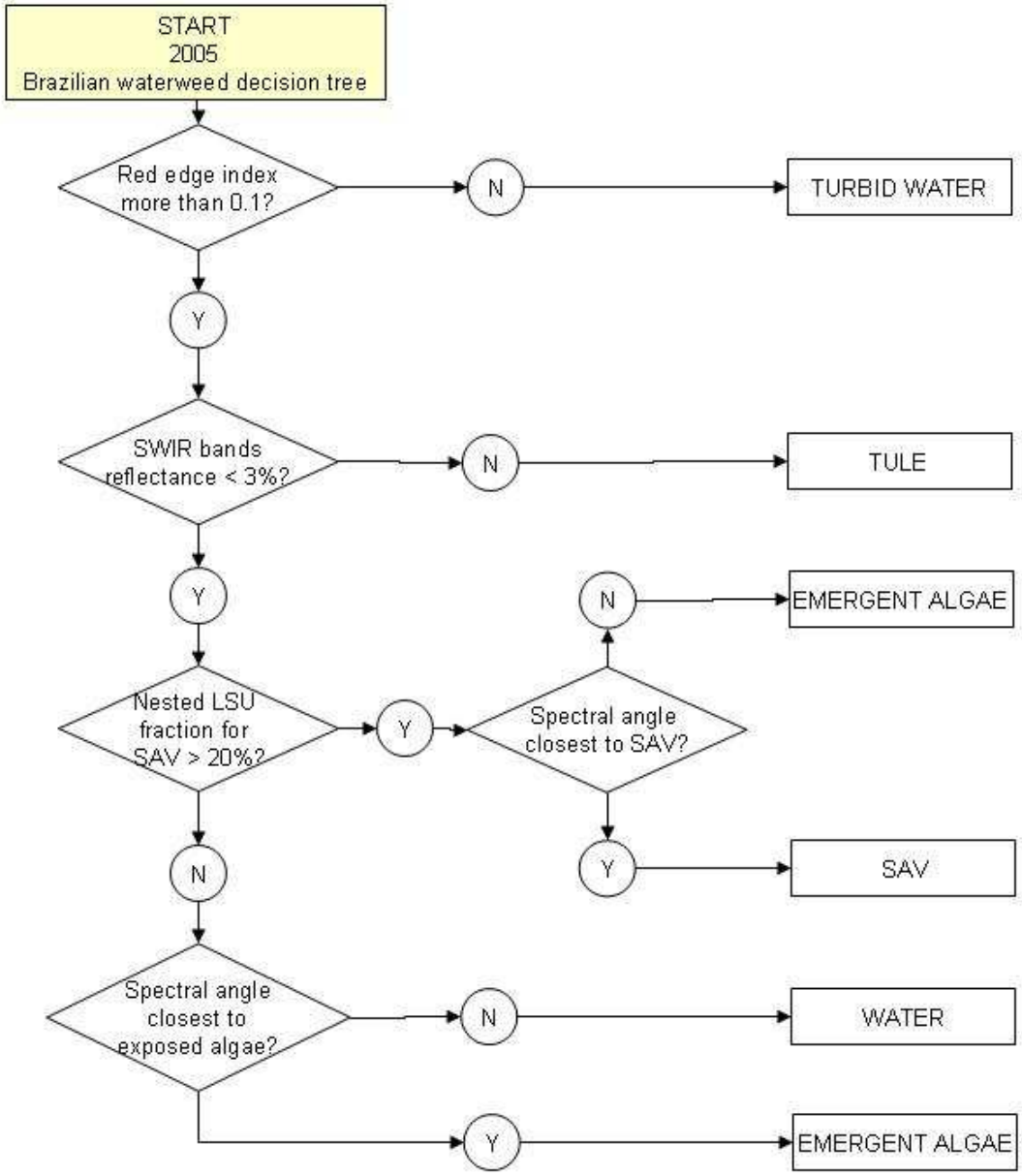

Figure 6: Schematic of the decision tree used to identify SAV in 2005 across 64 HyMap flightlines

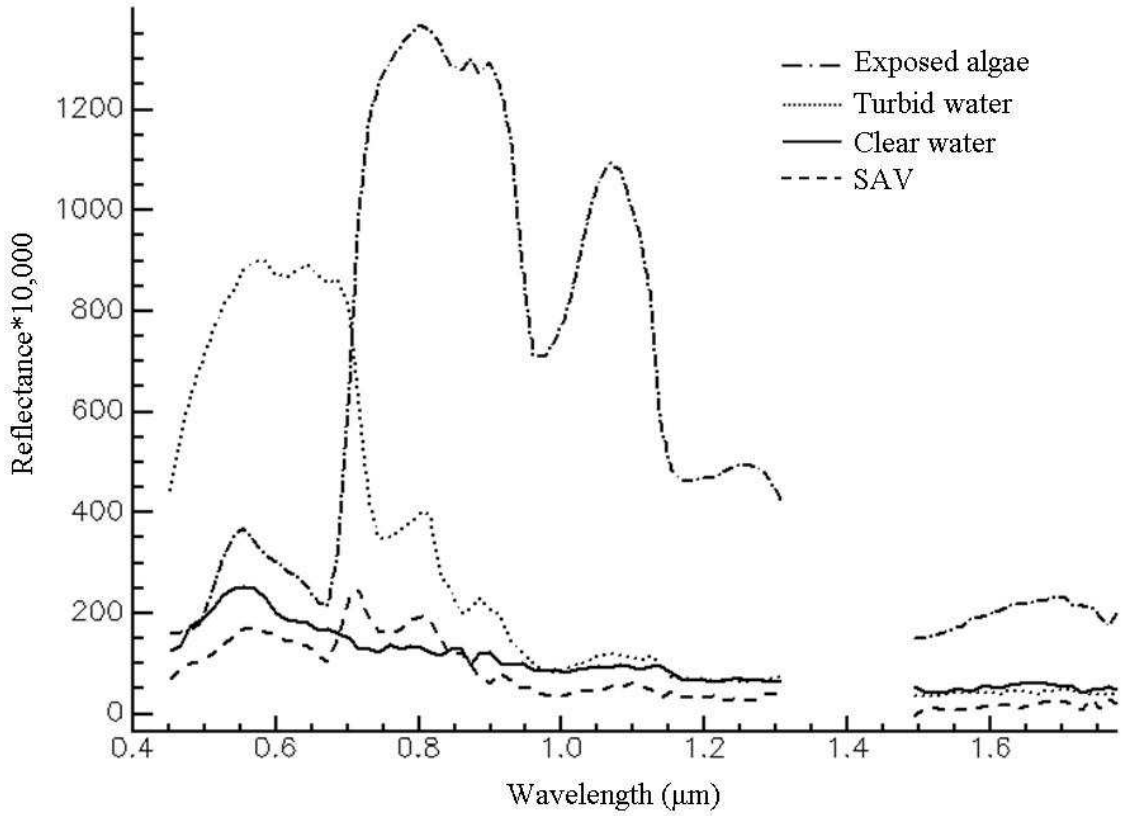

Figure 7: Endmembers of emergent algae, turbid water, relatively "clear" water, and SAV as used in a "nested" second spectral mixture analysis to identify SAV. Spectra were extracted from the HyMap imagery from ground reference data points.

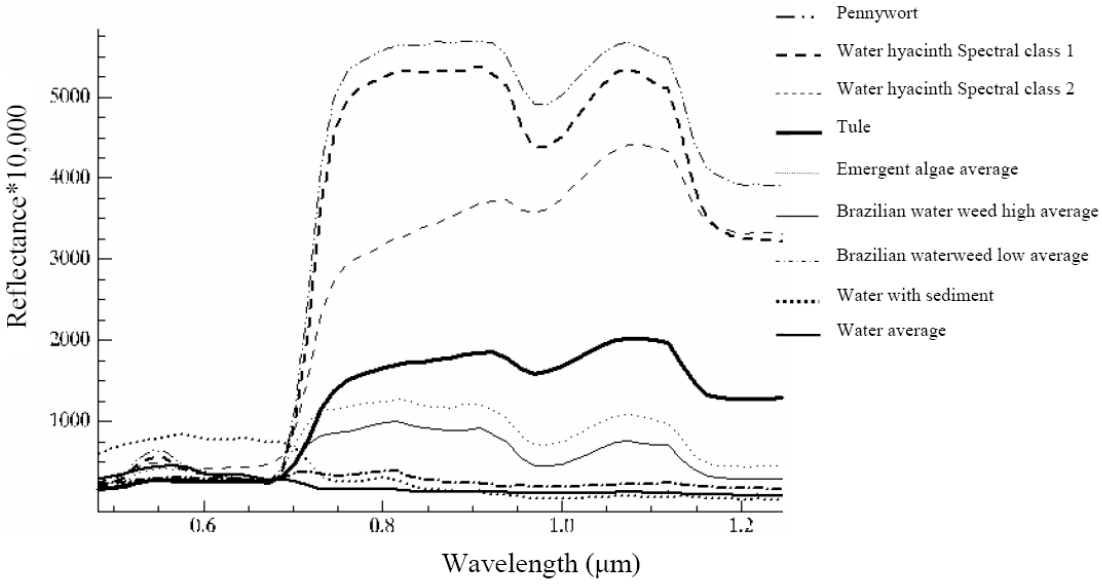

Figure 8: Endmembers used to train the Spectral Angle Mapper used in both the 2006 water hyacinth and SAV decision trees. Spectra were extracted from the HyMap imagery from ground reference data points.

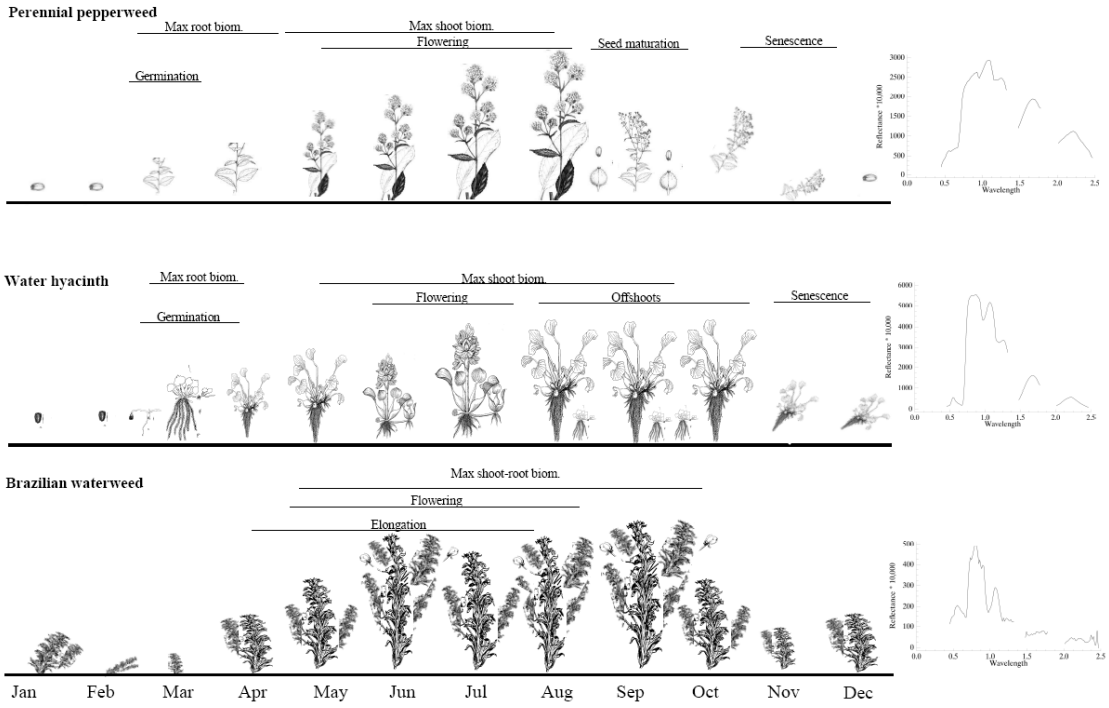

Figure 9: Case study invasive species annual life cycle and respective June spectra extracted from HyMap imagery using ground reference locations.

· Chapter 2 ·

Classification Trees for Aquatic Vegetation Community Prediction from Imaging Spectroscopy

Classification Trees for Aquatic Vegetation Community Prediction from Imaging Spectroscopy

Erin L. Hestir[a], Jonathan A. Greenberg[a], and Susan L. Ustin[a]

[a] Center for Spatial Technologies and Remote Sensing, Department of Land Air and Water Resources, University of California Davis.

ABSTRACT

Imaging spectroscopy provides the information needed to identify vegetation communities and functional groups. However, the high variability of the target classes, as well as the variability contained in multiple images acquired over large areas complicates classification, as the need for greater training data increases as the variability and feature space of the imagery increases. There is a need to find robust and easy-to-use classifiers that can account for data with high variability, non-normal distributions, and high dimensionality. We used the C5.0 algorithm to train and test ensemble classification trees with one collection of 48 imaging spectroscopy flightlines from a single year and corresponding ground reference data. The classifier achieved an overall accuracy of 84.6% on the test dataset. We then applied the classifier trained from that single year to four years of historic airborne imaging spectroscopy data sets of the same size over the same area and validated the resultant maps with corresponding historic ground reference data. Overall historic accuracies ranged from 78.8% to 85.9%, with target class kappa coefficients ranging from 0.71-0.83. This classification method was successful because the training dataset encompassed the range of variability of the study area and dataset and the relative frequency of occurrence of each of the cover classes.

1. INTRODUCTION

Identifying aquatic vegetation communities using remotely sensed imagery presents several challenges. Aquatic plants often co-occur in mixed patches with multiple species and phenologies present. Aquatic vegetation communities often have varying species composition and canopy sizes and densities in space. Differing water depth and quality, sun angle and wind conditions make detection of submerged aquatic vegetation especially problematic as the signal from the water surface and overlying water column deteriorate plant canopy reflectance signals (Han and Rundquist 2003, Hestir et al. 2008). To account for high spatial heterogeneity, phenological and canopy morphological variability, high spatial and spectral resolution imagery available from airborne imaging spectrometers is required to discriminate aquatic vegetation communities (Mundt et al. 2005, Becker et al. 2007, Chan and Paelinckx 2008, Hestir et al. 2008). However, land cover classification from airborne imaging spectroscopy is complicated by a number of factors. In order to acquire data over entire regions, multiple flight paths are often necessary. This results in mosaicked images composed of many flightlines with different view angles and acquisition dates, leading to differing sun angles, atmospheric, and environmental conditions. The combination of variability in both the image data and the target classes themselves make image classification challenging even when only a few classes are the target. Furthermore, although imaging spectroscopy provides more spectral information by providing hundreds of narrow bands, identifying which bands are informative for vegetation community detection is critical (Pal and Mather 2003, Becker et al. 2007).

In order to successfully detect aquatic vegetation communities using imaging spectroscopy, an image classification approach needs to 1) effectively use the information content in high dimensionality data; 2) make no distributional assumptions about the training set (i.e. a classifier that can handle land cover classes with multimodal distributions in spectral space exemplified by submerged aquatic vegetation in a heterogeneous environment); and 3) be stable, and not require year-to-year or flightline-to-flightline reclassification, as was the case in previous work by Hestir et al. (2008); so that the classifier can be trained and validated with a single year of data, and then accurately applied to datasets from other years (past or future). The purpose of this study was to classify three highly variable land cover classes (submerged aquatic vegetation, floating and emergent vegetation, and water) all with multi-modal distributions. We aimed to detect submerged aquatic vegetation communities and separate them from floating and emergent vegetation communities and water. We then tested whether classification trees (developed in C5.0, Rulequest Research) trained from a single year's airborne imaging spectroscopy data could be applied to other years with reasonable accuracy.

1.1 Motivation

The Sacramento-San Joaquin River Delta (henceforth, the Delta) provides approximately 80% of the freshwater to the San Francisco Bay (Knowles and Cayan 2002), comprising the largest estuary in the Western United States (Figure 1). The Delta provides habitat for a number of threatened and endangered fish species, migrating waterfowl along the Pacific Flyway, and serves as the freshwater hub for California's agricultural and growing urban sectors. The Bay-Delta system is also a gateway for

aquatic biological invasions (Cohen and Carlton 1998), and the recent expansion of invasive submerged aquatic vegetation may have contributed to the precipitous decline of the now endangered endemic fish, the delta smelt (*Hypomesus transpacificus*) (Brown and Michniuk 2007, Feyrer et al. 2007). Understanding the distribution of submerged aquatic vegetation during the period of decline of the delta smelt provides insights into the effects of the submerged aquatic vegetation invasion on habitat quality and its contribution to the smelt species decline. This in turn can help guide habitat management for successful species protection and recovery.

1.2 Classification Trees and C5.0

Classification trees have been recognized as a useful technique for remote sensing because they are non-parametric, can accommodate different types of variables (i.e. categorical and continuous), and frequently result in higher classification accuracies (Friedl and Brodley 1997, Friedl et al. 1999) and also (Brown de Colstoun et al. 2003) and references therein. Classification trees predict class membership by splitting a dataset into a sequence of Boolean decisions (interior nodes, or branches) that result in a final grouping of the data into membership classes (terminal nodes, or trees) (Tso and Mather 2001). In the C5.0 (See5 for Windows) (Quinlan 2009), Rulequest Research) classification tree algorithm, an automated method of creating classification trees, the split at the interior nodes of the tree is estimated using the "information gain ratio." The information gain considers the information after splitting subtracted from the information before splitting, and it uses this measure to test each possible subdivision of data until a subdivision with the greatest information gain is selected (Tso and Mather 2001). That is, at an interior node of the tree, C5.0 maximizes the homogeneity of resulting subsets by

choosing the split that maximizes the information gain. However, this metric favors tests that result in large number of splits, so the information gain is normalized by the instrinsic information of the split into account (i.e., how much information gain would occur if the training set were allocated into separate classes?). (DeFries and Chan 2000, Tso and Mather 2001). This is the information gain ratio. C5.0 uses the ratio to reduce bias toward oversplitting attributes by taking into account the number and size of branches and choosing a split that minimizes the branches. The dataset is recursively split until there is no decrease in information or until the terminal node contains observations from only a single class (DeFries and Chan 2000). Because of this recursive process, which attempts to develop a 100% match with the training data, classification trees can perform poorly when applied to independent, unseen data. This process is known as overfitting, a common problem for classification trees (Lawrence et al. 2006) especially if there is error or "noise" in the data (Liu et al. 2008), as is commonly the case with remote sensing data. Overfitting classification results may yield high statistical accuracies on both training and unseen data, but will produce maps that are spatially incoherent and incorrect by even cursory qualitative evaluation. Pruning classification trees helps eliminate some overfitting (DeFries and Chan 2000, Olden et al. 2008). C5.0 prunes, or creates simpler trees, by examining the trees initially produced and removing or pruning lower interior nodes that are predicted to have higher error rates and replacing them with terminal nodes or sub-interior nodes (Quinlan 2009).

An ensemble of classification trees is often used rather than a single tree because it improves classification accuracy (Breiman 2001). To create an ensemble, C5.0 uses an adaptive boosting algorithm, AdaBoost (Freund and Schapire 1996), to iteratively create

classification trees where each tree learns from the errors of the previous tree until an ensemble of classification trees is created which then vote to determine the predicted class membership for every pixel (e.g. water, vegetation, soil). Boosting typically enhances remote sensing classification success (DeFries and Chan 2000, Brown de Colstoun and Walthall 2006, Chan and Paelinckx 2008), however see (Moisen et al. 2006), and especially (Pal and Mather 2003) with regard to high-dimensional data. Attribute winnowing can be enabled to address the problems of high dimensional data, namely the requirement of a large training set, and feature selection for splitting decisions (Pal and Mather 2003). Before constructing its classifiers, attribute winnowing searches through feature space and discards variables that do not provide predictive information as well as those variables which have significant overlap. The result when applied to high-dimensional applications is improved predictive accuracy and smaller classifiers (Quinlan 2009) which are easier to interpret.

2. METHODS

Airborne imaging spectroscopy was collected annually over the Sacramento-San Joaquin Delta (~2,100 km^2) from 2004-2008 to map the distribution of several invasive species, both aquatic and terrestrial (Underwood et al. 2006, Andrew and Ustin 2008, Hestir et al. 2008, Khanna et al. 2010). Concurrent with the overflights, intensive field campaigns were conducted to gather ground reference data. This dataset provides a unique opportunity to test the robustness of a classification developed on and trained with a dataset from a single flight/field campaign and applied to historic imagery.

2.1 Image Data

Airborne spectroscopic imagery was acquired by the HyVista Corporation using the HyMap imaging spectrometer (Cocks et al., 1998) during morning and afternoon low tide periods between June 29 and July 7, 2008. HyMap measures radiance across 128 bands from 400 nm to 2500 nm and was flown at an altitude of ~1.5 km, resulting in a ground resolution of 3 meter pixels. A total area of 2,166 km^2 was covered by 48 flightlines. The imagery was atmospherically corrected to apparent reflectance using a modified version of the ATREM algorithm (Gao et al. 1993), HyCorr (HyVista Corp., Sydney, Australia). HyVista identified and removed noisy bands, leaving 126 usable bands. Additional geographic correction was made using orthophoto correction software developed specifically for the HyMap instrument (Analytical Imaging & Geophysics, CO), resulting in an RMSE of ± 1.5 m between the orthophoto and the HyMap image (~1/2 pixel). These same procedures were employed on all the historic HyMap data collected over the same area, with the same acquisition requirements.

In addition to the reflectance bands, six additional spectral indexes that were identified as important for submerged aquatic vegetation detection during previous mapping efforts (Hestir et al. 2008) were calculated. These spectral indexes were merged with the reflectance bands resulting in a 132 band image. Table 1 summarizes the spectral indices used as inputs.

2.2 Field Data Collection

Ground reference data (GRD) were collected between June 23 and July 8, 2008. In order to ensure the number of points sampled for each cover class (submerged aquatic vegetation, water, floating & emergent vegetation) were proportional to the cover of that

class in the field we used previous years classification results to randomly select sampling locations *a priori* for field sampling. Random points were generated in a Geographic Information System (GIS), stratified based on frequency of occurrence informed by studies conducted by Hestir et al. (2008), and field crews navigated to within 10 meters of the points using airboat and outboard motorboats. At each location the following information was recorded: the geographic position from a differential global positioning system (DGPS) unit, the cover class, percent cover (percent cover at the surface for submerged vegetation), a rake was used to sample the presence and absence of submerged plants and a visual estimate of the quantity, by approximating length and width of the patch at the water surface, and secondarily from a nadir and oblique digital photograph at each point. Figure 2 shows the geographic distribution of ground reference data collected. Table 2 summarizes the number of points collected for each cover class.

Historic ground reference data were collected concurrent with historic overflights during June and July 2004-2007 (Table 3-hymap overflight dates, and associated GRD). Similar field protocol was followed and similar attributes were recorded in the field as from 2008, with two key differences. 1) Rather than an *a priori* approach as used in 2008, opportunistic sampling was employed where field researchers recorded ground reference data of cover classes as they came upon them, resulting in a more equal distribution of cover classes rather than one proportional to the occurrence of cover classes. This approach was followed in earlier studies (Underwood et al. 2006, Andrew and Ustin 2008, Hestir et al. 2008, Khanna et al. 2010), which focused on defining the spectral properties and the variance of the classes. 2) GRD collected in 2004-2007 only recorded locations of cover classes and plant species where cover was greater than 75% and in the

case of submerged vegetation, only where it was present at the surface with 75% or greater cover as visually estimated. Rakes were not used to confirm submerged vegetation presence, density, or absence.

Submerged aquatic vegetation ground reference data from 2008 were screened by percent plant cover at the surface, and only points with greater than 75% cover were used in training and testing of the classifier, to make it comparable to the previous years' data. The 2008 ground reference data were split (50/50) into training and test subsets to develop and validate the classifier.

2.3 Imagery Classification

We developed the ensemble classifier in See5 version 2.02a (Rulequest Research) and applied it using ENVI 4.6 (ITT Visual Information Solutions). We used STARSPAN (http://starspan.casil.ucdavis.edu) to extract the band information from pixels which overlap ground reference data for input into the classifier. Once the classification tree was developed and tested, it was implemented on 2008 image subsets consisting of windows of 31 pixels (~90 square meters) around a ground reference data point using STARSPAN. The classification results of the subset images were qualitatively evaluated for spatial consistency and expected patterns. The classifier was then applied to all flightlines from 2008 as well as historic imagery 2004-2007. The resulting classification maps were masked to the applicable study area (the waterways) using a water and riparian tree shadow mask derived from LiDAR data collected by Airborne 1 for the California Department of Water Resources (CA DWR). The water mask was obtained from the last return DEM developed from the LiDAR dataset and rescaled to the same 3 m resolution as the HyMap imagery. The shadow mask was created using a ray tracing algorithm,

r.sun (Scharmer and Greif 2000) on the first return raster (rescaled to 3m) for the date of each HyMap image. Classification maps from historic imagery were validating using corresponding GRD for each of the years.

3. RESULTS AND DISCUSSION

Of the 132 bands provided to the classifier, 121 bands were winnowed. Of the 11 bands remaining, one band index calculated over a narrow wavelength interval between the red and red/near-infrared region (Normalized Difference Vegetation Index 2, $NDVI_2$, Table 1) which detects the "red edge" spectral feature of vegetation (Filella and Penuelas 1994), and one calculated using a more traditional longer near-infrared wavelength ($NDVI_1$, Table 1). The other bands came from the reflected visible, near-infrared, and shortwave infrared regions. The near infra-red region (0.9431 μm) and the shortwave infrared (2.4757 μm) were estimated to be the most important attributes contributing to the predictive power of the classifier. This was followed by the blue visible region (0.4417 μm). Of these 11 bands, only $NDVI_1$ was used by 100% of the trees, though this was followed by closely $NDVI_2$, shortwave infrared (2.4757 μm), and near infrared (0.9431 μm) which all had a frequency of use of 99% by the trees. Table 3 lists the important bands, as well as the frequency of use in the ensemble classification trees. The attributes selected by winnowing reveal the utility of imaging spectroscopy data for this particular classification problem; the classifier used several narrow regions throughout the reflected spectrum. Critical to discriminating water and submerged vegetation from other vegetation is the information contained in the shortwave-infrared bands, as was information contained within the near-infrared for detecting submerged vegetation in water.

The final classification of 2008 had an error of 15.4% for the test data set which meets acceptable land cover classification standards suggested by the literature (Thomlinson et al. 1999, Foody 2002). The overall kappa coefficient, a measure of agreement between ground reference data and map classes that takes into account the probability of chance agreement, for the training and test sets is 0.96 and 0.69, respectively, indicating "excellent" and "good" agreement (Monserud and Leemans 1992). The kappa coefficient for submerged aquatic vegetation is 0.54, which is considered "fair" agreement (Congalton 1991, Monserud and Leemans 1992). The 2008 test producer's and user's Accuracies (indicating the level of class omission and commission, respectively) were lowest for submerged vegetation. Despite the accuracy limitations, displays of the mini-rasters show the maps have spatially coherent patterns. Additionally, the distributions follow locations where submerged vegetation would likely be present due to channel conditions (e.g. shallow and low flow areas). The application of the ensemble classifier to the historic imagery resulted in overall errors ranging from 20.4% to 14.1%; overall kappa coefficients range from 0.69 to 0.77 ("good" to "very good") and kappa coefficients relative to submerged vegetation range from 0.71 to 0.83 ("very good") (Table 4).

The largest source of confusion in the classification is discriminating submerged vegetation from water (see Hestir et al., 2008 for a detailed discussion of this problem). In the test set, 24 submerged vegetation points were misclassified as water, and 25 water points were erroneously classified as submerged vegetation, resulting in producer's and user's accuracies of 61% and 56 %, respectively (Table 5). However, in contrast to the methodology presented in Hestir et al. (2008), training data for 2008 were not biased

toward surface submerged vegetation, which produced higher detection rates of submerged vegetation at depth. We suggest that detectability of submerged vegetation may be most limited by plant density and cover rather than the inherent optical properties of the overlying water column itself. Detectability of submerged vegetation diminishes as submerged vegetation cover or density decreases or water depth to the submerged vegetation canopy increases. This is evident in the unsuccessful classifications using training data with low estimated percent cover, and confirmed by rake data collected in 2008 (Figure 4). Submerged vegetation detection is most successful when plant density is highest and least successful when it occurs at low cover and density. This is further supported by the high accuracies observed for classification of historic imagery whose validation data only include patches with dense cover at the surface (for which the classifier has been optimally trained).

Although rarely discussed, we feel it is important to highlight some of the problems with common assumptions regarding remote sensing accuracy assessments. Ground reference data is commonly thought of as ground truth data, and is often presumed to have no inherent errors in it, which is, of course, incorrect (Foody 2002). Positional errors between the ground reference point and the pixel due to GPS positional errors from the boats' movement from wind, wave, and current action can result in errors that are not due to the thematic accuracy of the map (Loveland et al. 1999).

Classification trees are highly sensitive to the training data values (Olden et al. 2008), quantity (Pal and Mather 2003), and quality (Liu et al. 2008) (such as the positional accuracy of ground reference data). Small changes in the training data can result in significant changes in the variables used in the trees themselves and can

significantly impact the mapping results. Appropriately distributed and accurately collected training data is critical to the success of ensemble classification. The low submerged vegetation class accuracies are due, in part, to its infrequent occurrence in the Delta during the 2008 field campaign. Submerged vegetation was relatively sparse compared to previous years, and many of the patches sampled had low densities, and were deep in the water column. Although our sampling was structured to be representative of all classes, the lack of submerged aquatic vegetation points available for training contribute to decreased accuracies for that class relative to other classes which had more points. Another potential source of error is from the photo-interpreted water class training data, although the water training points were photo-interpreted from the center of deep channels where submerged vegetation does not occur, some classification error is possible.

4. CONCLUSIONS

Our study demonstrated the robustness of ensemble classification trees for historic aquatic vegetation classification when constructed with an appropriate training set. The high cost of obtaining ground reference data and the frequent unavailability of historic ground reference data require that classification techniques be sufficiently robust to be relied upon when validation data is unavailable. We were able to construct a classifier using a single year of airborne imaging spectroscopy (48 flightlines) and correspondent ground reference data, and apply that classifier to the four years of historic spectroscopic imagery covering the same site, with high agreement between the predicted distribution and the real distribution of submerged vegetation in the Delta. Classification maps were

successfully constructed in spite of the flightline-to-flightline or year-to-year calibration and environmental and climate-hydrological heterogeneity.

Using C5.0 on the 2008 data to construct a classifier was successful due to the sampling strategy used during ground reference data collection. As a basic function of the algorithm, C5.0 considers the probability that a set of training data for a particular class (e.g. submerged vegetation) is the relative frequency of observations in that class (Tso and Mather 2001). In order to successfully implement the classifier, it was important to ensure that our sampling strategy reflected the relative distribution of classes (submerged vegetation, emergent and floating vegetation, and water) present in the system. Capturing the variability within the study area through a carefully planned field campaign was necessary to construct a classifier robust enough to apply to highly variable, high dimensional historic imagery. *A priori* understanding of the cover classes and variability of the system allowed us to estimate the relative frequency of each of the classes and stratify our field sampling techniques accordingly. The historic classification validation enabled us to test the robustness of the training data and classifier.

5. ACKNOWLEDGEMENTS

This study benefited greatly from insightful input from Maria J. Santos. The staff and field crews of the Center for Spatial Technologies and Remote Sensing at UC Davis, the California Department of Boating and Waterways, and the California Department of Food and Agriculture provided critical support in the field. We are grateful to Carlos Rueda for developing a program to apply C5.0 classification trees to image data. This study was funded by the California Department of Water Resources contract

4600008137-T4, and California Department of Boating and Waterways agreement 03-105-114.

6. REFERENCES

Andrew, M. E. and S. L. Ustin. 2008. The role of environmental context in mapping invasive plants with hyperspectral image data. Remote Sensing of Environment **112**: 4301-4317.

Becker, B. L., D. P. Lusch, and J. Qi. 2007. A classification-based assessment of the optimal spectral and spatial resolutions for Great Lakes coastal wetland imagery. Remote Sensing of Environment **108**: 111-120.

Breiman, L. 2001. Random Forests. Machine Learning **45**: 5-32.

Brown de Colstoun, E. C., M. H. Story, C. Thompson, K. Commisso, T. G. Smith, and J. R. Irons. 2003. National Park vegetation mapping using multitemporal Landsat 7 data and a decision tree classifier. Remote Sensing of Environment **85**: 316-327.

Brown de Colstoun, E. C. and C. L. Walthall. 2006. Improving global scale land cover classifications with multi-directional POLDER data and a decision tree classifier. Remote Sensing of Environment **100**: 474-485.

Brown, L. and D. Michniuk. 2007. Littoral fish assemblages of the alien-dominated Sacramento-San Joaquin Delta, California, 1980–1983 and 2001–2003. Estuaries and Coasts **30**: 186-200.

Chan, J. C.-W. and D. Paelinckx. 2008. Evaluation of Random Forest and Adaboost tree-based ensemble classification and spectral band selection for ecotope mapping using airborne hyperspectral imagery. Remote Sensing of Environment **112**: 2999-3011.

Cohen, A. N. and J. T. Carlton. 1998. Accelerating Invasion Rate in a Highly Invaded Estuary. Science **279**: 555-558.

Congalton, R. G. 1991. A review of assessing the accuracy of classifications of remotely sensed data. Remote Sensing of Environment **37**: 35-46.

DeFries, R. S. and J. C.-W. Chan. 2000. Multiple Criteria for Evaluating Machine Learning Algorithms for Land Cover Classification from Satellite Data. Remote Sensing of Environment **74**: 503-515.

Feyrer, F., M. L. Nobriga, and T. R. Sommer. 2007. Multidecadal trends for three declining fish species: habitat patterns and mechanisms in the San Francisco Estuary, California, USA. Canadian Journal of Fisheries and Aquatic Sciences **64**: 723-734.

Filella, I. and J. Penuelas. 1994. The red edge position and shape as indicators of plant chlorophyll content, biomass and hydric status. International Journal of Remote Sensing **15**: 1459 - 1470.

Foody, G. M. 2002. Status of land cover classification accuracy assessment Remote Sensing of Environment **80**: 185-201.

Freund, Y. and R. E. Schapire. 1996. Experiments with a new boosting algorithm. Pages 148-156 *in* Machine Learning: Proceedings of the Thirteenth International Conference.

Friedl, M. A. and C. E. Brodley. 1997. Decision Tree Classification of Land Cover from Remotely Sensed Data. Remote Sensing of Environment **61**: 399-409.

Friedl, M. A., C. E. Brodley, and A. H. Strahler. 1999. Maximizing land cover classification accuracies produced by decision trees at continental to global scales. Geoscience and Remote Sensing, IEEE Transactions on **37**: 969-977.

Gao, B. C., K. B. Heidebrecht, and A. F. H. Goetz. 1993. Derivation of scaled surface reflectances from AVIRIS data. Remote Sensing of Environment **44**: 165-178.

Han, L. and D. C. Rundquist. 2003. The spectral responses of Ceratophyllum demersum at varying depths in an experimental tank. International Journal of Remote Sensing **24**: 859-864.

Hestir, E. L., S. Khanna, M. E. Andrew, M. J. Santos, J. H. Viers, J. A. Greenberg, S. S. Rajapakse, and S. L. Ustin. 2008. Identification of invasive vegetation using hyperspectral remote sensing in the California Delta ecosystem. Remote Sensing of Environment **112**: 4034-4047.

Khanna, S., M. J. Santos, S. Ustin, and P. J. Haverkamp. 2010. An integrated approach to biophysiologically based classification of floating aquatic macrophytes. International Journal of Remote Sensing **In press**.

Knowles, N. and D. R. Cayan. 2002. Potential effects of global warming on the Sacramento/San Joaquin watershed and the San Francisco estuary. Geophys. Res. Lett. **29**: 4p.

Lawrence, R. L., S. D. Wood, and R. L. Sheley. 2006. Mapping invasive plants using hyperspectral imagery and Breiman Cutler classifications (randomForest). Remote Sensing of Environment **100**: 356-362.

Liu, K., X. Li, X. Shi, and S. Wang. 2008. Monitoring mangrove forest changes using remote sensing and GIS data with decision tree-learning. Wetlands **28**: 336-346.

Loveland, T. R., Z. Zhu, D. O. Ohlen, J. F. Brown, B. C. Reed, and L. Yang. 1999. An analysis of the IGBP global land-cover characterization process. Photogrammetric Engineering and Remote Sensing **65**: 1021-1032.

Moisen, G. G., E. A. Freeman, J. A. Blackard, T. S. Frescino, N. E. Zimmermann, and J. T. C. Edwards. 2006. Predicting tree species presence and basal area in Utah: A comparison of stochastic gradient boosting, generalized additive models, and tree-based methods. Ecological Modelling **199**: 176-187.

Monserud, R. A. and R. Leemans. 1992. Comparing global vegetation maps with the Kappa statistic. Ecological Modelling **62**: 275-293.

Mundt, J. T., N. F. Glenn, K. T. Weber, T. S. Prather, L. W. Lass, and J. Pettingill. 2005. Discrimination of hoary cress and determination of its detection limits via hyperspectral image processing and accuracy assessment techniques. Remote Sensing of Environment **96**: 509-517.

Olden, J. D., J. J. Lawler, and N. L. Poff. 2008. Machine learning methods without tears: a primer for ecologists. Quarterly Review of Biology **83**: 171-193.

Pal, M. and P. M. Mather. 2003. An assessment of the effectiveness of decision tree methods for land cover classification. Remote Sensing of Environment **86**: 554-565.

Quinlan, J. R. 2009. C5.0 An Informal Tutorial. Rulequest Research.

Scharmer, K. and J. Greif, editors. 2000. The European solar radiation atlas, Vol. 2: Database and exploitation software. Les Presses de l' École des Mines, Paris.

Thomlinson, J. R., P. V. Bolstad, and W. B. Cohen. 1999. Coordinating Methodologies for Scaling Landcover Classifications from Site-Specific to Global: Steps toward Validating Global Map Products. Remote Sensing of Environment **70** :16-28.

Tso, B. and P. M. Mather. 2001. Classification Methods for Remotely Sensed Data. Taylor and Francis, New York.

Underwood, E., M. Mulitsch, J. Greenberg, M. Whiting, S. Ustin, and S. Kefauver. 2006. Mapping Invasive Aquatic Vegetation in the Sacramento-San Joaquin Delta using Hyperspectral Imagery. Environmental Monitoring and Assessment **121** :47-64.

Table 1. Spectral indices used as inputs into C5.0. $\rho_{0.649}$ indicates reflectance value at wavelength 0.649 µm.

Index	Equation
$NDVI_1$, Normalized Difference Vegetation Index	$\frac{(\rho_{0.862} - \rho_{0.649})}{(\rho_{0.862} + \rho_{0.649})}$
$NDVI_2$, Normalized Difference Vegetation Index	$\frac{(\rho_{0.710} - \rho_{0.649})}{(\rho_{0.710} + \rho_{0.649})}$
Green/red ratio	$\frac{\rho_{0.528}}{\rho_{0.650}}$
Normalized green/red ratio	$\frac{(\rho_{0.650} - \rho_{0.528})}{(\rho_{0.650} + \rho_{0.528})}$
Average SWIR Reflectance 1	Average($\rho_{1.62}$ to $\rho_{1.77}$)
Average SWIR Reflectance 2	Average($\rho_{2.165}$ to $\rho_{2.25}$)

Table 2. Summary of HyMap acquisition and concurrent ground reference data collection. For each "water" point, a rake was dropped to the bottom to ascertain definitively the presence or absence of submerged plant material.

	Ground Reference Data			
Image Acquisition	Submerged vegetation	Floating & Emergent	Water	Total
June 25, 2004-July 10, 2004	795	1106	99	2000
June 22, 2005-July 8, 2005	796	1335	52	2183
June 21, 2006-June 26, 2006	1387	1163	335	2885
June 19, 2007-June 26, 2007	320	423	226	969
June 29, 2008-July 7, 2008	347	191	726	1264

Table 3. HyMap reflective and index bands remaining after attribute winnowing, and their frequency of use by the ensemble of classification trees.

Band	Frequency
$NDVI_1$	100%
2.4757 µm	99%
$NDVI_2$	99%
1.6855 µm	94%
2.2843 µm	94%
0.4971 µm	88%
1.9652 µm	84%
0.5584 µm	82%
2.4135 µm	81%

Table 4. A summary of the classification accuracies for 2008 and historic HyMap imagery.

	2008_{Train}	2008_{Test}	2007	2006	2005	2004
Overall Accuracy	97.7%	84.6%	79.6%	85.9%	84.3%	78.8%
Overall Kappa	0.96	0.69	0.69	0.77	0.70	0.65
$Kappa_{SAV}$	0.97	0.54	0.71	0.83	0.79	0.83
Producer's $Accuracy_{SAV}$	98.1%	55.8%	72.2%	82.4%	80.0%	64.7%
User's $Accuracy_{SAV}$	97.8%	60.6%	80.5%	90.9%	86.7%	89.5%

Table 5. Classification confusion matrices between the ground reference data (columns), and the predicted class membership (rows) for 2008-2004.

2008_{Test}	**Ground Reference Data**			
Classified Data	Submerged Vegetation	Water	Floating & Emergent	Total
Submerged Vegetation	43	24	4	71
Water	25	320	6	351
Floating & Emergent	9	13	83	105
Total	77	357	93	527
2007				
Submerged Vegetation	231	22	34	287
Water	81	203	52	336
Floating & Emergent	8	1	337	346
Total	320	226	423	969
2006				
Submerged Vegetation	1143	17	97	1257
Water	147	317	48	512
Floating & Emergent	97	1	1018	1116
Total	1387	335	1163	2885
2005				
Submerged Vegetation	637	1	97	735
Water	88	51	86	225
Floating & Emergent	71	0	1152	1223
Total	796	52	1335	2183
2004				
Submerged Vegetation	514	5	55	574
Water	255	93	82	430
Floating & Emergent	26	1	969	996
Total	795	99	1106	2000

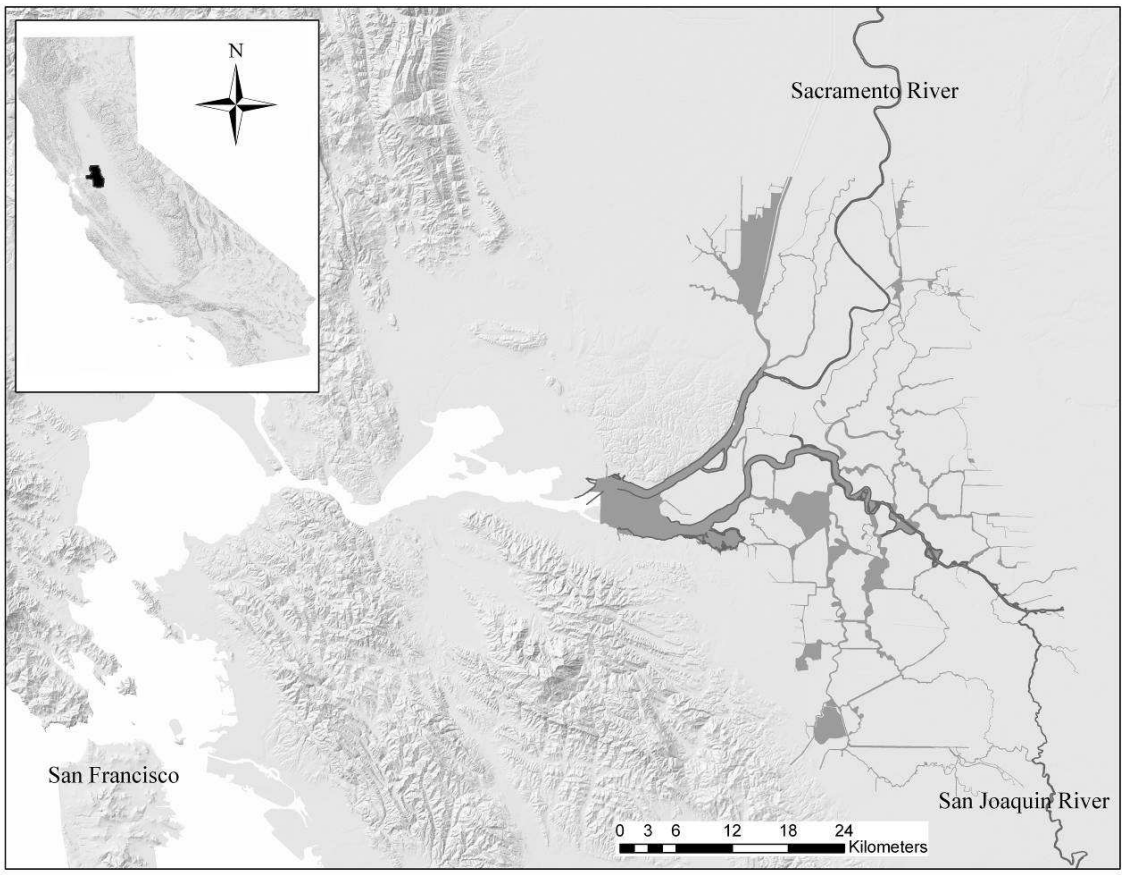

Figure 1. A map of the Sacramento-San Joaquin River Delta and upper San Francisco Bay. The inset map indicates the study area's location (in black) within California. The Delta's watersheds drain nearly 40% of California, over 160,000 km^2.

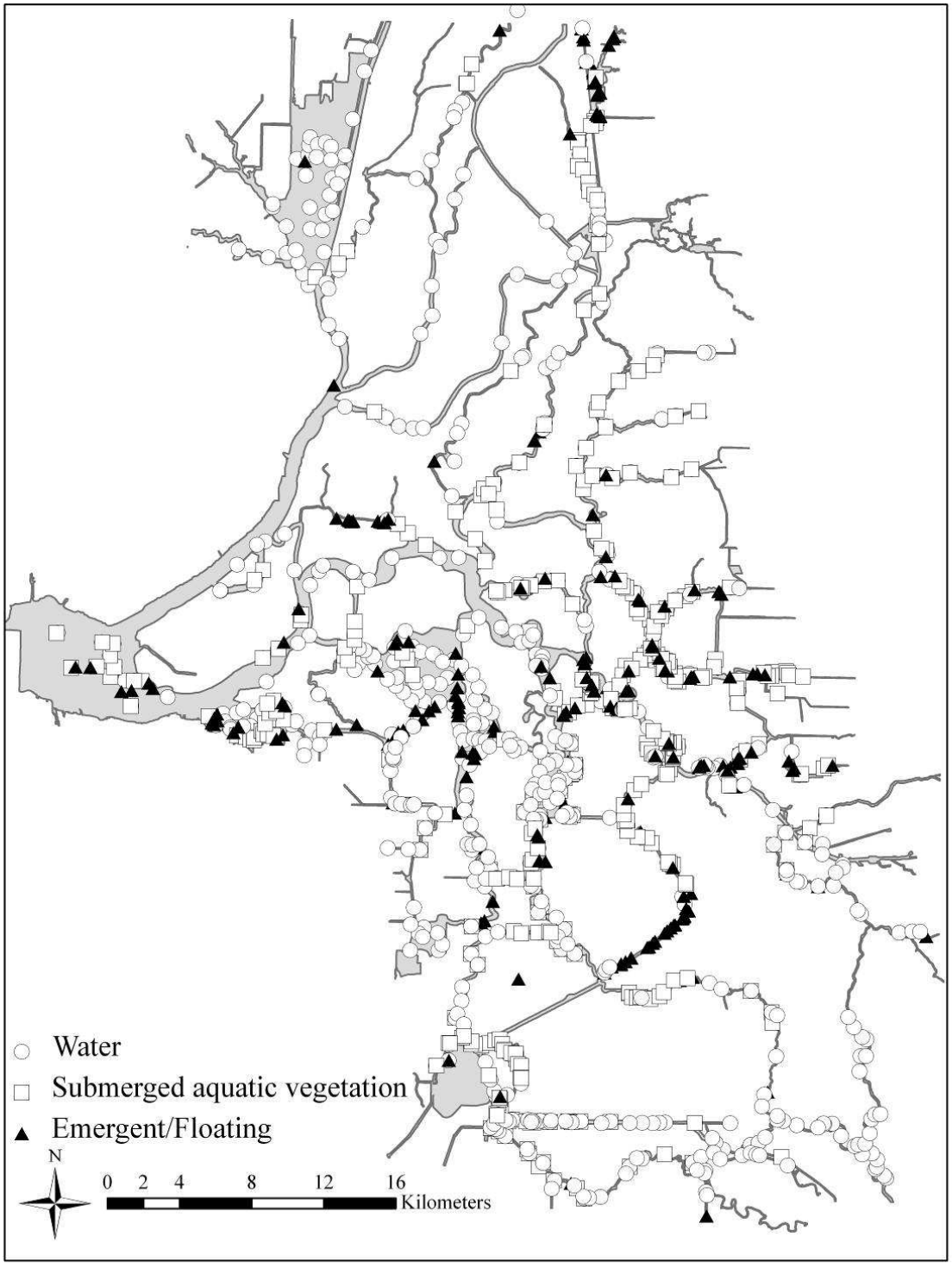

Figure 2. Ground reference data collected 23 June-8 July 2008. Stratified random points of the target cover classes (submerged aquatic vegetation, water, floating and emergent vegetation) were selected *a priori* to the field campaign and navigated to using boats. The actual cover class and percent cover were recorded with handheld differential GPS devices.

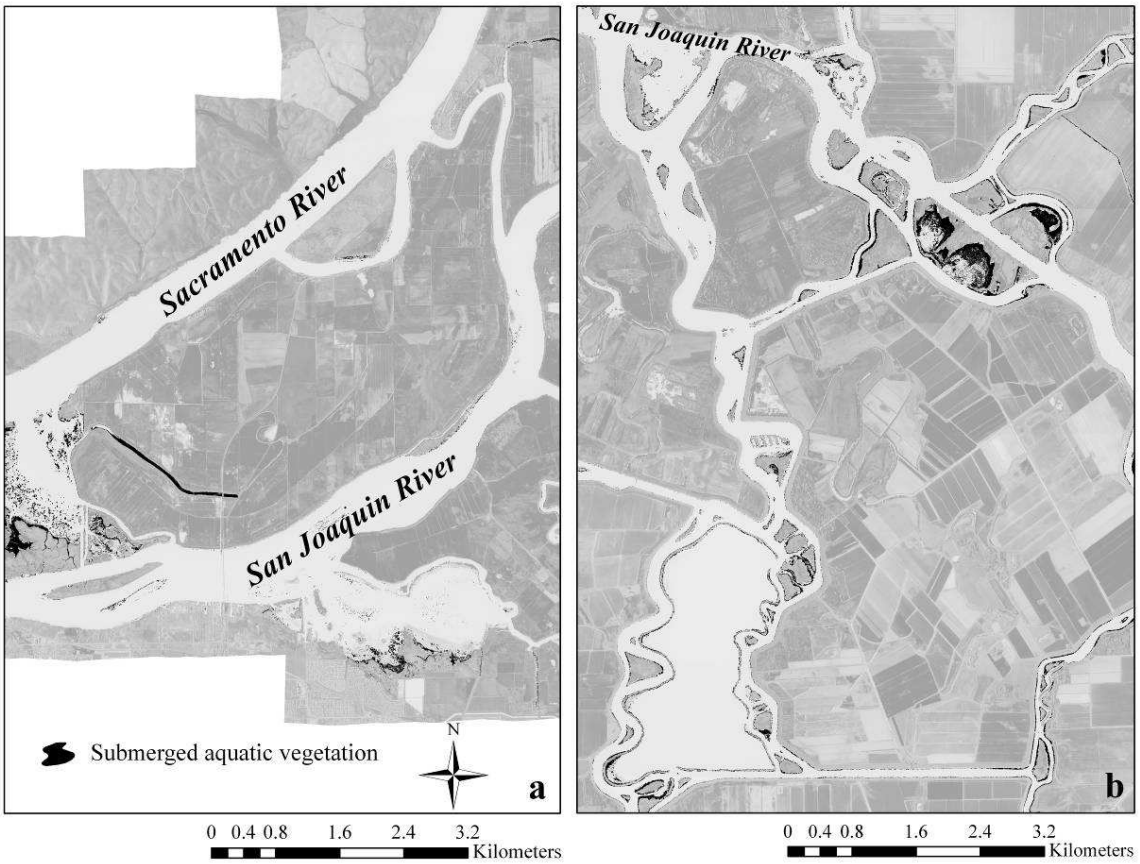

Figure 3. Two maps of predicted submerged aquatic vegetation distribution (in black) from the 2008 spectroscopic imagery. The spatial patterns of submerged vegetation occurrence match those expected from field observation and previous study (Hestir et al. 2008); submerged vegetation does not occur in fast flowing or deep channels or lakes, it inhabits shallow channel margins and backwater areas of slow flow. These patterns were also observed for submerged aquatic vegetation distribution predicted from the historic imagery.

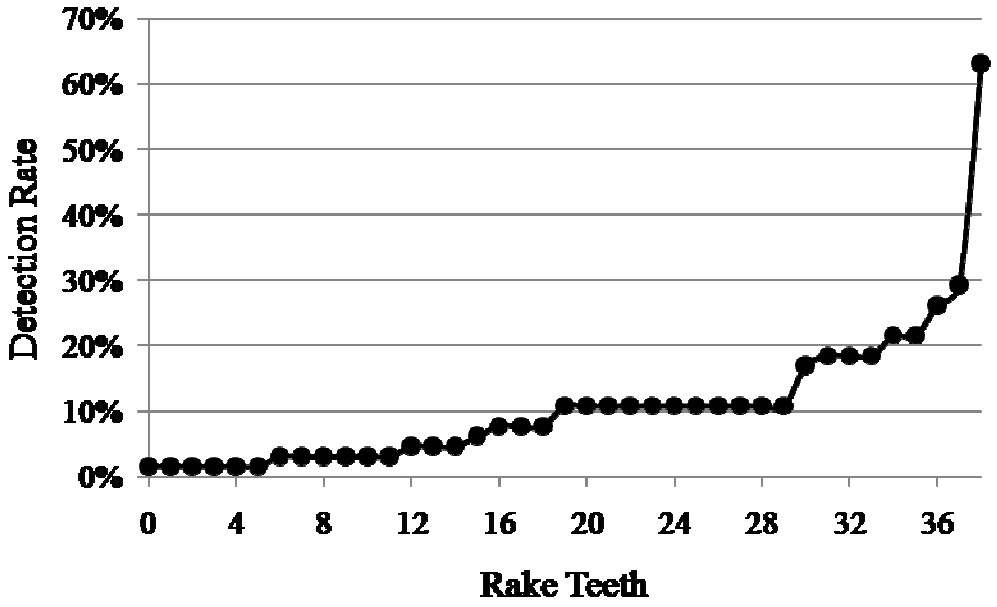

Figure 4. The cumulative detection rate of submerged aquatic vegetation by the number of rake teeth covered by submerged vegetation during a sample. Rake teeth are a proxy for submerged plant density in the water column at the sampling location. Detection rates are highest at sample locations with high submerged aquatic vegetation density.

· Chapter 3 ·

Interactions between Submerged Vegetation, Turbidity, and Water Movement in a Tidal River Delta

Interactions between Submerged Vegetation, Turbidity, and Water Movement in a Tidal River Delta

Erin Lee Hestir[a], David H. Schoellhamer[b], Jonathan Greenberg[a], Tara Morgan-King[b], and Susan L. Ustin[a]

a Center for Spatial Technologies and Remote Sensing, University of California, Davis 95616
b California Water Science Center, United States Geological Survey, 95819

ABSTRACT

The interactions between water velocity, submerged vegetation, and turbidity are commonly described as a feedback in which the presence of submerged vegetation at lower velocities further decreases turbidity, which then promotes continued persistence and growth of submerged vegetation. However, these interactions are determined by spatial variability in hydrology and plant distributions. This study examines submerged vegetation cover, water velocity, and turbidity in the Sacramento-San Joaquin River Delta, a tidal river delta with high inter-and intra-annual hydrologic variability, as well as variable submerged vegetation distribution to determine whether these interactions are detectable. We found annual maximum water velocity limits submerged vegetation cover above 0.49 $m \cdot s^{-1}$. We also found submerged vegetation cover has a negative linear relation with turbidity, and limits high turbidities (13.8-15.8 NTU). This limiting relation between submerged vegetation cover and turbidity negatively affects endangered fish species habitat (i.e., delta smelt, *Hypomesus transpacificus*), although removal of the vegetation may not affect sufficient increases in turbidity to restore fish habitat.

1. INTRODUCTION

Turbidity, or the optical clarity of a water body, is an important ecological indicator for freshwater and estuarine systems. Turbidity controls light penetration

through the water column which limits the growth and survival of submerged vegetation (Dennison et al. 1993). Once established, submerged vegetation can reduce water velocity both within the plant bed (Madsen et al. 2001) and at the channel scale (Chambers et al. 1991), thus decreasing turbidity, increasing sedimentation (Madsen et al. 2001, Crooks 2002, Schulz et al. 2003) and light availability, and promoting further growth. Conversely, high velocities mediate the establishment, growth, and distribution of submerged plants (Biggs 1996), resulting in higher sediment resuspension and turbidity, limited light availability, and limited submerged plant productivity. Additional factors contribute to the establishment and growth of submerged vegetation, but these tend to strengthen feedback loops that either amplify or dampen submerged vegetation growth and persistence. For example, high current velocity also changes bed composition (Chambers et al. 1991), leading to reduced sediment and fertility (Barko et al. 1991), and high velocities present direct physiological and mechanical limits to submerged vegetation establishment and growth (Koch 2001). However, recent studies suggest the interaction between water movement, sediment, and submerged vegetation, although regional in scope, may be of only second-order importance and the relations are dependent on the biomass and distribution of submerged vegetation (Havens 2004, Gurnell et al. 2006). Given the spatial variability of submerged vegetation distribution at the ecosystem scale, the influence of submerged vegetation on increased water clarity is likely to vary spatially as well. Therefore, we ask: are the feedbacks between submerged vegetation, velocity, and turbidity detectable in a hydrologically variable tidal river delta with variable submerged vegetation distribution?

1.1 Study Site

The Sacramento-San Joaquin River Delta is formed by the confluence of four rivers in the Central Valley of California: the Sacramento, San Joaquin, the Cosumnes, and the Mokelumne Rivers (Figure 1). Historically a vast tidal marsh which drained to the Pacific Ocean via the San Francisco Bay, the Delta is now a network of levee-bound rivers and man-made channels, reclaimed agricultural tracts of land (islands), and shallow lakes formed by flooded islands (Wright and Schoellhamer 2005). Hydraulics in the Delta are altered by cross-Delta conveyance channels, freshwater export pumping, and agricultural consumption and drainage within the Delta. The hydrology is dominated by freshwater inflows from the Sacramento and San Joaquin rivers with extreme seasonal (1700 ± 300 $m^3 \cdot s^{-1}$ in the winter and 540 ± 40 $m^3 \cdot s^{-1}$ in summer) and interannual (230 $m^3 \cdot s^{-1}$ in a low flow year to 2700 $m^3 \cdot s^{-1}$ in a high flow year) variability (Jassby and Cloern 2000). Tides propagate eastward through the estuary, dampening as they move inland, and disseminating over most of the Delta during low river inflow (Wright and Schoellhamer 2005). Water velocities range from 0.02 $m \cdot s^{-1}$ during slack tides to 5.5 $m \cdot s^{-1}$ during ebb tides. Turbidity in the Delta is primarily controlled by suspended sediments, which are essentially equivalent to total suspended solids in this system (Gray et al. 2000).

The altered hydrology of the Delta has resulted in an increase in exotic plant and animal species (Santos et al. 2010), and the expansion of submerged vegetation over the past three decades, particularly of the invasive Brazilian waterweed (*Egeria densa*)(Jassby and Cloern 2000), has led to increased concern about its possible role in altering aquatic habitat (Service 2007, Santos et al. 2009). Of particular concern is the

impact submerged vegetation has on turbidity, which has become one of the focal habitat indicators for the endangered endemic fish, delta smelt (*Hypomesus transpacificus*) (Nobriga et al. 2005, Feyrer et al. 2007). The submerged vegetation community is comprised of four exotic rooted submerged plant species, *Egeria densa* (which accounts for approximately 85% of the submerged vegetation community biomass [Hestir et al. unpublished data]), *Myriophyllum spicatum*, *Potamogeton crispus*, and *Cabomba caroliniana,* and four rooted native species, *Stuckenia pectinatus, Stuckenia filiformis, Potamogeton nodosus,* and *Elodea canadensis,* as well a fifth, free floating submerged plant, *Ceratophyllum demersum.* Understanding how submerged vegetation interacts with turbidity and water velocity can inform endangered species habitat conservation, invasive plant management strategies, and may provide insight into the impact of proposed water diversion projects on submerged vegetation in the Delta.

2. METHODS

2.1 Submerged vegetation distribution data

We used submerged vegetation distribution maps derived from airborne imaging spectroscopy to determine submerged vegetation distribution. The HyVista Corporation acquired HyMap imaging spectrometer (Cocks et al. 1998)data during morning and afternoon low tides during late June and early July of each year 2004-2008 with a ground resolution of 3 meter pixels ($9m^2$). The images were classified using ensemble classification trees developed in C5.0 (Rulequest Research), and validated with ground reference data collected concurrent with image acquisition. The overall classification accuracies for all years range from 79%-86%, with Kappa coefficients (an indicator of the level of agreement between ground data and map data that accounts for the

probability of random agreement) ranging from 0.65-0.77 indicating "good" to "very good" agreement with ground reference data (Monserud and Leemans 1992). Table 1 details the image acquisition dates and accuracies of classifications. The final submerged vegetation classes were exported to shapefiles. Image data calibration and corrections are described in (Hestir et al. 2008). For ground reference data collection and classifier development and performance, see (Hestir et al. 2010).

To quantify the coverage of submerged vegetation near sites where turbidity is measured, we used the fraction of water area containing submerged vegetation within a 1 km radius by generating a 1 km buffer around each turbidity station, and then clipping the submerged vegetation maps within these buffers using ArcMap 9.2 (ESRI, Redlands, CA). We selected a 1 km radius because the time it takes a parcel of water to move 1 km [1000 m/0.3 ms^{-1} ≈ O (1hr)] is the same order of magnitude as the time it would take a particle to settle from the water surface to bottom [5 m/10^{-3} ms^{-1} ≈ O (1hr)] in typical Delta channels. Thus, 1 km is a sufficient distance for suspended sediment concentration to adjust to the conditions in the reach of the channel. The same buffer size (1 km) was used for velocity measurement stations. We tested whether there were significant differences in submerged vegetation cover between years (using Tukey's HSD pairwise test) for both the turbidity and velocity buffers, and found none. Therefore we treated each year of submerged vegetation cover as a replicate for a given site.

2.2 Turbidity data

The California Department of Water Resources conducts monthly water quality sampling cruises in the Delta and northern San Francisco Bay. Measured parameters include turbidity 1 meter below the surface. Data are made available at

http://bdat.ca.gov/. A total of ten sites were active within the study area for the period of interest, 2004-2008, and we calculated the mean turbidity during the growing season (April-October) of submerged vegetation for each site, based on the submerged vegetation maps produced from the spectroscopic imagery (Hestir et al. 2010).

2.3 Velocity data

The US Geological Survey measures water velocity using hydroacoustic velocity meters at 31 stations within the study area, beginning in June 2006. Data were downloaded from the California Data Exchange Center (http://cdec.water.ca.gov). Velocity data is recorded every 15 minutes. The data were run through a low-pass filter, and the annual maximum water flow velocity for each year (2006-2008) at each site was determined.

2.4 Turbidity and submerged vegetation interactions

We related turbidity values averaged over the submerged vegetation growing season with the percent cover of submerged vegetation within each 1 km buffer around the 10 turbidity sites to determine if submerged vegetation cover controls turbidity. We hypothesized that, once established, submerged vegetation cover constrains, or limits turbidity in the Delta. We used quantile regression (Koenker and Bassett 1978, Koenker and Hallock 2001), to model the upper limit of the turbidity response to SAV cover. Quantile regression is a form of least absolute deviation (LAD) regression (Cade et al. 1999) that predicts a range of conditional distribution of responses, rather than just the conditional mean of responses (as provided by ordinary least squares (OLS) regression) given a set of predictor variables (Yu et al. 2003). While OLS regression models the

central tendency of a distribution of data, quantile regression can model the outer edge of a distribution (Cade et al. 1999), represented by an upper quantile (e.g. 75% of the observations), which indicates the limiting condition of the predictor variable on the response variable (Cade and Noon 2003). We implemented linear quantile regression using the quantreg package (Koenker 2009) in R (version 2.9.2, R: A Language and Environment for Statistical Computing, http://www.R-project.org). To calculate the standard errors of the model coefficients, we used the (x,y)-pair bootstrap method (Koenker and Hallock 2001) in quantreg. Similar to OLS regression, the parameter estimates in linear quantile regression provide estimates for the rates of change conditional on adjusting for the effects of the other variable in the model, but for a specific quantile. We selected the regression quantile with the lowest variance in slope estimation from among the upper quantiles to use as our limitation model (Koenker and Hallock 2001, Bryce et al. 2008).

2.5 Velocity threshold identification

Water velocity has long been recognized as a habitat constraint for submerged vegetation (Chambers et al. 1991), and high water velocities can impede submerged vegetation establishment and persistence through both mechanical and physiological damage (Sand-Jensen 2008). We tested whether there was a maximum water velocity critical to submerged vegetation cover in the Delta. We binned maximum water velocity measurements into 0.03 $m \cdot s^{-1}$ increments, and performed a t-test to determine the significance of the separation between submerged vegetation cover above and below each velocity bin. This t-test was iterated through each water velocity bin from 0.0 $cm \cdot s^{-1}$ to 1.2 $m \cdot s^{-1}$. We hypothesized that if there is a velocity threshold that controls submerged

vegetation cover, there should be a discernible value at which maximum separation of covers occurs. The velocity position that yielded the most significant separation is the velocity threshold on submerged vegetation establishment and persistence, and the p-value is the significance of this threshold.

3. RESULTS

3.1 Submerged vegetation constraint on growing season turbidity

From the upper quantiles we regressed, we found that all estimated regression parameters were significant, and the estimated slope from 90^{th} quantile regression model had lowest standard error (Table 2). Therefore, we take the 90^{th} regression quantile as the most appropriate model for the constraint submerged vegetation cover has on growing season turbidity. This model shows a negative relation between increased submerged vegetation cover and growing season turbidity, and describes a significant, linear upper limit of turbidity by submerged vegetation cover (Figure 2). The slope from the 90^{th} regression quantile represents decreases in turbidity associated with the constraints of increased submerged vegetation cover. Figure 3 shows the estimated slope and the intercept of the linear quantile regression as a function of quantiles from 0.02-0.98, incremented every 0.01, and shown with 95% confidence interval bands. This figure demonstrates the variability of slopes and intercepts over the full range of turbidity quantiles and its sensitivity to submerged vegetation cover. Figure 3 reveals the upper distributional limit of turbidity to be a function of a limiting factor, in this case, submerged vegetation cover (Cade et al. 1999, Koenker and Hallock 2001). For example, the rate of decrease in turbidity (slope) at the 10^{th} quantile (-0.08 ± 0.08 NTU change in turbidity per unit change in submerged vegetation) is much less than at the 90^{th} quantile

of the turbidity distribution (-0.6 ± 0.07 NTU). The gray horizontal solid line and confidence interval (dashed lines) shows the least squares regression estimate for the slope and intercept coefficients, illustrating the mean response.

3.2 Velocity thresholds on submerged vegetation cover

As we iterated the t-tests through the 3.0 $cm \cdot s^{-1}$ velocity bins, the significance of separation of submerged vegetation cover increased (p-values decreased), until it reached a maximum separation of submerged vegetation cover at 0.49 $m \cdot s^{-1}$ (a minimum p-value of 3.4×10^{-6}), after which the significance of separation of cover decreased again (Figure 4).

4. DISCUSSION

4.1 Velocity controls submerged vegetation distribution

Submerged vegetation cover is highly variable throughout the Delta, and the distribution of submerged vegetation in the Delta is controlled, at least in part, by water velocity. Our iterative t-tests found a discernible value at which maximum separation of submerged vegetation cover occurs. We interpret this to be the velocity threshold controlling submerged vegetation cover in the Delta. In channels where the annual maximum velocity exceed 0.49 $m \cdot s^{-1}$, submerged vegetation cover is significantly lower than at sites with lower velocity. The observed velocity threshold for the submerged vegetation community cover in the Delta falls within the range of velocities observed in other studies; in streams intermediate current velocities (> 0.3 $m \cdot s^{-1}$) reduced (Nilsson 1987), or even proscribed submerged vegetation (>0.28 $m \cdot s^{-1}$) (Gantes and Caro 2001). In larger rivers, submerged vegetation occurrence was rare at current velocities of 0.4-0.6 $m \cdot s^{-1}$ (French and Chambers 1996) or was absent where current velocities exceeded 1

$m \cdot s^{-1}$ (Chambers et al. 1991, Fortin et al. 1993). The effects of variable flow due to flooding, or in this study tides, on submerged vegetation distribution are not well understood (Madsen et al. 2001) but in large rivers the direct effects of velocity on submerged vegetation might be very localized; a weak (Gantes and Caro 2001) or even no response (Sprenkle et al. 2004) to velocity may be detected if measurements are not made within the plant bed. In such systems velocity may have secondary effects on submerged vegetation growth by altering bed sediment composition (Chambers et al. 1991) even if a strong linear correlation is not observed.

In the Delta velocity events above 0.49 $m \cdot s^{-1}$ constrain submerged vegetation cover, but below that threshold cover is controlled by other variables; sites with high velocity events have little or no submerged vegetation (mean cover = 1.76%), whereas sites with low velocity have much more vegetation (mean cover = 7.23%). Additionally, the variance in the low velocity sites is much higher than low velocity sites (64% and 44% respectively). That is, submerged vegetation occurs in a range of cover in low velocity sites, but there is little or no submerged vegetation in high velocity sites. In the low velocity sites, other environmental conditions (such as light limitation, sediment quality, and nutrient availability) (Sprenkle et al. 2004), as well as species-specific plant traits (including dispersal and recruitment strategies, resistance to flow) (Sand-Jensen 2008) influence submerged vegetation distribution. We imagine that some of the variation in response observed in this study is due to the varying species composition of the submerged vegetation community. Velocity reduction in submerged vegetation canopies is biomass and species dependent: plant and canopy morphology strongly influence the reduction in drag forces in the plant beds (Madsen et al. 2001, Sand-Jensen

2008). Although the community is dominated by *Egeria densa*, a ramifying species with dense canopy growth throughout the water column, some native species such as *Stuckenia pectinatus* and *Stuckenia filiformis* have more streamlined canopies with blade-like leaves. It is likely that variations in community composition across the Delta contribute to the variation in responses to water velocity.

4.2 Submerged vegetation cover constrains high turbidity

There is a significant negative relation between submerged vegetation cover and turbidity, and the results of the quantile regression suggest that submerged vegetation cover limits high turbidity in the Delta. This is a response that would be underestimated by ordinary least squares regression; submerged vegetation cover has a greater impact on higher turbidity values than on lower ones as demonstrated by Figure 3 in which the slope of the regression increases with increasing turbidity quantiles (Figure 3). Just as submerged vegetation cover is controlled by a number of factors (including velocity), there are many possible variables contributing to the variability of turbidity in this system. The Delta is characterized by high inter- and intra-annual hydrodynamic variability, and local variability in channel morphology and water velocity, as well as proximity to external sources of suspended sediment from the Sacramento River (upstream) and the Suisun Bay (downstream) all are likely to determine turbidity. Turbidity at some sites may be low or high without the presence of submerged vegetation due to these other explanatory variables, but at higher turbidities in the Delta, submerged vegetation cover will always constrain turbidity values. The 90^{th} regression quantile is the best model for estimating changes in turbidity when submerged vegetation cover is the limiting factor. Cause and effect is not proven here, but submerged vegetation cover as a

limiting factor on turbidity supports the hypothesized feedback in which submerged vegetation decreases turbidity which allows submerged vegetation to persist and possibly spread without the impediment of light limitation.

Unfortunately velocity and turbidity were not measured in the same locations, save for one site in Old River, which makes direct conclusions about the interactions and proposed feedbacks between velocity, submerged vegetation and turbidity difficult to make. However, Old River where all three factors are measured, velocity is high (1.0-1.8 $m \cdot s^{-1}$) and should be limiting, submerged vegetation cover is low-moderate (4.5%), and turbidity is moderate (5-7 NTU). It will be useful to conduct more turbidity and velocity measurements in the same location. Such data would provide the information needed to conduct multivariate analyses which may shed further light on the interplay between these three factors.

Our study is observational, which leads us to conclude correlation, but not causation. An experiment which removed submerged vegetation from the environment and then recorded subsequent changes in turbidity would allow us to test predictions made from the submerged vegetation-turbidity feedback model. The application of herbicides to manage *Egeria densa* in the Delta by the California Department of Boating and Waterways (CDBW) *Egeria densa* Control Program (EDCP) has been successful in one location (Frank's Tract) in the Delta beginning in 2007 (Santos et al. 2009). Successful treatment of *Egeria densa* at Frank's tract resulted in a decrease in areal submerged vegetation cover from 2006 to 2007 of 47% (Santos et al. 2009) and continuation of treatment has resulted in a further decrease of 56% from 2007 to 2008. The reductions in submerged vegetation at Frank's Tract provide a natural experiment in

which we can examine the effects of submerged vegetation removal on turbidity. Turbidity station D19 is located in the central-eastern portion of Frank's Tract, a flooded island, or lake, which is now a popular recreation site for boaters and anglers. At site D19, submerged vegetation cover decreased from 4.7% in 2006 to 1.1% in 2007 (a 77% decrease) and mean growing season turbidity decreased from 6.6 (SD =5.3) NTU to 5.1 NTU (SD = 2.4). However, from 2007 to 2008, submerged vegetation cover was reduced again from 1.1% to 0.1% (a 91% decrease), and turbidity increased to 8.3 NTU (SD=3.9). This appears to at least follow the general linear relation we observe for turbidity response to submerged vegetation cover in a situation where submerged vegetation cover is the confirmed independent variable. In this case, turbidity at D19 for all of these years is not in the upper quantiles of turbidity distribution in the Delta (below the 50^{th} quantile-the median-for all years), which means that it may be influenced by factors in addition to or other than submerged vegetation cover (all points fall in the left corner of the wedge-shaped distribution of points). However, when submerged vegetation cover is decreased an order of magnitude, the effects on turbidity become apparent, and turbidity increases by almost a full standard deviation.

4.3 Impacts on endangered species habitat

The impact of submerged vegetation on turbidity may have consequences on habitat suitability for the endemic endangered delta smelt (*Hypomesus transpacificus*). High summertime water clarity, and the trend in increasing water clarity over the past several decades has contributed to the decline of the delta smelt (Jassby et al. 2002, Nobriga et al. 2005, Nobriga et al. 2008) and several studies have speculated that submerged vegetation has figured into this decline by acting as a water filter to reduce

turbidity (Nobriga et al. 2005, Brown and Michniuk 2007, Nobriga et al. 2008). Turbidities during the growing season range from 4.3 to 17.5 NTU, with the upper range of these turbidities (75^{th}-90^{th} quantile = 13.8-15.8 NTU) limited by submerged vegetation cover. This range of turbidities is the same range that is important to delta smelt: turbidities exceeding 12-15 NTU are a functional cue for delta smelt spawning migration (CALFED 2009), and reductions to these levels of turbidities may restrict the amount of habitat available to delta smelt (Nobriga et al. 2005). Submerged vegetation cover has the greatest impact on the habitat range most important to delta smelt; thus submerged vegetation may be directly reducing habitat quality for this endangered fish species.

5. CONCLUSION

Submerged vegetation distribution in the tidal Sacramento-San Joaquin River Delta is controlled by high water velocity events. Most likely the variation in response of submerged vegetation cover results from channel morphology and hydrology, bed composition, and vegetation community composition. The estimated velocity threshold of 0.49 $m \cdot s^{-1}$ comes from velocity measurements made at the channel-scale rather than from within the plant bed itself. Although this measurement may result in a loss of information about the interaction with water movement and the canopy and bed, it does provide us with a useful, quantifiable value that may inform invasive species management through altered flow regimes. Similarly, this value allows evaluation of potential impacts from proposed hydrologic diversions and restored or altered flows on submerged vegetation cover in the Delta. Additionally, submerged vegetation cover is negatively associated with turbidity, and limits high turbidity in the Delta. This leads us to conclude that submerged vegetation cover has a direct impact on endangered delta smelt habitat by

constraining the amount of available habitat during the growing season (April-October). Although this may induce some to suggest system-wide removal of invasive submerged vegetation, removal success is unlikely (Santos et al. 2009). Even if successful, such an effort may not result in a sufficient increase in turbidities. Despite the eventual increase in turbidity upon reduction and then near removal of submerged vegetation in Frank's Tract, water clarity was not sufficiently reduced to levels critical to delta smelt. Further, sediment supply to the Delta has been decreasing over the past 50 years due to upstream dam construction and flood control channels, diminishment of the hydraulic mining sediment pulse, and bank protection from extensive levee and rip rap construction (Wright and Schoellhamer 2004, McKee et al. 2006, Florsheim et al. 2008, Singer et al. 2008). The existing sediment supply may not provide enough suspended matter to the Delta to increase turbidities to levels needed for delta smelt habitat in spite of submerged vegetation removal. This motivates us to encourage further research into the interactions between water velocity, submerged vegetation, and turbidity to determine how changing flows, sediment supply, and submerged vegetation invasion affect turbidity in the Delta, and how these may be managed to conserve and restore delta smelt habitat.

6. ACKNOWLEDGEMENTS

Funding for this research was provided by the interagency ecological program under California Department of Water Resources contract 4600008137-T4.

REFERENCES

Barko, J. W., D. Gunnison, and S. Carpenter. 1991. Sediment interactions with submersed macrophyte growth and community dynamics. . Aquatic Botany **41**: 41-65.

Biggs, B. J. F. 1996. Hydraulic habitat of plants in streams. Regulated River Research and Management **12**: 131-144.

Brown, L. R. and D. Michniuk. 2007. Littoral fish assemblages of the alien-dominated sacramento - San Joaquin Delta, California, 1980-1983 and 2001-2003. Estuaries and Coasts **30**: 186-200.

Bryce, S. A., G. A. Lomnicky, P. R. Kaufmann, L. S. McAllister, and T. L. Ernst. 2008. Development of Biologically Based Sediment Criteria in Mountain Streams of the Western United States. North American Journal of Fisheries Management **28**: 1714-1724.

Cade, B. S. and B. R. Noon. 2003. A gentle introduction to quantile regression for ecologists. Frontiers in Ecology and the Environment **1**: 412-420.

Cade, B. S., J. W. Terrell, and R. L. Schroeder. 1999. Estimating Effects of Limiting Factors with Regression Quantiles. Ecology **80**: 311-323.

CALFED. 2009. 2-Gates Fish Protection Demonstration Project. CALFED Science Program, Sacramento.

Chambers, P. A., E. E. Prepas, H. R. Hamilton, and M. L. Bothwell. 1991. Current velocity and its effect on aquatic macrophytes in flowing water. Ecological Applications **1**: 249-257.

Cocks, T., R. Jenssen, A. Stewart, I. Wilson, and T. Shields. 1998. The HyMap airborne hyperspectral sensor: the system, calibration, and performance. Pages 1-5 *in* 1st EARSEL workshop on imaging spectroscopy., Zurich.

Crooks, J. A. 2002. Characterizing ecosystem-level consequences of biological invasions: the role of ecosystem engineers. Oikos **97**: 153-166.

Dennison, W. C., R. J. Orth, K. A. Moore, J. C. Stevenson, V. Carter, S. Kollar, P. W. Bergstrom, and R. A. Batiuk. 1993. Assessing water quality with submerged aquatic vegetation. Bioscience **43**: 86-94.

Feyrer, F., M. L. Nobrigia, and T. R. Sommer. 2007. Multidecadal trends for three declining fish species: habitat patterns, and mechanisms in the San Francisco Estuary, California, USA. Canadian Journal of Fisheries and Aquatic sciences **64**: 723-734.

Florsheim, J. L., J. F. Mount, and A. Chin. 2008. Bank erosion as a desirable attribute of rivers. Bioscience **58**: 519-529.

Fortin, G. R., L. Saint-Cyr, and M. Leclerc. 1993. Distribution of Submersed Macrophytes by Echo-sounder Tracings in Lake Saint-Pierre, Quebec. Journal of Aquatic Plant Management **31**: 232-240.

French, T. and P. Chambers. 1996. Habitat partitioning in riverine macrophyte communities. Freshwater Biology **36**: 509-520.

Gantes, H. P. and A. S. Caro. 2001. Environmental heterogeneity and spatial distribution of macrophytes in plain streams. Aquatic Botany **70**: 225-236.

Gray, J. R., G. D. Glysson, L. M. Turcois, and G. E. Schwarz. 2000. Comparibility of suspended-sediment concentration and total suspended solids data. US Geological Survey

Gurnell, A. M., M. P. Van Oosterhout, B. De Vlieger, and J. M. Goodson. 2006. Reach-scale interactions between aquatic plants and physical habitat: River Frome, Dorset. River Research and Applications **22**: 667-680.

Havens, K. E. 2004. Submerged aquatic vegetation correlations with depth and light attenuating materials in a shallow subtropical lake. Hydrobiologia **493**: 1573-5117.

Hestir, E. L., J. A. Greenberg, and S. L. Ustin. 2010. Classification Trees for Aquatic Vegetation Community Prediction from Imaging Spectroscopy. IEEE Journal of Applied Remote Sensing **In Review**.

Hestir, E. L., S. Khanna, M. E. Andrew, M. J. Santos, J. H. Viers, J. A. Greenberg, S. Rajapakse, and S. L. Ustin. 2008. Identification of invasive vegetation using hyperspectral remote sensing in the California Delta ecosystem. Remote Sensing of Environment **112**: 4034-4047.

Jassby, A. D. and J. E. Cloern. 2000. Organic matter sources and rehabilitation of the Sacramento-San Joaquin Delta (California, USA). Aquatic Conservation: Marine and Freshwater Ecosystems **10**: 323-352.

Jassby, A. D., J. E. Cloern, and B. E. Cole. 2002. Annual primary production: Patterns and mechanisms of change in a nutrient-rich tidal ecosystem. Limnology and Oceanography **47**: 698-712.

Koch, E. W. 2001. Beyond light: Physical, geological, and ceochemical parameters as possible submersed aqautic vegetation habitat requirements. Estuaries **24**: 1-17.

Koenker, R. 2009. quantreg: Quantile regression and related methods.

Koenker, R. and G. Bassett, Jr. 1978. Regression Quantiles. Econometrica **46**: 33-50.

Koenker, R. and K. Hallock. 2001. Quantile Regression. Journal of Economic Perspectives **15**: 143-156.

Madsen, J. D., P. A. Chambers, W. F. James, E. W. Koch, and D. F. Westlake. 2001. The interaction between water movement, sediment dynamics and submersed macrophytes. Hydrobiologia **44**: 71-84.

McKee, L. J., N. K. Ganju, and D. H. Schoellhamer. 2006. Estimates of suspended sediment flux entering the San Francisco Bay from the Sacramento and San Joquin Delta, San Francisco Bay, California. Journal of Hydrology **323**: 335-352.

Monserud, R. A. and R. Leemans. 1992. Comparing global vegetation maps with the Kappa statistic. Ecological Modelling **62**:275-293.

Nilsson, C. 1987. Distribution of Stream-Edge Vegetation Along a Gradient of Current Velocity. Journal of Ecology **75**: 513-522.

Nobriga, M. L., F. Feyrer, R. D. Baxter, and M. Chotkowski. 2005. Fish community ecology in an altered river delta: Spatial patterns in species composition, life history strategies, and biomass. Estuaries **28**: 776-785.

Nobriga, M. L., T. R. Sommer, F. Feyrer, and K. Fleming. 2008. Long-term Trends in Summertime Habitat Suitability for Delta Smelt (*Hypomesus transpacificus*). San Francisco Estuary and Watershed Science **6**: 1.

Sand-Jensen, K. 2008. Drag forces on common plant species in temperate streams: consequences of morphology, velocity and biomass. Hydrobiologia **610**: 307-319.

Santos, M. J., L. W. Anderson, and S. L. Ustin. 2010. Community effects of invasive species: an example using submerged aquatic plants at the regional scale. Biological Invasions **in review**.

Santos, M. J., S. Khanna, E. L. Hestir, M. E. Andrew, S. Rajapakse, J. A. Greenberg, L. W. Anderson, and S. L. Ustin. 2009. Use of hyperspectral remote sensing to evaluate efficacy of aquatic plant management. Invasive Plant Science and Management **2**: 216-229.

Schulz, M., H. Kozerski, T. Pluntke, and K. Rinke. 2003. The inlfuence of macrophytes on sedimentation and nutrient retention in the lower River Spree (Germany). Water Research **37**: 569-578.

Service, F. 2007. Delta blues, California style. Science **317**: 442-444.

Singer, M. B., R. Aalto, and L. A. James. 2008. Status of the Lower Sacramento Valley Flood-Control System within the Context of Its Natural Geomorphic Setting. Natural Hazards Review **9**: 104-115.

Sprenkle, E. S., L. A. Smock, and J. E. Anderson. 2004. Distribution and Growth of Submerged Aquatic Vegetation in the Piedmont Section of the James River, Virginia. Southeastern Naturalist **3**: 517-530.

Wright, S. A. and D. H. Schoellhamer. 2004. Trends in the sediment yield of the Sacramento River, CA, 1975-2001. San Francisco Estuary and Watershed Science **2**: 2.

Wright, S. A. and D. H. Schoellhamer. 2005. Estimating sediment budgets at the interface between rivers and estuaries with application to the Sacramento-San Joaquin River Delta. Water Resources Research **41**: W09428.09421-W09428.09417.

Yu, K., Z. Lu, and J. Stander. 2003. Quantile Regression: Applications and Current Research Areas. Journal of the Royal Statistical Society. Series D (The Statistician) **52**: 331-350.

Table 1. Image acquisition dates and classification accuracies. The Kappa statistic ranges between 0-1.0, and is an indicator of the level of agreement between ground data and map data that accounts for the probability of random agreement. Both the overall kappa coefficient and the kappa coefficient relative to the submerged vegetation class are presented. The Producer's and User's accuracies for the submerged vegetation class detail the error of omission and commission (respectively). For a detailed discussion of image classification and performance see Hestir et al. (2010).

Image Acquisition	Overall Accuracy	Overall Kappa	Kappa submerged vegetation	Producer's Accuracy submerged vegetation	User's Accuracy submerged vegetation
June 25, 2004-July 10, 2004	78.8%	0.65	0.83	64.7%	89.5%
June 22, 2005-July 8, 2005	84.3%	0.70	0.79	80.0%	86.7%
June 21, 2006-June 26, 2006	85.9%	0.77	0.83	82.4%	90.9%
June 19, 2007-June 26, 2007	79.6%	0.69	0.71	72.2%	80.5%
June 29, 2008-July 7, 2008	84.6%	0.69	0.54	55.8%	60.6%

Table 2. Estimated regression parameters for 6 upper quantile regressions, the standard error for the estimated slope, and the t-statistic and probability that for H_0: slope = 0 for each model.

Quantile	Intercept	Slope	Slope Standard error	t	p
0.70	14.59	-0.533	0.109	-4.87	0.00001
0.75	15.17	-0.569	0.102	-5.56	0.00000
0.80	15.39	-0.489	0.098	-4.96	0.00001
0.85	15.73	-0.510	0.086	-5.89	0.00000
0.90	16.74	-0.576	0.073	-7.86	0.00000
0.95	16.98	-0.592	0.499	-11.86	0.00000

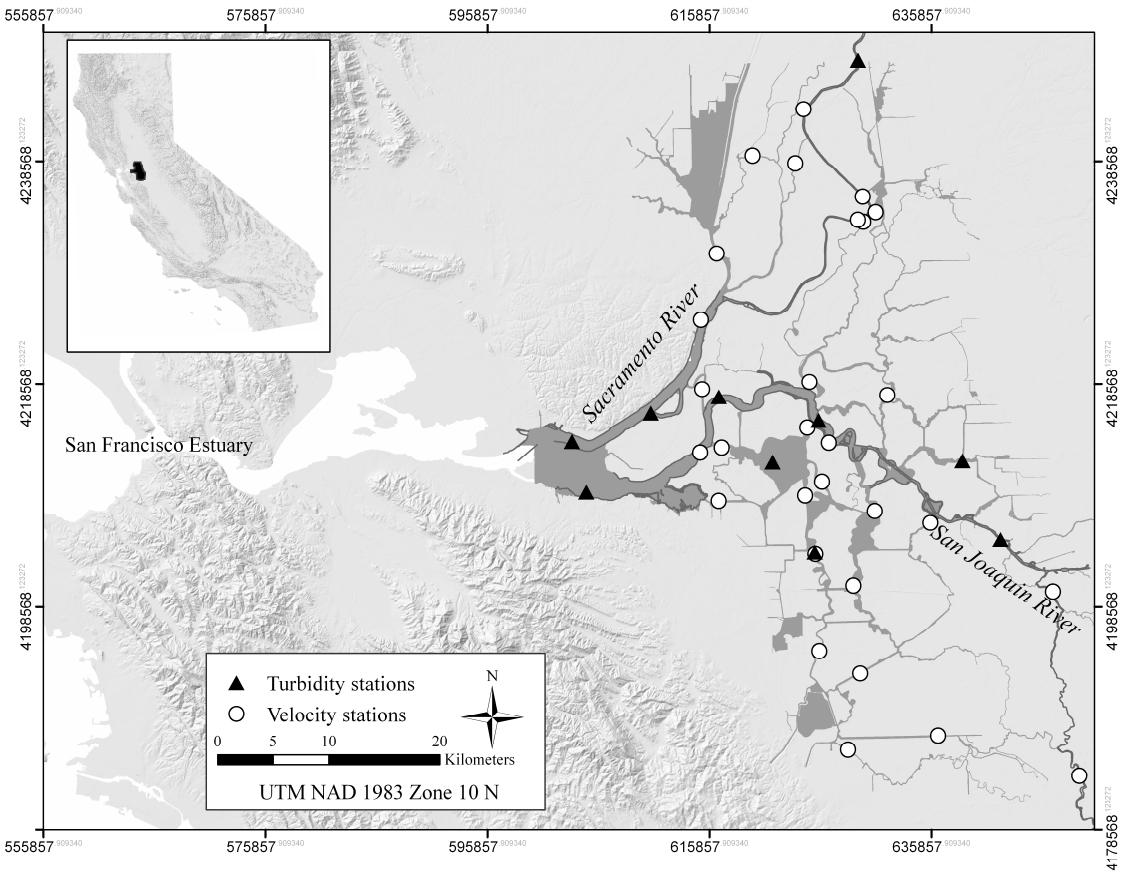

Figure 1. The Sacramento-San Joaquin River Delta and the upper San Francisco Estuary. The area of waterways mapped for submerged vegetation is highlighted in grey. Within the mapping area, there are 10 turbidity stations indicated by black triangles, and 31 water velocity stations indicated by white circles. Submerged vegetation cover within a 1 km buffer around these stations was used for the study.

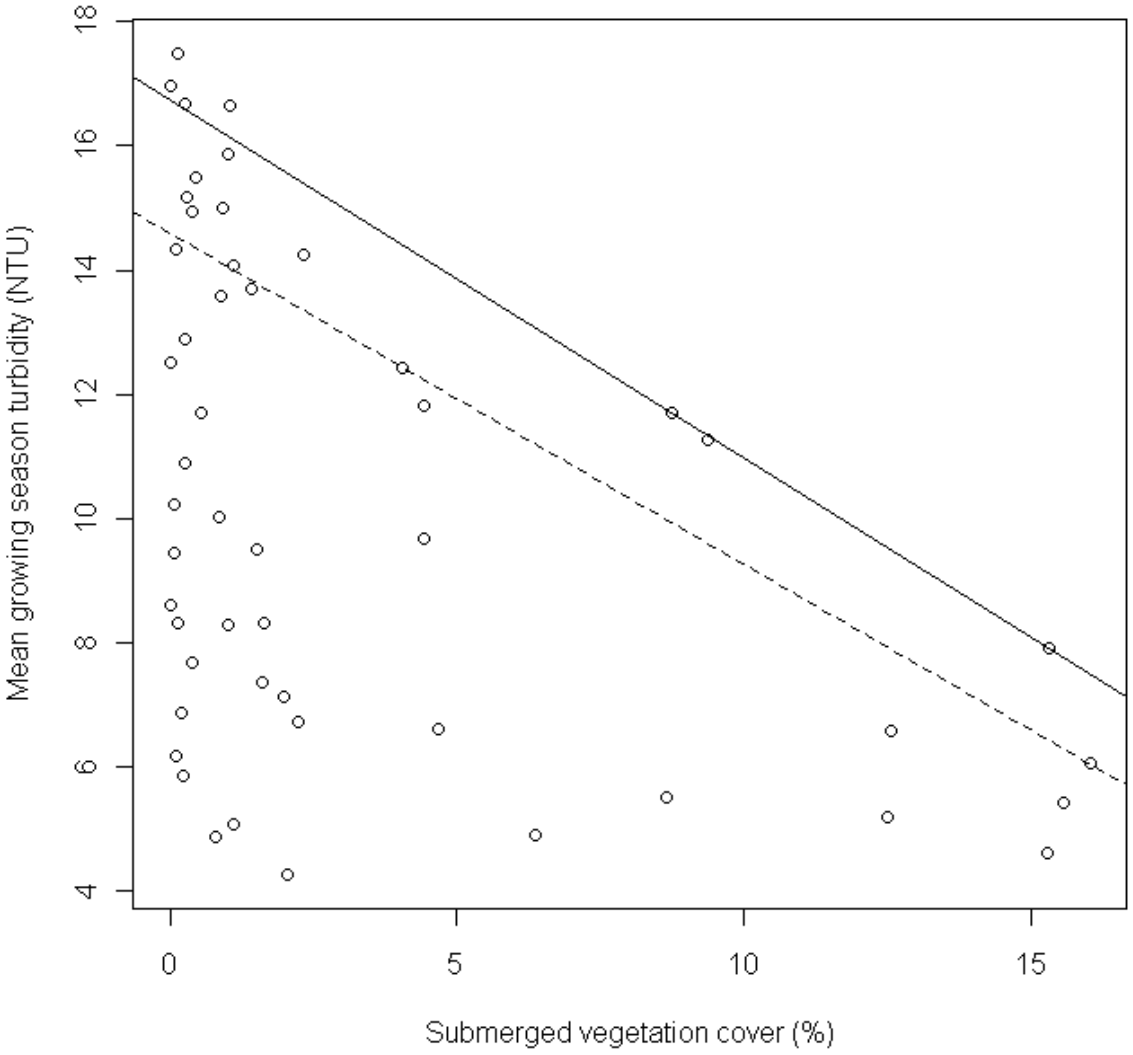

Figure 2. Mean submerged vegetation growing season turbidity (April-October) measured in NTU and submerged vegetation cover contained within a 1 km buffer around each turbidity station for 10 sites between 2004 and 2008 (n=60). There is no statistically significant difference in submerged vegetation cover between years, so each year was treated as replicate for each station. The 70th regression quantile is shown with a dashed line, and the 90th regression quantile is shown with a solid line. The 90th regression quantile describes the limiting condition of submerged vegetation cover on turbidity. The scatter of points below the quantile represents conditions under which turbidity is limited by a factor other than, or in addition to, submerged vegetation.

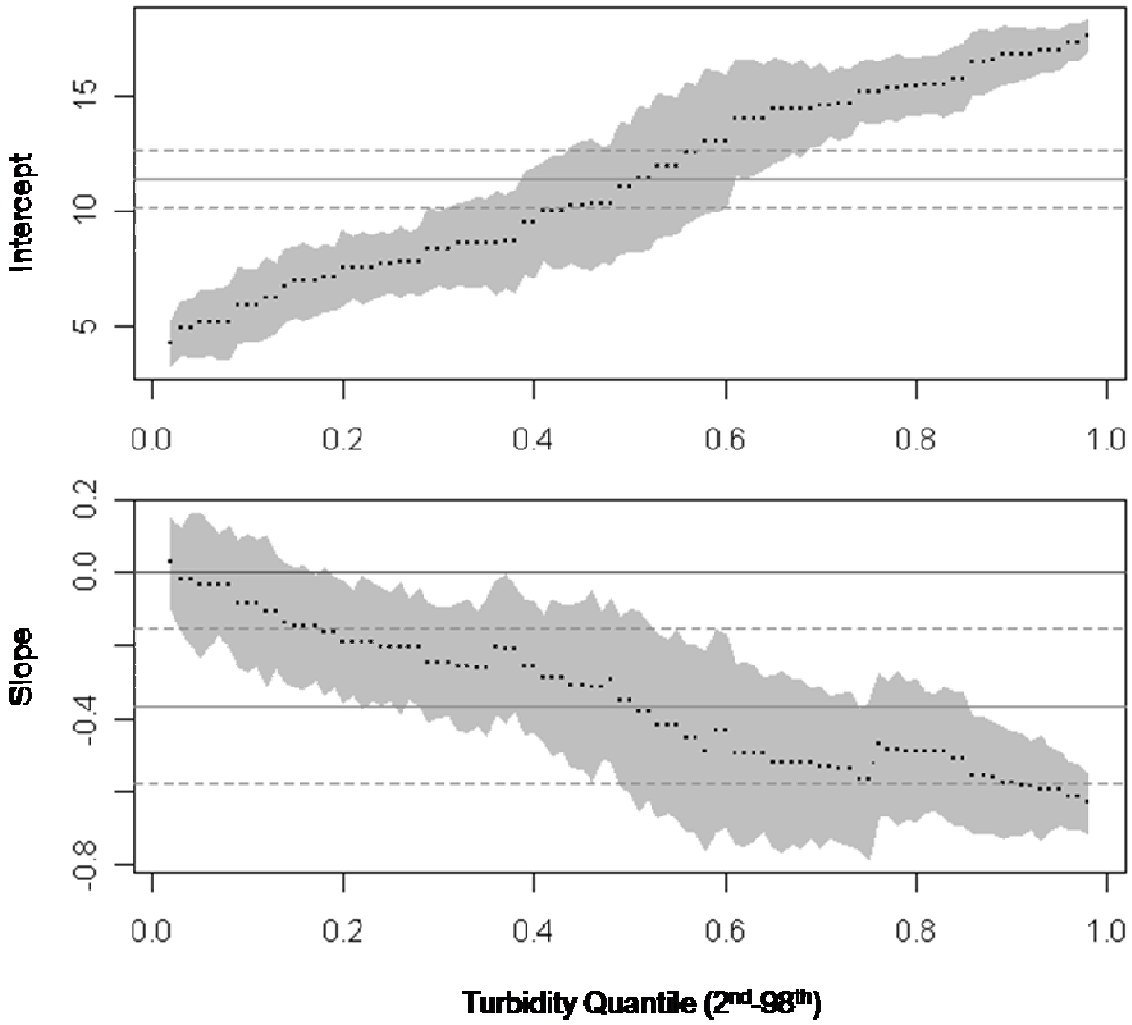

Figure 3. Estimated regression coefficients, intercept (top), and slope (bottom) from the linear quantile regression from 2nd-98th quantile (dots). The gray area shows the 95% point-wise confidence band. The gray solid line shows the estimated value from ordinary least squares estimates with the confidence intervals (dashed line). The upper black line in the slope plot shows the null hypothesis (H_0: slope = 0).

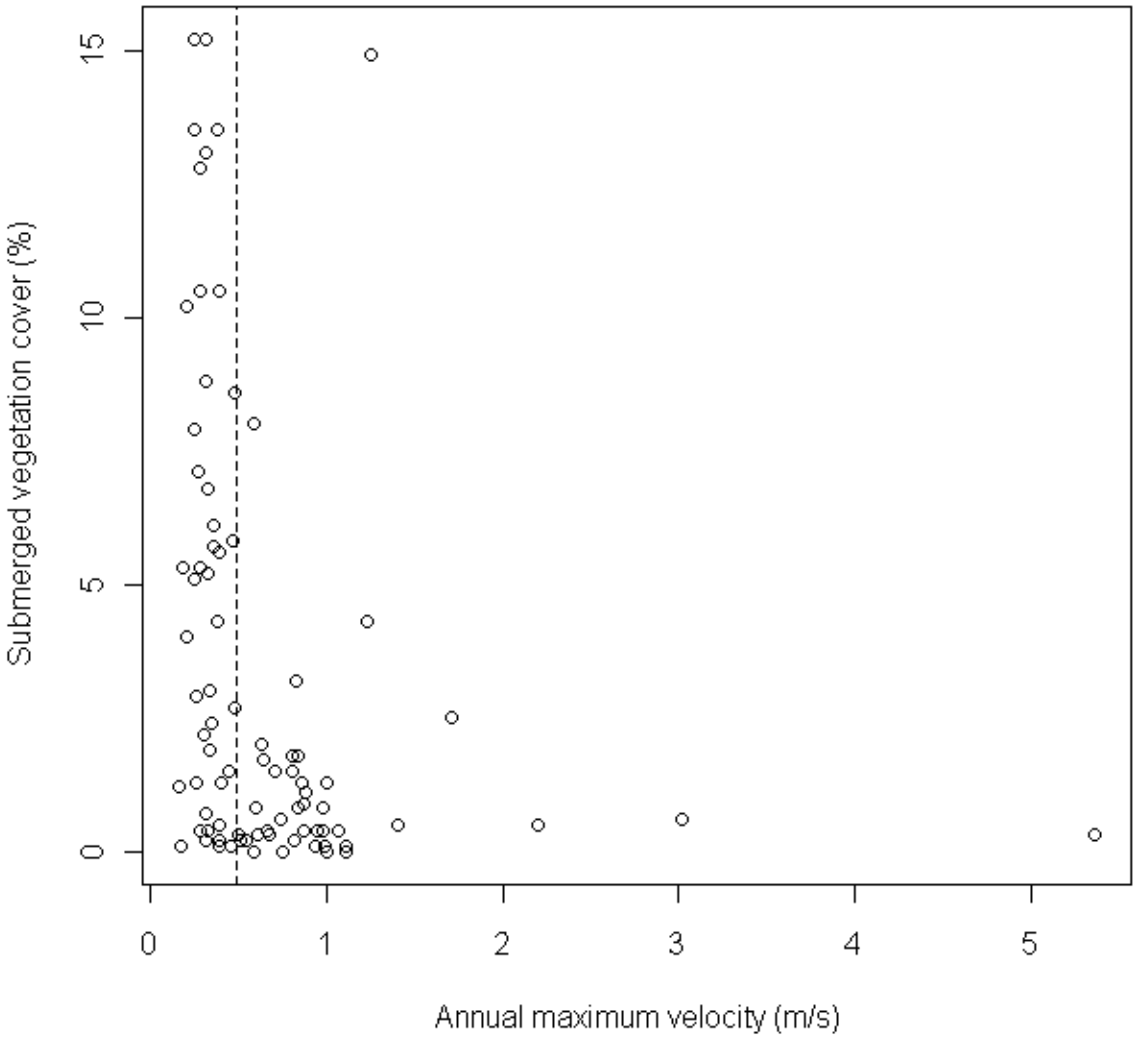

Figure 4. Submerged vegetation cover and annual maximum water velocity measured in 31 locations throughout the Delta from 2006-2008. The dashed line represents the velocity (0.49 $m \cdot s^{-1}$) at which the iterative t-test produced the most significant separation in submerged vegetation cover. We interpret this to be the velocity threshold that controls submerged vegetation cover in the Delta. The mean submerged vegetation cover below this threshold is 7.23% (n=48), and the mean above is 1.76% (n=38).

· Chapter 4 ·

Turbidity Declines and Submerged Aquatic Vegetation Expansion in a Tidal River Delta

Turbidity Declines and Submerged Aquatic Vegetation Expansion in a Tidal River Delta

Erin Lee Hestir[a], David H. Schoellhamer[b], Jonathan Greenberg[a], Tara Morgan-King[b], and Susan L. Ustin[a]

a. Center for Spatial Technologies and Remote Sensing, University of California, Davis 95616
b. California Water Science Center, United States Geological Survey, 95819

ABSTRACT

External forcings on aquatic ecosystems with submerged aquatic vegetation (SAV) can promote an ecosystem shift to an alternative meta-stable state (e.g. from a high-turbidity-low SAV state to a low turbidity-high SAV state) from which it is unlikely to revert back to its previous state (ecological hysteresis). We analyzed historic turbidity data from a tidal river delta in the San Francisco Estuary which has had both an anthropogenically-induced decline in sediment supply and an expansion of primarily invasive SAV over the past three decades. We found a significant negative trend in turbidity from 1975-2008, and when we removed the sediment supply signal from the trend we found the trend to still be significant and negative. The decreasing turbidity trend is correlated with SAV cover (R^2=0.90), and we estimate the relative contribution of SAV to the decreasing turbidity trend is 21-70% of the total trend. We suggest the decreasing sediment supply favored SAV expansion and triggered an ecosystem regime shift into a state of low turbidity-high SAV.

1. INTRODUCTION

The interaction between turbidity, water movement and submerged vegetation is a positive feedback loop that often results in two different ecosystem states: high turbidity, low submerged vegetation; or low turbidity, high submerged vegetation (Scheffer et al.

1993, Madsen et al. 2001, Scheffer and van Nes 2007). In the first case, submerged vegetation is sparse, velocity is high, sediment resuspension is high and turbidity is high, all of which further limit the growth of submerged vegetation. In the second case submerged vegetation is dense which can reduce water velocity, thus decreasing turbidity, increasing sedimentation and increasing light availability which promotes further plant growth (Madsen et al. 2001, Crooks 2002, Schulz et al. 2003). The strength of the feedback results in a strong biomodality of ecosystem regimes (e.g. high vegetation and clear water, or low vegetation and turbid water) (Figure 1). This propensity of aquatic ecosystems to occur in one of these two states and be reinforced through feedbacks has been well described in alternative stable state theory (Scheffer et al. 1993, Scheffer and Carpenter 2003, Scheffer and van Nes 2007). Alternative stable states make aquatic ecosystems vulnerable to catastrophic regime shifts and ecological hysteresis, an ecological condition under which a shift to an alternative state driven by a change in an external variable cannot be reversed to its previous state simply by reversing the modification of that variable (*sensu* Scheffer and Carpenter 2003, Scheffer et al., 2001). Ecological hysteresis presents complications to ecosystem management and restoration projects because the feedbacks that promote alternative stable states may make it impossible to restore an ecosystem by simply restoring environmental conditions to their previous circumstances (Scheffer et al. 2001).

Catastrophic regime shifts are usually modeled for submerged aquatic vegetation and turbidity in shallow lakes in which nutrient loading is the external force that triggers the shift into hysteresis. Estuaries have multiple external controls on turbidity that complicate this model such as high mineral contribution to turbidity, sensitivity to

watershed (upstream) and coastal (downstream) inputs, tidal fluctuations, short residence times and strong top down control by benthic suspension feeders (Jassby et al. 2002). Additionally, estuaries are often characterized by high hydrodynamic and sediment variability. Such environmental heterogeneity can determine hysteresis and may smooth ecosystem responses, weakening the potential for catastrophic regime shifts (van Nes and Scheffer 2005). In this study we used remote sensing submerged vegetation maps and field monitoring data from a highly modified, ecologically impaired tidal river delta to investigate trends in turbidity and submerged vegetation in the context of submerged vegetation-turbidity feedbacks. We then appraised the implications of our findings to the possibility of hysteresis and observed ecosystem shifts.

1.1 Site Description

The Sacramento-San Joaquin River Delta (henceforth, "the Delta") drains over 160,000 km^2 of California into the Pacific Ocean via the San Francisco Bay (Figure 2). The Delta is a tidal river network of levee-bound channels, rivers, and flooded tracts of lands (or lakes) that comprise the upstream component of the San Francisco Estuary, the largest estuary in the Western United States. The hydrodynamic heterogeneity of the Estuary is manifest in a wide variety of salinities, tidal fluxes, and seasonal and intra-annual inflows reflecting the Mediterranean climate of California. The Delta is critical habitat to several threatened and endangered species. In the Delta, turbidity has become one of the focal water quality indicators for the endemic and endangered Delta smelt (*Hypomesus transpacificus*). Since 2000, the abundances of four key pelagic fish species in the Delta, including the Delta smelt, have declined precipitously (Sommer et al. 2007), and reduced suspended sediment concentrations and turbidity have been identified as one

of the critical contributors (Nobriga et al. 2005). Delta smelt are dependent on highly turbid water (>18 NTU) for successful feeding (Baskerville-Bridges et al. 2004), and their habitat use is directly linked to regions in the Delta with higher turbidities (Nobriga et al. 2005, Feyrer et al. 2007). Additionally, increasing water clarity in the Estuary has contributed to a shift in species composition, timing, and variability of primary production (Jassby et al. 2002) which raises serious concerns about the stability of the food web and the importance of nutrient inputs in a traditionally light-limited estuary.

The concentration of total suspended solids, the primary factor controlling turbidity in the Delta, has decreased from 1975-1995 (Jassby et al. 2002). At this same time, two events have occurred that may explain the decrease in turbidity: 1) expansion of submerged aquatic vegetation (SAV), and 2) decreased sediment supply. The expansion of SAV includes the invasive Brazilian waterweed (*Egeria densa*) which has been actively changing aquatic habitat in the Delta (Service 2007, Santos et al. 2009). First reported in the Delta in 1946 as a result of aquaria release (Light et al. 2005), Brazilian waterweed has been rapidly expanding in the Delta over the past three decades (Jassby and Cloern 2000), and acting as an ecosystem engineer by aiding the establishment of other native and submersed species (Santos et al. 2009). Brazilian waterweed is the dominant submerged aquatic plant species in the Delta: 85% of the submerged aquatic vegetation community biomass is contributed by Brazilian waterweed (Hestir et al., *unpublished data*). We hypothesized that a feedback loop between turbidity and SAV in this estuary may explain the decrease in turbidity. However, the supply of suspended sediment, considered equivalent to suspended solids in this estuary (Gray et al. 2000), has also decreased. The Sacramento River is the primary source of suspended

sediment and the dominant sediment pathway to the Delta (Wright and Schoellhamer 2004, 2005). Sediment supply from this river decreased 50% from 1957-2001 due to diminishment of the hydraulic mining sediment pulse (McKee et al. 2006), sediment trapping behind dams in the upper watershed (Wright and Schoellhamer 2004), deposition in flood bypasses (Singer et al. 2008), and bank protection from riprap construction (USFWS 2000, Florsheim et al. 2008). Therefore we considered the effect of decreased sediment supply in our study in order to address the alternate hypothesis that external, upstream controls on turbidity explain decreased turbidity.

2. METHODS

2.1 SAV distribution data

We used SAV maps from Hestir et al. (2010) for the contemporary SAV distribution, and a review of previous field surveys and reports to infer historical SAV distribution. The contemporary SAV maps were derived from classification of airborne imaging spectroscopy collected in June and July 2004-2007. The maps have a ground resolution of 3 x 3 m ($9m^2$), and the overall classification accuracies for each year ranges from 79-85%, with target class (SAV) Kappa coefficients (an indicator of the level of agreement between ground data and map results that accounts for the probability of random agreement) ranging from 0.71-0.83, indicating very good agreement with ground reference data (Monserud and Leemans 1992) (Table 1) (Hestir et al. 2010a). Final SAV maps were exported to shapefiles.

We generated a 1 km radius around each turbidity station using ArcMap 9.2 (ESRI, Redlands, CA) and calculated the percent cover of water area covered by SAV. Based on average settling rates and water velocity, we selected 1 km as a sufficient

distance for suspended sediment to adjust to the conditions of the channel; in a typical Delta channel, the amount of time it takes a particle to settle from the water surface to bottom [5 m/10^{-3} m/s ≈ O (1hr)] is on the same order of magnitude as the time it takes a parcel of water to move 1 km [100 m/0.3 m/s ≈ O (1hr)] (Hestir et al. 2010b).

In order to estimate the SAV trend from 1975-2008 we first calculated the average SAV cover from 2004-2008 within each of the turbidity sites in order to minimize the influence of year to year fluctuations in SAV cover, even though these were minimal. Using a pair-wise Student's t-test, we found no statistically significant difference in SAV cover between years at each site, thus the average cover of 2004-2008 is representative of the contemporary SAV cover at the turbidity monitoring stations. Field surveys conducted in the 1970s and reported in 1979 found one occurrence of Brazilian waterweed with negligible cover (no patches greater than 10m^2), minimal occurrence and cover of exotic milfoil (*Myriophyllum spicatum*) (three 10-20 m^2 sites with < 5% cover, and one with 6-25%), and minimal occurrence of native sago pondweed (*Pomatogeton/Stuckenia pectinatus*) and native waterweed (*Elodea canadensis*) (Atwater et al. 1979). Brazilian waterweed and SAV cover was minimal until the 1990s (Jassby and Cloern 2000, Brown and Michniuk 2007) when a significant expansion occurred: 35 of 204 reaches, i.e. 17.2% of reaches (1000 m) sampled in 1980-1983 had SAV present at any percent cover and most had less than 50% cover, whereas 133 of 389 (34.2%) reaches sampled in 2001-2003 had 100% SAV cover (Brown and Michniuk 2007). By the late 1990s the rapid expansion of SAV resulted in a Delta-wide SAV cover of approximately 1830 ha in 1997 as estimated from color-infrared aerial photos (Jassby and Cloern 2000), a cover which appears to have stabilized. Mapping results from Hestir et

al. (2010) show fluctuation in SAV cover between the years 2004-2008, but the mean total cover for all of those years was 1817 ha. Based on this review of past studies we assumed the mean 2004-2008 SAV cover represents the trend in SAV from 1975, when there was little or no SAV present prior to its rapid expansion to 2008. [($SAV_{2004-2008}$-SAV_{1975})/33yrs = $SAV_{2004-2008}$/33yrs].

2.2 Turbidity data

Turbidity, 1 m below the surface, is measured monthly by the California Department of Water Resources (http://bdat.ca.gov/) (Figure 3). Eight sites in the Delta were active from 1975-2008 and were within the SAV mapping area used in this analysis (Figure 1). A ninth site, D10, is west of the SAV mapping area, but was included in the trend analysis. For the San Francisco Bay, Ganju et al. (2007) found a linear relation between SSC and turbidity. Thus we considered trends of turbidity and SSC in units of percent mean value per year to be comparable.

2.3 River sediment data

The US Geological Survey measures daily average suspended sediment concentrations (SSC) and suspended sediment discharge in the Sacramento River at Freeport (site 1147650) and on the San Joaquin River at Vernalis (site 11303500) (http://waterdata.usgs.gov/nwis). The Freeport station began operation in 1979. From water years 1957-1978, data were collected at a station upstream, but the two stations are considered equivalent (Wright and Schoellhamer 2004).

2.4 Turbidity trend test

We used the Seasonal Kendall test, a nonparametric method used to identify monotonic trends in water quality data that accounts for seasonal variability (Helsel and

Hirsch 1992) to determine whether there was a decreasing turbidity trend in the Delta. The tests were implemented in the ESTREND program (Schertz et al. 1991) for SPlus (TIBCO Spotfire S+ 8.1) (http://bwtst.usgs.gov/apps/s-plus/index.html). We considered a trend to be significant if $p<0.05$. We applied the trend test to Delta turbidity and turbidity corrected for sediment supply to identify whether there was a significant decreasing trend in turbidity that is not explained by decreased sediment supply. For the sediment supply correction, we used the mean SSC at Freeport in the Sacramento River for the five days prior to collection of the turbidity sample. A five day mean was used as travel time from the Sacramento River into the Delta, which varies by 1-6 days (Kuivila and Foe 1995), varying by location in the Delta and river flow. We applied linear regression to the log transformed 5 day mean flow and SSC at Freeport which removed the effect of variable flow from the SSC data, thus improving the statistical significance of the trend in decreasing sediment supply. At each turbidity site in the Delta, we applied linear regression to the log-transformed turbidity and to the Freeport residual SSC. We then applied the Seasonal Kendall test to the residual turbidity to determine the sediment supply corrected trend.

3. RESULTS

3.1 Turbidity trend without sediment supply adjustment

Turbidity in the Delta significantly decreased at eight of nine sites from 1975-2008 (Table 2). The only site without significant decrease was D22 on the Sacramento River, which had a decreasing trend but with a slightly higher p-value ($p=0.06$). At the sites with a significant downward trend, the slope of the trend ranged from -1.1% to -2.3% of the mean site turbidity per year.

3.2 River sediment supply trend with and without flow adjustment

Flow correction proved to be necessary to detect a significant downward trend of SSC in the Sacramento River with the Seasonal Kendall test. The 5-day mean suspended sediment concentration in the Sacramento River from 1975-2008 had a downward trend that had a p-value 0.064, slightly greater than 0.05. Regression of log-transformed 5-day mean SSC and discharge had an R^2 of 0.56. The downward trend p-value was 0.0065 when SSC was corrected for the 5-day mean discharge. The slope of the downward trend was -1.3% of the mean SSC per year.

The 5-day mean SSC in the San Joaquin River from 1975-2008 had a downward trend that had a p-value of < 0.0010. The slope of the downward trend was also -1.3% of the mean SSC per year. Flow and SSC are poorly correlated in this river, thus flow correction has a negligible effect on trend.

3.3 Turbidity trend adjusted for sediment supply

Most sites still had a significant downward trend in turbidity after adjusting for sediment supply (Table 2). Adjusting for sediment supply made the trends less significant (increased p-values). Sites in the Sacramento River, (D22 and D4) and downstream from the confluence of the Sacramento and San Joaquin Rivers (D10) did not have significant downward trends in supply adjusted turbidity. Sites upstream from the confluence and not in the Sacramento River retained a less significant downward turbidity trend. The slope of the downward trend at these sites ranges from -0.83% to -2.07% of the mean site turbidity per year.

Turbidity in the Sacramento San Joaquin River Delta has decreased from 1975-2008. The downward trend in turbidity increased, and the significance of the downward

trend in turbidity increased as SAV cover at monitoring sites increased (Table 2). Correcting turbidity for the Sacramento River sediment supply reduced the downward trend, and decreased the significance of the trend downstream of the Sacramento River. Among those sites with a significant trend, the average trend in decreased turbidity unadjusted for sediment supply was -1.6%/year of the mean site turbidity per year, and the average decreasing trend when adjusted for sediment supply was -1.3% of mean site turbidity per year. These decreasing trends correspond to an observed expansion of SAV from little or no cover at the beginning of the time series (1975) to its current distribution in which SAV infests approximately 6% of the water surface. Furthermore, stations with higher rates of invasion (larger values of % cover/year) had steeper and more significant trends.

To estimate the relative effect of SAV on the turbidity trend relative to decreasing sediment supply, we can use two approaches to retrieve the upper and lower bounds for the effect of SAV relative to decreased sediment supply. First the trend in river sediment supply, -1.3%/year is assumed to be equal to the unadjusted turbidity trend throughout the Delta. This assumption overestimates the effect of river supply, and underestimates the effect of SAV because river waters mix with Bay waters in the Delta. Where the unadjusted turbidity trend is less negative than -1.3%/year, the trend due to SAV is assumed to be zero. The difference between the unadjusted turbidity trends and the sediment supply trend is the turbidity trend due to SAV: 0.0 to -1.0%/year; up to 44% of the strongest trend (figure 4). The second approach assumes the adjusted turbidity trend contains only the effect of the SAV. The turbidity trend due to decreased sediment supply is then the difference in the unadjusted and adjusted trends. This assumption

overestimates the effect of the SAV, as the adjusted turbidity trend likely includes factors other than SAV. The trend due to SAV is -0.83 to -2.07%/year, or 40%-100% of the strongest trend (Figure 4).

4. DISCUSSION

Trends in suspended sediment concentration (SSC) in the Sacramento River and unadjusted turbidity in the Delta support findings from previous studies that observed significant declines in turbidity and suspended sediments in this system. Wright and Schoellhamer (2004) found the sediment yield of the Sacramento River decreased by about one-half from 1957-2001, and the trend was -1.1% of the mean value per year. This is similar to the -1.3%/year trend found for 1975-2008 in this study. Unlike the Sacramento River, the San Joaquin River watershed did not experience hydraulic mining, but it is much more regulated and impounded than the Sacramento River, which may explain the identical declining SSC trends. Jassby et al (2002) analyzed total suspended solids (TSS) data from many of the same sites used in this study and also found a 50% decrease from 1975-1995. They found a TSS (equivalent to the SSC trend (Gray et al. 2000)) trend of -2.4%/year which is near the upper limit of turbidity trends found in this study (Table 2). The present study is the first to examine turbidity trends with the supply signal removed, and our findings support the hypothesis that the expansion of submerged aquatic vegetation in the Delta may be contributing to the observed increase in water clarity.

Even with the sediment supply signal removed from the trend analysis, significant decreasing trends were still identified at 6 of the 9 sites. Of the three sites that did not have a significant trend after supply adjustment, two had information available about

associated SAV cover (D22 and D4), and both of these sites had mean SAV cover below both the average (2.47%) and median (1.35%) cover of all the sites. The two sites with the strongest decreasing turbidity trend, D28A and D19 both had significantly higher mean SAV cover than the other sites (pairwise Student's t). When the turbidity trend is adjusted for sediment supply, the strength of the trend between sites switches: D28, which has higher cover, has a larger trend than D19. This indicates the importance of SAV cover to the decreased turbidity trend. Furthermore, SAV cover and decreased turbidity trends are collocated; sites with greater SAV cover have higher trend significance (smaller p-value), and a stronger trend (steeper slope). This can be quantified with linear regressions between log-transformed p-values and mean SAV cover for both supply adjusted and unadjusted turbidity trends, which are significant, as are linear regressions between the slope and mean SAV cover (Table 3). Most meaningfully, 2004-2008 mean SAV cover explains 90% of the supply adjusted turbidity trend variation for sites with a significant decreasing turbidity trend (Figure 5). That is, after removal of one explanatory variable for declining turbidity (sediment supply), turbidity is still significantly decreasing at 6 sites, and this decline is highly correlated with SAV cover. Our results are consistent with a previous study using experimental ponds that found turbidity decreased with increased vegetation volume (Nakamura et al. 2008).

The sediment supply from the Sacramento River can be considered an external (upstream) variable controlling turbidity trends. Therefore, the removal of this upstream variable and the resulting decreasing turbidity trend implies an internal (instream) control of turbidity. Water optical properties in the Delta, as in most estuaries, are explained primarily by suspended minerals (Cloern 2001, Jassby et al. 2002), and since the vast

majority of river banks within the Delta are riprap that effectively eliminates bank erosion, turbidity is most likely a function of water column-bed sediment settling and resuspension dynamics. These dynamics are influenced by the presence and density of SAV. One factor we do not consider in this analysis is the interaction of the Delta and the San Francisco Bay, the downstream variable. Tides exchange water and suspended sediment between the two, and a decrease in Bay SSC would decrease SSC in the western Delta within several kilometers (one tidal excursion) of the Bay. There was a statistically significant step change in the water year mean SSC between 1998 and 1999 at station D10 (Mallard Island, where SSC is monitored continuously) (Schoellhamer 2009). This decline in SSC may contribute to some of the decreasing turbidity trend identified in this study, especially for the westernmost Delta sites.

We estimate the relative contribution of SAV to the decreasing turbidity trend averages between 21%-70% of the total trend (the median of the estimated upper and lower bounds in figure 4), and that this contribution varies with SAV cover; the fraction of decreasing turbidity trend attributable to SAV increases as SAV cover increases. For SAV cover less than 2%, upstream influences may be more important to the turbidity trend, whereas for cover greater than 5%, instream influences contribute more to the decreasing turbidity trend. Eighty-five percent of the surface area of channels with SAV present have greater than 5% SAV cover (4.9% of the total surface area of Delta waters) (Figure 6) and in these areas we expect SAV to play the dominant role in increasing water clarity, and the subsequent ecologic impacts observed: decreased phytoplankton (Jassby et al. 2003), decreased fish abundances (Sommer et al. 2007), increased harmful

algal blooms (Jassby et al. 2003), and persistent and increasing SAV distribution (Santos et al. 2009).

4.1 Regime shift

There are clear linkages between submerged aquatic vegetation (SAV) and increased water clarity; SAV is light limited and can be controlled by high turbidity, but SAV can also increase water clarity, promoting its own expansion. It is suggested that spatial heterogeneity of the environment reduces the chance of a regime shift, and change may be more characteristic of a smooth large-scale response rather than an abrupt shift (Scheffer and van Nes 2007). However, intense dispersion of matter and organisms may counteract the heterogeneity of a system, and a large-scale regime shift may still occur (van Nes and Scheffer 2005). This is a likely scenario in a tidal river system. Although at a Delta-wide scale, SAV cover significantly decreased from 2006-2007 (Tukey-Kramer HSD test) from a total of 2324 ha to 1827 ha and significantly decreased again from 2007-2008 (1827 ha-927.6 ha). We do not observe a significant difference in turbidity between any years 2004-2008. This may be due to the fact that there is no significant difference in SAV cover in the 1 km buffers at turbidity monitoring sites between any of the years; however, it may also indicate the current stability of the new ecosystem regime. That is, SAV cover is changing in certain areas which are geographically dispersed (a heterogeneous environment in terms of cover), but if the ecosystem has undergone a regime shift, then it may be in hysteresis and may not revert back to its previous high-turbidity state even with a reduction in SAV cover.

In shallow lake models, nutrient loading leads to changes in turbidity, thus forcing an ecosystem regime shift to its alternative meta-stable state. Estuaries, on the other hand,

have other external controls that complicate this model, such as high mineral contribution to turbidity such that they are not considered nutrient limited (Jassby et al. 2002), and are sensitive to both watershed (upstream) (Li et al. 2007, Loverde-Oliveira et al. 2009) and coastal (downstream) influences (Cho and Poirrier 2005). For example, in Lake Pontchartrain, Louisiana, SAV cover was dominated by sensitivity to climate forcing on inflow and salinity rather than nutrient loading and light limitation (Cho and Poirrier 2005). Nonetheless, our results provide a preponderance of evidence that leads us to suggest that we have observed a regime shift in the Delta from a state of high turbidity, low SAV at or prior to 1975 to that of low turbidity, high SAV in its current state. Historic sediment inputs to the estuary were high, which limited SAV. As the hydraulic mining sediment pulse moved through the estuary and sediments were trapped upstream, light conditions began to favor expansion of SAV. Our study demonstrates that the trend in turbidity declines after 1975 may be largely explained by this expansion of SAV. We postulate that a tipping point was reached, and a new ecologic regime of high SAV-low turbidity is now in place. Furthermore, the current state is at a sort of equilibrium in which SAV cover is limiting high turbidity, and SAV cover is currently controlled by channel flow velocities, rather than light limitation (Hestir et al. 2010b) and may not revert to its previously turbid state, even upon removal or reduction of SAV cover.

ACKNOWLEDGEMENTS

Funding for this research was provided by the Interagency Ecological Program through the California Department of Water Resources contract 4600008137-T4 to UC Davis and through the US Bureau of Reclamation to the US Geological Survey. Additional support

was provided by the California Department of Boating and Waterways agreement 03-105-114.

REFERENCES

Atwater, B. F., S. G. Conrad, J. N. GDowden, C. W. Hedel, R. L. MacDonald, and W. Savage. 1979. History, landforms and vegetation of the estuary's tidal marshes. Pages 347-385 *in* T. J. Conomos, editor. San Francisco Bay: The urbanized estuary. Pacific Division AAAS, San Francisco.

Baskerville-Bridges, B., J. C. Lindberg, and S. I. Doroshov. 2004. The affect of light intensity, algal concentration, and prey density on the feeding behavior of delta smelt larvae. American Fisheries Society Symposium **36**: 219-227.

Brown, L. R. and D. Michniuk. 2007. Littoral fish assemblages of the alien-dominated sacramento - San Joaquin Delta, California, 1980-1983 and 2001-2003. Estuaries and Coasts **30**: 186-200.

Cho, H. J. and M. A. Poirrier. 2005. Response of submersed aquatic vegetation (SAV) in Lake Pontchartrain, Louisiana to the 1997-2001 El Nino Southern Oscillation shifts. Estuaries **28**: 215-225.

Cloern, J. E. 2001. Our evolving conceptual model of the coastal eutrophication problem. Marine Ecology-Progress Series **210**: 223-253.

Crooks, J. A. 2002. Characterizing ecosystem-level consequences of biological invasions: the role of ecosystem engineers. Oikos **97**: 153-166.

Feyrer, F., M. L. Nobriga, and T. R. Sommer. 2007. Multidecadal trends for three declining fish species: habitat patterns, and mechanisms in the San Francisco Estuary, California, USA. Canadian Journal of Fisheries and Aquatic sciences **64**: 723-734.

Florsheim, J. L., J. F. Mount, and A. Chin. 2008. Bank erosion as a desirable attribute of rivers. Bioscience **58**: 519-529.

Ganju, N. K., D. H. Schoellhamer, M. C. Murrell, J. W. Gartner, and S. A. Wright. 2007. Constancy of the relation between floc size and density in San Francisco Bay. Proceedings in Marine Science **8**: 75-92.

Gray, J. R., G. D. Glysson, L. M. Turcois, and G. E. Schwarz. 2000. Comparibility of suspended-sediment concentration and total suspended solids data. US Geological Survey

Helsel, D. R. and R. M. Hirsch. 1992. Statistical methods in water resources. Elsevier, Amsterdam.

Hestir, E. L., J. A. Greenberg, and S. L. Ustin. 2010a. Classification Trees for Aquatic Vegetation Community Prediction from Imaging Spectroscopy. IEEE Journal of Applied Remote Sensing **in review**.

Hestir, E. L., D. H. Schoellhamer, J. A. Greenberg, T. Morgan, and S. L. Ustin. 2010b. Interactions between Submerged Vegetation, Turbidity, and Water Movement in a Tidal River Delta. Water Resources Research **in review**.

Jassby, A. D., J. Cloern, and A. Mueller-Solger. 2003. Phytoplankton Fuels Delta Food Web. California Agriculture **57**: 104-109.

Jassby, A. D. and J. E. Cloern. 2000. Organic matter sources and rehabilitation of the Sacramento-San Joaquin Delta (California, USA). Aquatic Conservation: Marine and Freshwater Ecosystems **10**: 323-352.

Jassby, A. D., J. E. Cloern, and B. E. Cole. 2002. Annual primary production: Patterns and mechanisms of change in a nutrient-rich tidal ecosystem. Limnology and Oceanography **47**: 698-712.

Kuivila, K. M. and C. G. Foe. 1995. Concentrations, transport, and biological effects of dormant spray pesticides in the San Francisco Estuary, California. Environmental Toxicology and Chemistry **14**: 1141-1150.

Li, X. Y., D. E. Weller, C. L. Gallegos, T. E. Jordant, and H. C. Kim. 2007. Effects of watershed and estuarine characteristics on the abundance of submerged aquatic vegetation in Chesapeake Bay subestuaries. Estuaries and Coasts **30**: 840-854.

Light, T., T. Grosholz, and P. Moyle. 2005. Delta Ecological Survey (Phase I): Non-indigenous aquatic species in the Sacramento-San Joaquin Delta, a literature review. US Fish and Wildlife Service, Sacramento.

Loverde-Oliveira, S. M., V. L. M. Huszar, N. Mazzeo, and M. Scheffer. 2009. Hydrology-Driven Regime Shifts in a Shallow Tropical Lake. Ecosystems **12**: 807-819.

Madsen, J. D., P. A. Chambers, W. F. James, E. W. Koch, and D. F. Westlake. 2001. The interaction between water movement, sediment dynamics and submersed macrophytes. Hydrobiologia **44**: 71-84.

McKee, L. J., N. K. Ganju, and D. H. Schoellhamer. 2006. Estimates of suspended sediment flux entering the San Francisco Bay from the Sacramento and San Joquin Delta, San Francisco Bay, California. Journal of Hydrology **323**: 335-352.

Monserud, R. A. and R. Leemans. 1992. Comparing global vegetation maps with the Kappa statistic. Ecological Modelling **62**: 275-293.

Nakamura, K., Y. Kayaba, J. Nishihiro, and N. Takamura. 2008. Effects of submerged plants on water quality and biota in large-scale experimental ponds. Landscape and Ecological Engineering **4**: 1-9.

Nobriga, M. L., F. Feyrer, R. D. Baxter, and M. Chotkowski. 2005. Fish community ecology in an altered river delta: Spatial patterns in species composition, life history strategies, and biomass. Estuaries **28**: 776-785.

Santos, M. J., S. Khanna, E. L. Hestir, M. E. Andrew, S. Rajapakse, J. A. Greenberg, L. W. Anderson, and S. L. Ustin. 2009. Use of hyperspectral remote sensing to evaluate efficacy of aquatic plant management. Invasive Plant Science and Management **2**: 216-229.

Scheffer, M., S. Carpenter, J. A. Foley, C. Folke, and B. Walker. 2001. Catastrophic shifts in ecosystems. Nature **413**: 591-596.

Scheffer, M. and S. R. Carpenter. 2003. Catastrophic regime shifts in ecosystems: linking theory to observation. Trends in Ecology & Evolution **18**: 648-656.

Scheffer, M., S. H. Hosper, M. L. Meijer, B. Moss, and E. Jeppesen. 1993. Alternative equilibria in shallow lakes. Trends in Ecology & Evolution **8**: 275-279.

Scheffer, M. and E. H. van Nes. 2007. Shallow lakes theory revisited: various alternative regimes driven by climate, nutrients, depth and lake size. Hydrobiologia **584**: 455-466.

Schertz, T. L., R. B. Alexander, and D. J. Ohe. 1991. The computer program estimate trend (ESTREND), a system for the detection of trends in water quality data US Geological Survey Water Resources Investigations Report 91-4040.

Schoellhamer, D.H. 2009. Suspended sediment in the Bay: Past a tipping point. The Pulse of the Estuary: Monitoring and Managing Water Quality in the San Francisco Estuary, San Francisco Estuary Institute, Oakland, Calif., 56-65. http://sfei.org/rmp/pulse/2009/RMP_Pulse09_no583_final4web.pdf

Schulz, M., H. Kozerski, T. Pluntke, and K. Rinke. 2003. The inlfuence of macrophytes on sedimentation and nutrient retention in the lower River Spree (Germany). Water Research **37**: 569-578.

Service, F. 2007. Delta blues, California style. Science **317**: 442-444.

Singer, M. B., R. Aalto, and L. A. James. 2008. Status of the Lower Sacramento Valley Flood-Control System within the Context of Its Natural Geomorphic Setting. Natural Hazards Review **9**: 104-115.

Sommer, T. R., C. Armor, R. D. Baxter, R. Breuer, L. Brown, M. Chotkowski, S. Culberson, F. Feyrer, M. Gingras, B. Herbold, W. Kimmerer, A. Mueller-Solger, M. L. Nobriga, and K. Souza. 2007. The collapse of pelagic fishes in the upper San Francisco estuary Fisheries **32**: 270-277.

USFWS. 2000. Impacts of riprapping to ecosystem functioning, lower Sacramento River, California. United States Fish and Wildlife Service, Sacramento.

van Nes, E. H. and M. Scheffer. 2005. Implications of spatial heterogeneity for catastrophic regime shifts in ecosystems. Ecology **86**: 1797-1807.

Wright, S. A. and D. H. Schoellhamer. 2004. Trends in the sediment yield of the Sacramento River, CA, 1975-2001. San Francisco Estuary and Watershed Science **2**: 2.

Wright, S. A. and D. H. Schoellhamer. 2005. Estimating sediment budgets at the interface between rivers and estuaries with application to the Sacramento-San Joaquin River Delta. Water Resources Research **41**: W09428.09421-W09428.09417.

Table 1. Image acquisition dates and classification accuracies for SAV distribution maps. The Kappa statistic ranges between 0-1.0, and is an indicator of the level of agreement between ground data and map data that accounts for the probability of random agreement. Both the overall kappa coefficient and the kappa coefficient relative to the submerged vegetation class are presented. The Producer's and User's accuracies for the submerged vegetation class detail the error of omission and commission (respectively). For details about image classification and performance see Hestir et al. (2010).

Image Acquisition	Overall Accuracy	Overall Kappa	Kappa submerged vegetation	Producer's Accuracy submerged vegetation	User's Accuracy submerged vegetation
June 25, 2004-July 10, 2004	78.8%	0.65	0.83	64.7%	89.5%
June 22, 2005-July 8, 2005	84.3%	0.70	0.79	80.0%	86.7%
June 21, 2006-June 26, 2006	85.9%	0.77	0.83	82.4%	90.9%
June 19, 2007-June 26, 2007	79.6%	0.69	0.71	72.2%	80.5%
June 29, 2008-July 7, 2008	84.6%	0.69	0.54	55.8%	60.6%

Table 2. SAV and turbidity trends from 1975-2008 at the nine monitoring stations. The SAV cover trend is given in percent cover per year. The significance (p) from the Seasonal Kendall trend test, and the resulting slope of the trend given in percent of the mean site turbidity per year for turbidity with and without suspended sediment supply adjustment. Asterisks (*) denote significant p-values ($p < 0.05$).

Site	Mean SAV cover within 1 km, 2004-2008	SAV cover trend (%/yr) 1975-2008	No supply adjustment		Adjusted for supply	
			p	Trend (%/yr)	p	Trend (%/yr)
D16	0.84%	0.03	< 0.001*	-1.44	0.008*	-1.08
D19	5.99%	0.18	< 0.001*	-2.33	< 0.001*	-1.84
D22	0.19%	0.01	0.066	-0.90	0.43	-0.37
D26	1.46%	0.04	< 0.001*	-1.33	0.048*	-0.83
D4	1.24%	0.04	0.006*	-1.15	0.12	-0.66
D10	-	-	0.019*	-1.10	0.17	-0.60
D12	1.67%	0.05	< 0.001*	-1.67	0.024*	-0.92
D28A	7.26%	0.22	< 0.001*	-2.22	0.0001*	-2.07
P8	1.08%	0.03	< 0.001*	-1.35	0.014*	-1.15

Table 3. Summary of linear regressions between significance (p value) and trend (slope) of trend test for sediment supply adjusted and unadjusted turbidity versus 204-2008 mean SAV cover. All regressions were significant ($p<0.05$, noted with an asterisk *), and SAV cover is most strongly correlated with the sediment supply adjusted turbidity trend.

	Supply adjusted?	Equation	R^2	Significance
p-value vs SAV	No	Log(p) = -5.65-0.75(SAV)	0.56	0.032*
p-value vs SAV	Yes	Log(p) = -2.11-0.93(SAV)	0.82	0.002*
Trend (slope) vs SAV (all sites)	No	Trend = -1.11-0.18(SAV)	0.85	0.001*
Trend (slope) vs SAV (all sites)	Yes	Trend = -0.61-0.20(SAV)	0.86	<0.001*
Trend (slope) vs SAV (significant sites)	No	Trend = -1.19-0.16(SAV)	0.86	0.003*
Trend (slope) vs SAV (significant sites)	Yes	Trend = -0.78-0.17(SAV)	0.90	0.003*

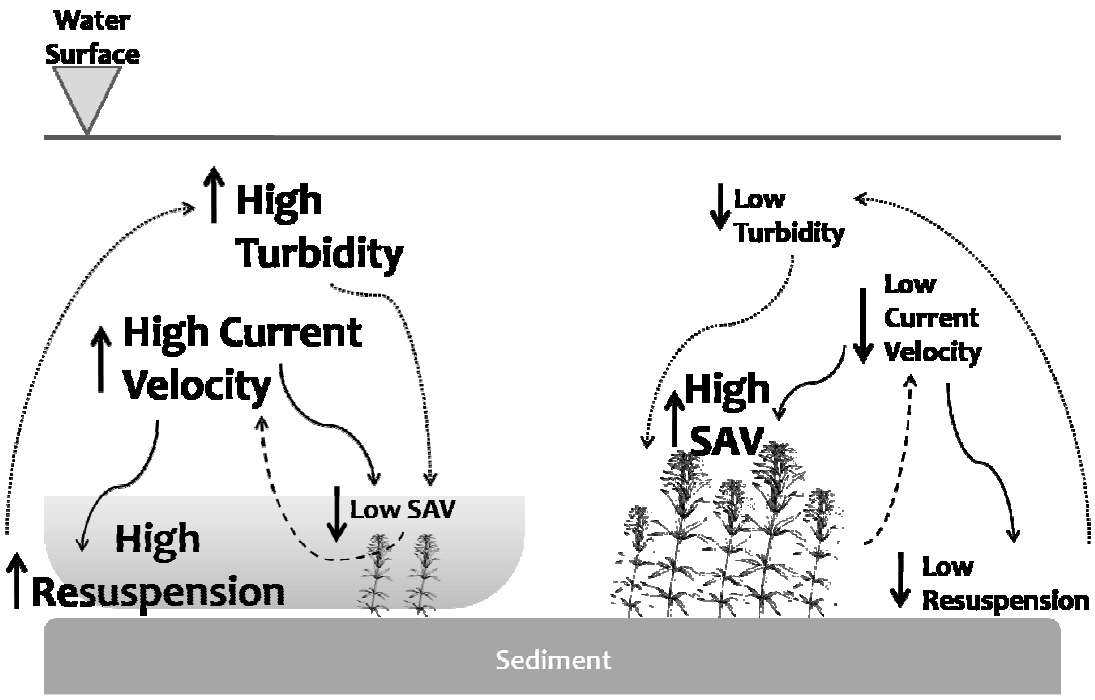

Figure 1. Two aquatic ecosystem regimes reinforced by feedbacks between water velocity, submerged aquatic vegetation amd turbidity. In the first state, submerged aquatic vegetation is sparse, water velocity is high, sediment resuspension is high, and turbidity is high. In the second state submerged vegetation is dense, water velocity is low, and turbidity is low. The potential for two possible ecosystem regimes makes ecosystems with these feedbacks vulnerable to catastrophic regime shifts once a change in an external factor reaches a critical tipping point. Conceptualized from Madsen et al. (2001) and Scheffer et al. (1993).

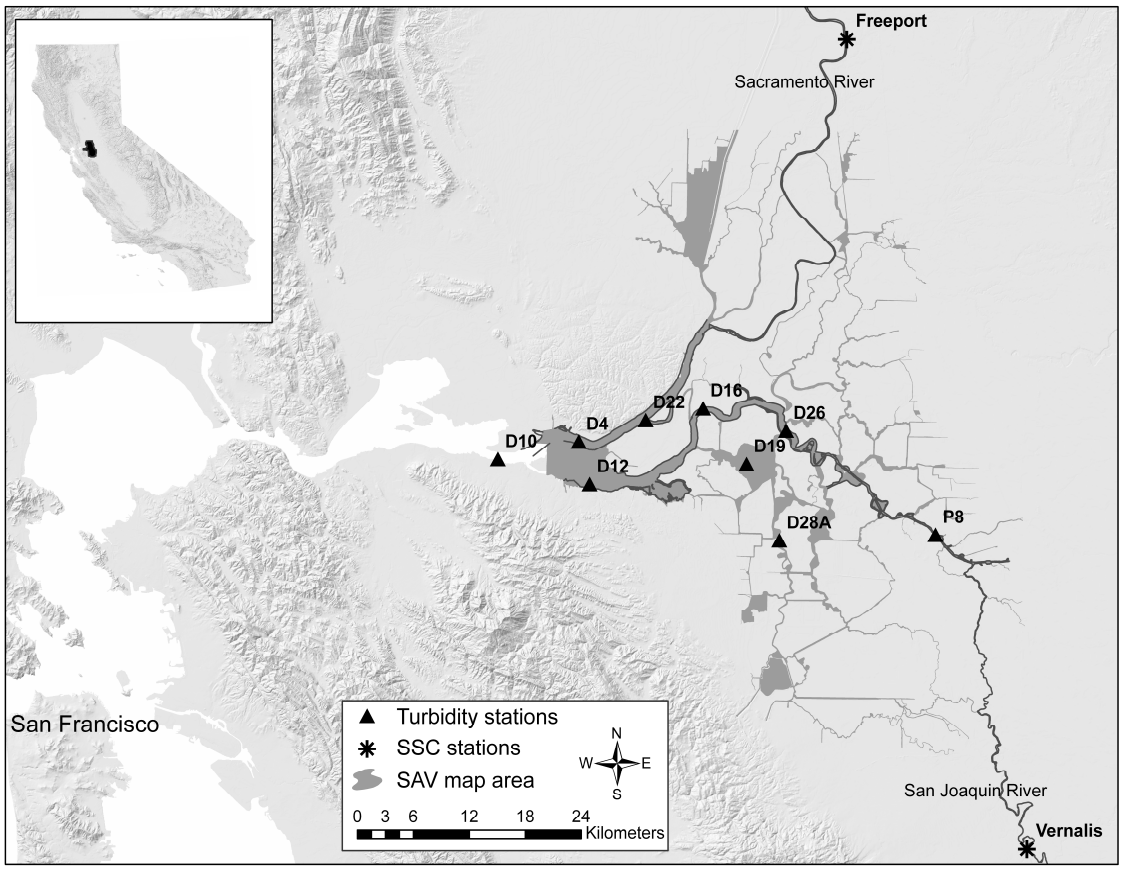

Figure 2. The upper San Francisco Estuary, including the Sacramento-San Joaquin River Delta is located in the Central Valley and coast of California. The SAV mapping area is indicated in grey, monthly turbidity monitoring stations are represented by black triangles, and suspended sediment concentration stations are designated by stars.

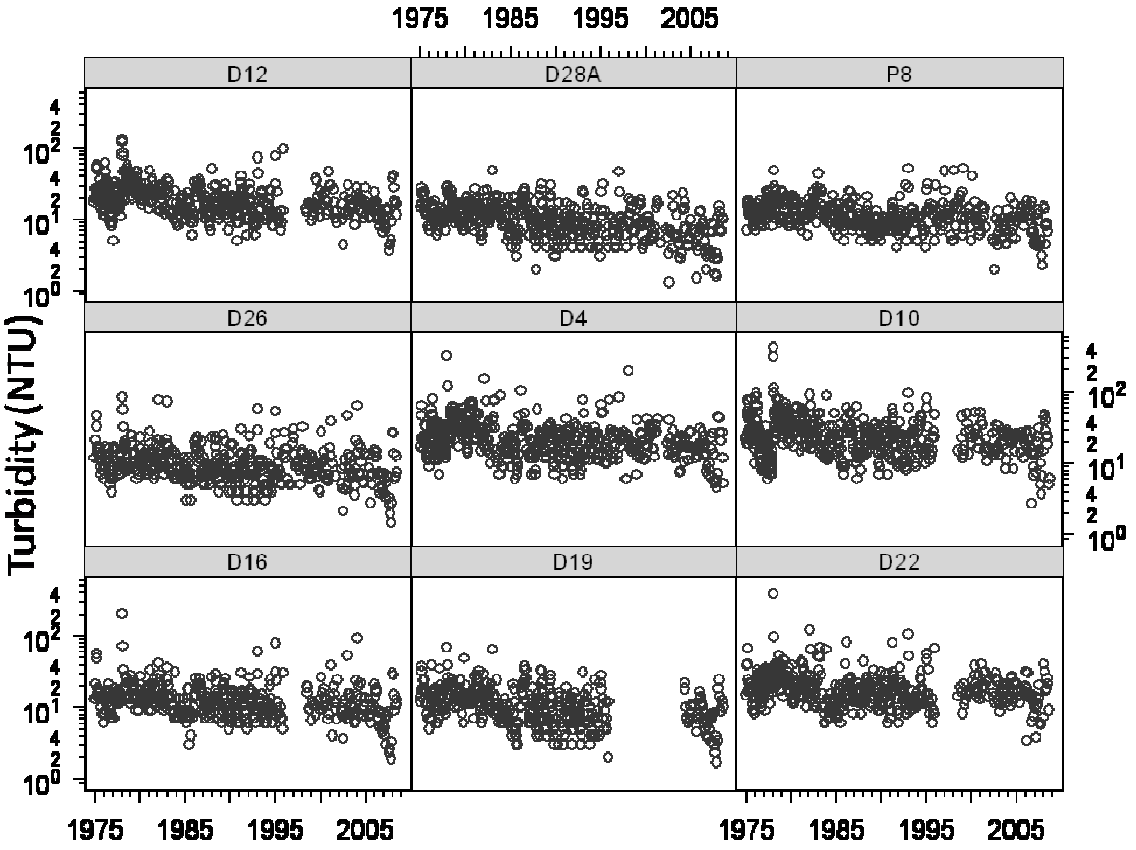

Figure 3. Monthly turbidity measurements at nine monitoring stations in the Delta (see Figure 1 for station location information) from 1975-2008. Gaps in the time series (blank regions) are periods when data were not collected. Note turbidity (in NTU) is displayed on log-scale on the y-axes.

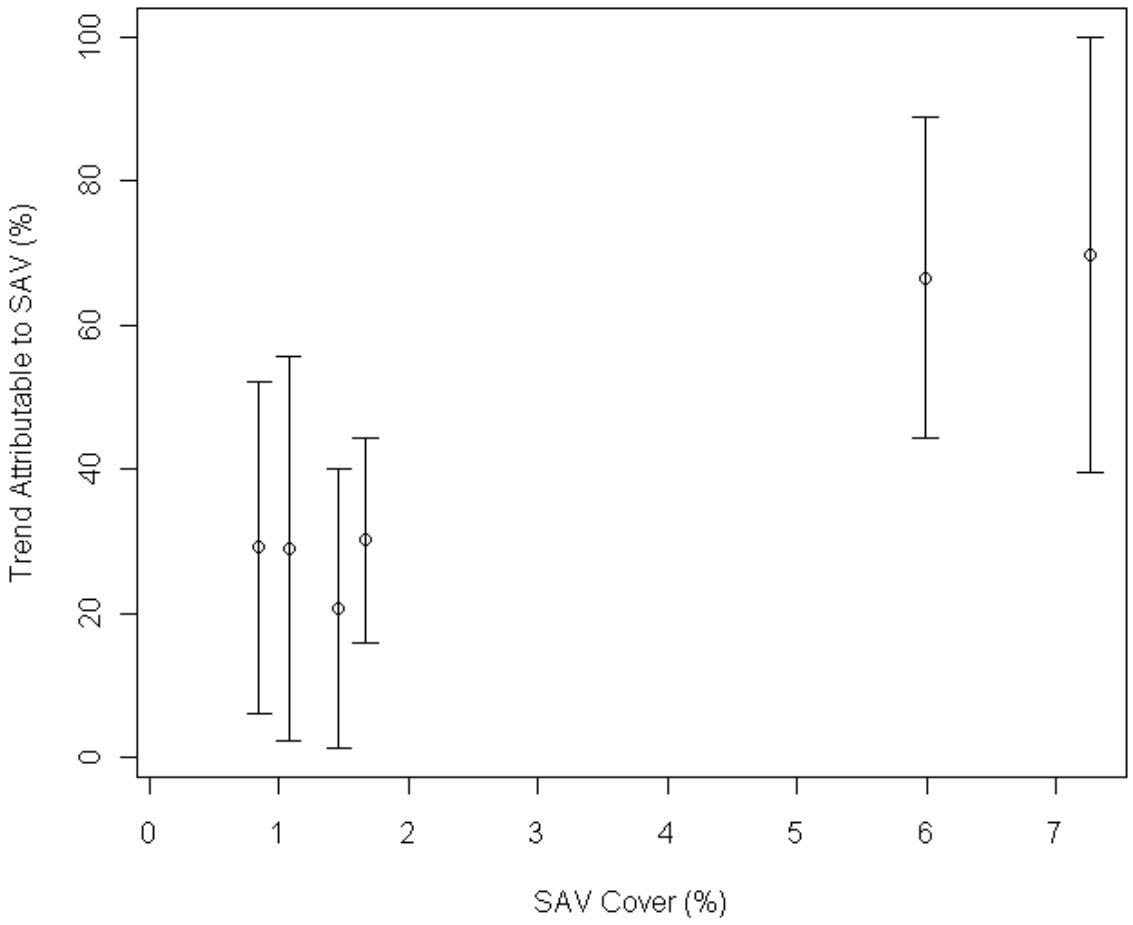

Figure 4. The portion of the decreasing turbidity trend attributable to submerged aquatic vegetation (SAV) as a function of contemporary SAV cover at sites with significant supply-adjusted trends. The lower bound assumes the trend in river sediment supply is equal to the supply turbidity trend, overestimating the effect of river supply and underestimating the effect of SAV. The upper bound assumes the turbidity trend adjusted for sediment supply is due entirely to SAV, overestimating the effect of SAV on the trend. The mean of these two estimates is represented by open circles.

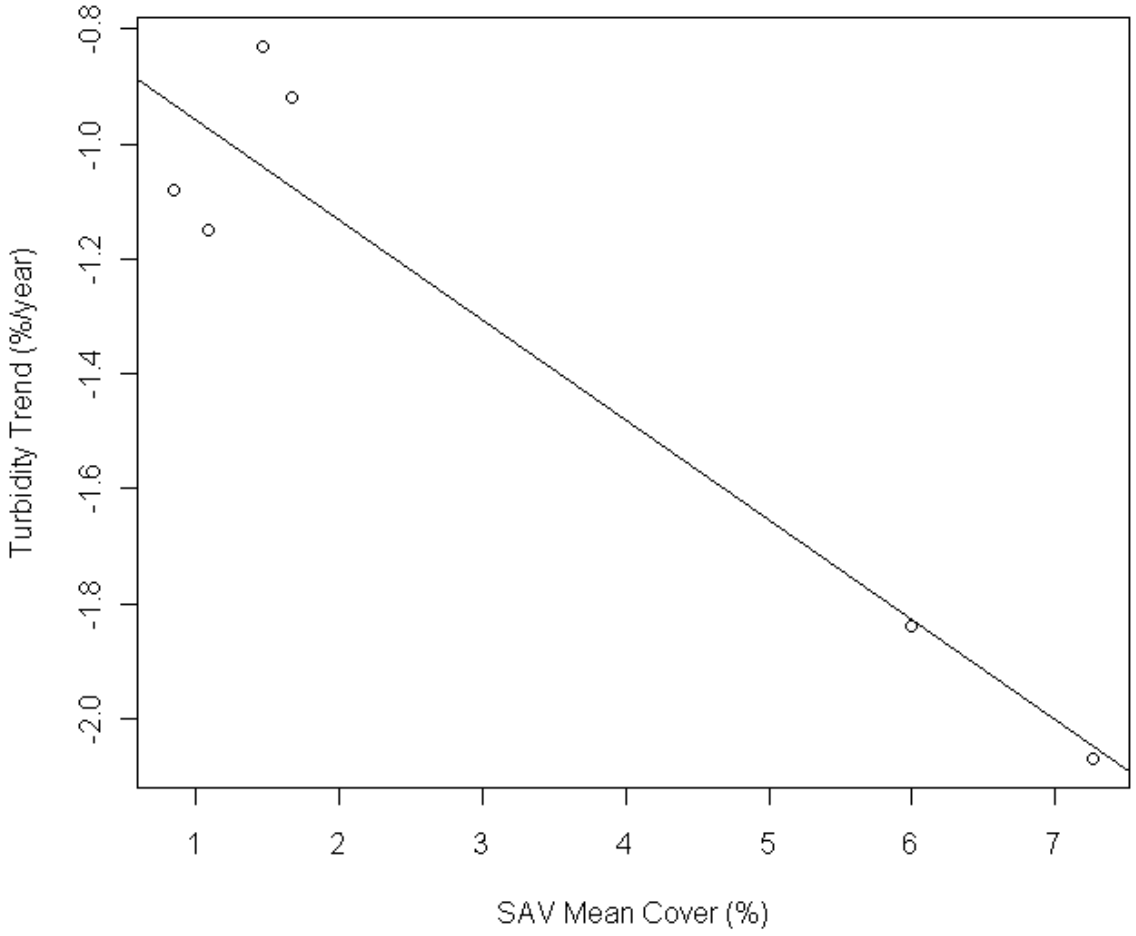

Figure 5. A plot of the slope of the sediment supply adjusted turbidity trend (in percent of the mean site turbidity per year) at sites with significant decreasing trends against the corresponding 2004-2008 mean submerged aquatic vegetation (SAV) cover in percent. SAV cover and the declining turbidity trend are negatively correlated ($R^2 = 0.90$); sites with greater SAV cover have stronger, more significant decreasing turbidity trends.

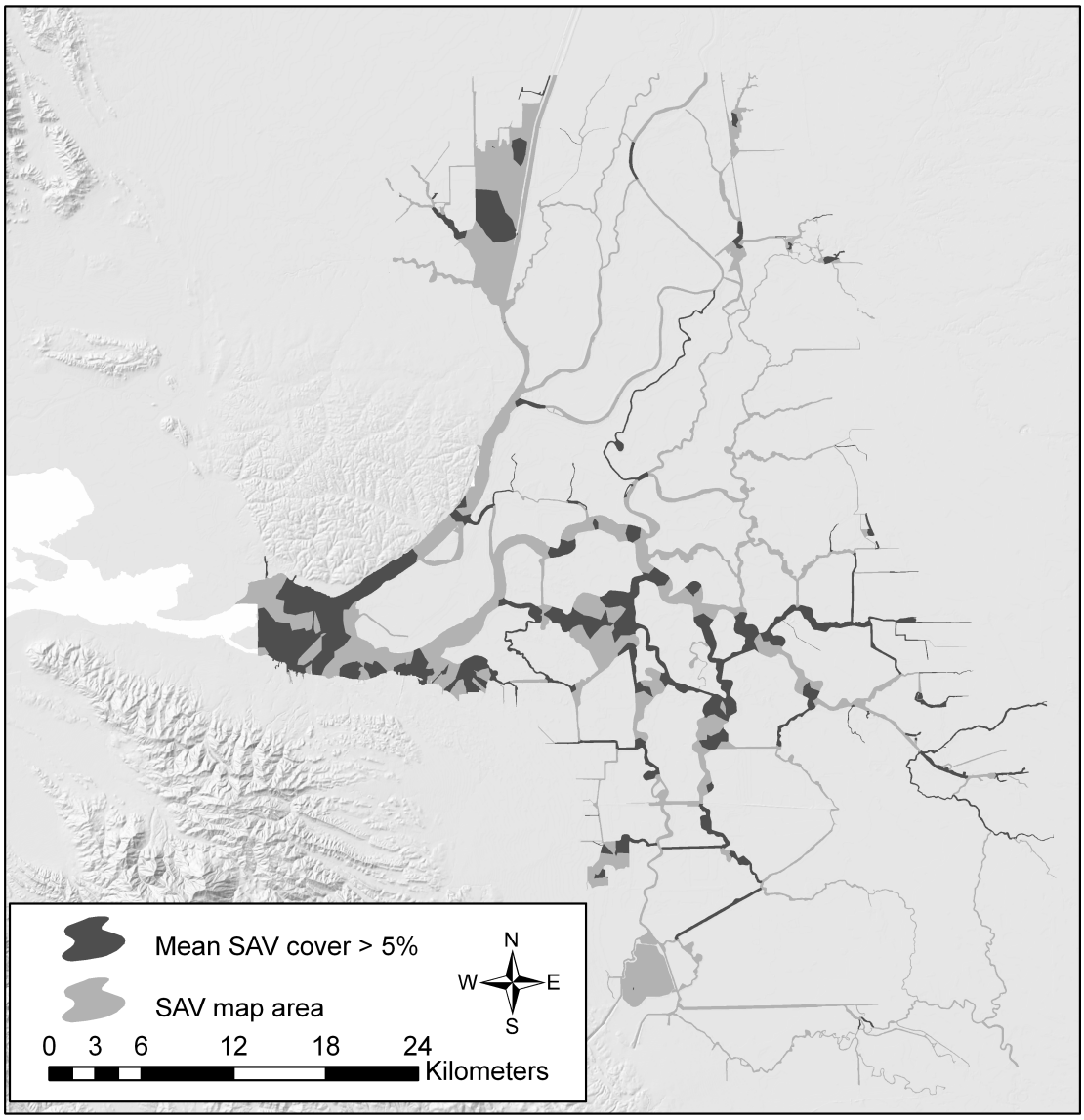

Figure 6. Reaches of the Delta that contain greater than 5% SAV cover (in dark grey). These reaches constitute 85% of all channels with any SAV present; 4.9% of the total water surface area. In these reaches, we expect SAV to have a considerable impact on increased water clarity.

CONCLUSIONS

Remote sensing provides a synoptic solution for monitoring submerged aquatic vegetation distribution over extensive river networks. However, mapping and monitoring the distribution of submerged aquatic vegetation (SAV) is difficult due to limited access to aquatic field sites, as well as the added problem of additional weed dispersal upon boat contact with vegetation patches. There are additional remote sensing challenges associated with successful SAV detection, including meterological conditions, water depth and water clarity, and pixel mixing. Appropriately distributed training data, as well as narrow-band reflectance data across the visible-shortwave infrared spectrum, is needed to successfully detect SAV. Constraining flight times for image acquisition to morning and afternoon low tide conditions can further improve detection.

I used a systematic, automated machine learning classification to detect SAV from hyperspectral remote sensing imagery with reasonable accuracies. However, discrimination between SAV and water still remains challenging, especially when SAV patches are sparse, or very deep in the water column.

There are feedbacks between SAV, water movement, and turbidity in estuaries, despite the sediment-dominated turbidity as well as the spatial and temporal variability in hydrology and SAV distribution. Furthermore, these feedbacks have contributed to the decreasing turbidity trend in the Sacramento-San Joaquin River Delta, negatively impacting endangered Delta smelt (*Hypomesus transpacificus*) habitat. Annual maximum water velocities exceeding 0.49 $m \cdot s^{-1}$ control SAV cover for the years 2004-2006. In reaches with annual maximum velocities below this threshold, other environmental conditions and species specific plant traits influence SAV distribution. There is also a

significant negative relation between SAV cover and turbidity, and SAV cover from 2004-2008 is limiting turbidities in the peak growing season: SAV is most limiting on turbidities ranging from 13.8-15.8 NTU. Recent research attributes the decline of the Delta smelt to high summertime water clarity and the trend in increasing water clarity over the past several decades (Jassby et al. 2002, Nobriga et al. 2005, Nobriga et al. 2008). The constraint SAV places on turbidities in the peak growing season is likely contributing to the degradation of Delta smelt habitat quality, thus negatively impacting this endangered fish.

Not only do the feedbacks between SAV, turbidity, and water velocity impact current ecosystem quality in the Delta, but it is likely that these feedbacks contributed to the decline of the ecosystem's health over the past 30 years, and may have forced a shift in the ecosystem regime. Turbidity in the Delta experienced a significant decreasing trend from 1975-2008, and the expansion of SAV contributed to 21-71% of the total trend. Sediment supply to the Delta has decreased approximately 50% since 1957 (Wright and Schoellhamer 2004) due primarily to anthropogenic activities in the watershed including dam construction on nearly every tributary into the Delta, upstream diversions, rip-rap bank protection and the diminishment of the hydraulic mining pulse. These disturbances to the sediment supply led to an increase in light availability and a rapid expansion of invasive SAV, and the positive feedback between SAV, turbidity, and water movement likely caused the system to shift from a low-SAV, high turbidity state into a high-SAV, low-turbidity state.

Alternative stable-state theory predicts ecosystem hysteresis in systems with two potential ecosystems states reinforced by positive feedbacks, such as aquatic ecosystems

dominated by SAV (Scheffer et al. 1993, Scheffer et al. 2001, Scheffer and Carpenter 2003). Under ecosystem hysteresis, instead of a dynamic ecosystem that responds smoothly to a change in external conditions, an ecosystem is likely shift into an alternative regime once a change in the external factor reaches a critical tipping point. This shift is called "catastrophic regime shift" because once shifted, the system is unlikely to switch back to its previous state, even if there is a modification in the external condition (Scheffer et al. 2001). It is very likely that the Delta has or may soon undergo such a shift; if this happens, then in spite of current efforts to remove invasive SAV from the system by state agencies it is unlikely to transition back to its previous light limited condition.

More research is needed to better understand the multivariate interaction between water velocity, turbidity, and SAV, and how those interactions vary across SAV species and community composition. Does species composition influence the strength of the feedbacks? How might changing flows, sediment supply, and SAV species composition affect the interactions between water movement, SAV, and turbidity? Are there possible ways to manage these external variables in such a way that promotes regime shift in a "desirable" direction that aids species conservation efforts? This dissertation is but a first step in understanding the interactions between SAV, turbidity, and water movement in highly modified estuaries. The implications of the potential for ecosystem hysteresis in the Delta cannot be ignored by resource managers in the face of plans to drastically alter water conveyance through the system while conserving and restoring Delta smelt habitat, and planning for the impacts of climate change on the Delta's water quality and water quantity.

REFERENCES

Jassby, A. D., J. E. Cloern, and B. E. Cole. 2002. Annual primary production: Patterns and mechanisms of change in a nutrient-rich tidal ecosystem. Limnology and Oceanography **47**:698-712.

Nobriga, M. L., F. Feyrer, R. D. Baxter, and M. Chotkowski. 2005. Fish community ecology in an altered river delta: Spatial patterns in species composition, life history strategies, and biomass. Estuaries **28**:776-785.

Nobriga, M. L., T. R. Sommer, F. Feyrer, and K. Fleming. 2008. Long-term Trends in Summertime Habitat Suitability for Delta Smelt (*Hypomesus transpacificus*). San Francisco Estuary and Watershed Science **6**:1.

Scheffer, M., S. Carpenter, J. A. Foley, C. Folke, and B. Walker. 2001. Catastrophic shifts in ecosystems. Nature **413**:591-596.

Scheffer, M. and S. R. Carpenter. 2003. Catastrophic regime shifts in ecosystems: linking theory to observation. Trends in Ecology & Evolution **18**:648-656.

Scheffer, M., S. H. Hosper, M. L. Meijer, B. Moss, and E. Jeppesen. 1993. Alternative equilibria in shallow lakes. Trends in Ecology & Evolution **8**:275-279.

Wright, S. A. and D. H. Schoellhamer. 2004. Trends in the sediment yield of the Sacramento River, CA, 1975-2001. San Francisco Estuary and Watershed Science **2**:2.